HEINRICH HEINE
UNIVERSITÄT DÜSSELDORF

Accessing possible protective functions and interaction partners of Progranulin

Inaugural-Dissertation

zur Erlangung des Doktorgrades
der Mathematisch-Naturwissenschaftlichen Fakultät
der Heinrich-Heine-Universität Düsseldorf

vorgelegt von

Julia Seegel
aus Fulda

Düsseldorf, Juni 2017

aus dem Institut für Neuropathologie
der Heinrich-Heine-Universität Düsseldorf

Gedruckt mit der Genehmigung der
Mathematisch-Naturwissenschaftlichen Fakultät der
Heinrich-Heine-Universität Düsseldorf

Referent: Prof. Dr. Sascha Weggen
Korreferent: Prof. Dr. Vlada Urlacher

Tag der mündlichen Prüfung:

Betreffend die vorgelegte Dissertation:

Accessing possible protective functions and interaction partners of Progranulin

Ich versichere an Eides Statt, dass die Dissertation von mir selbständig und ohne unzulässige fremde Hilfe unter Beachtung der "Grundsätze zur Sicherung guter wissenschaftlicher Praxis“ an der Heinrich-Heine-Universität Düsseldorf" erstellt worden ist.

Des Weiteren versichere ich, dass diese Dissertation zuvor keiner anderen Universität oder Fakultät vorgelegt wurde und ich bislang keinerlei andere Promotionsversuche getätigt habe.

Düsseldorf, den 13. Juni 2017 Julia Seegel

Contents

Summary

Frontotemporal dementia (FTD) is a fatal brain disease responsible for 5-10% of all dementia cases. FTD patients suffer from neurodegeneration in the frontal and temporal cortex and progressive abnormalities in behavior, personality and language. Progranulin (GRN) plays an important role in the pathogenesis as patients with familial forms of FTD harbor inactivating mutations in the GRN gene causing reduced protein levels. GRN is a secreted glycoprotein with growth factor-like properties. It is comprised of 7.5 repeats of a conserved cysteine-rich granulin motif and can be cleaved by proteases into small granulin peptides. At the start of this thesis project not much was known about the pathological mechanisms through which reduced GRN expression might cause neuronal loss. The aims of this thesis were to develop a functional bioassay for GRN and to identify novel interaction partners of GRN in order to improve the understanding of its physiological and pathological functions.

As a precondition to establish a bioassay, a protocol for the expression of human GRN in HEK293T cells and for its purification by affinity chromatography was developed. The highly pure recombinant protein was then tested for protective activity against oxidative glutamate toxicity. In this assay, treatment of the murine hippocampal HT22 cell line with glutamate promotes the accumulation of intracellular reactive oxygen species resulting in cell death. Recombinant full-length GRN did not rescue HT22 cells from glutamate toxicity. Importantly, granulin peptides generated by *in vitro* proteolysis of recombinant GRN were strongly neuroprotective in this assay, fully preserving the viability of HT22 cells in the presence of glutamate concentrations that killed > 50% of control cells.

To identify novel binding partners of GRN, a yeast-2-hybrid (Y2H) screen was performed. First, to establish the Y2H method in the laboratory, the APP C-terminus was used as bait and screened against a human brain cDNA library. In this control screen, FE65L1, a known binding partner of APP was repeatedly isolated, indicating that the multi-step Y2H procedure was successfully implemented. The full-length human GRN protein was not suitable for screening because of auto-activation of the Y2H reporter genes. However, through extensive deletion analysis, the granulin F domain was identified as responsible and eliminated from the final bait construct. In the GRN Y2H screen a high background of non-specific interactions was observed. 10 proteins were classified as true positive hits with a cellular localization allowing interaction with GRN in the secretory pathway or the extracellular space. Three of these candidates displayed a receptor-like structure (TMEFF2, NRXN1, LRRN3).

In summary, in the scope of this thesis, the expression and purification of recombinant GRN was optimized in mammalian cells and used to establish a cell-based bioactivity assay for granulin peptides. This assay is potentially adaptable to genetic screening and could be

employed to isolate specific receptors for granulin peptides. In addition, confirmation of GRN binding partners within the Y2H candidate proteins could lead to a better understanding of GRN and provide a starting-point for the development of novel therapeutic interventions.

Zusammenfassung

Frontotemporale Demenz (FTD) ist eine letale und unheilbare Erkrankung des Gehirns und verantwortlich für 5-10% aller Fälle von Demenz. FTD-Patienten zeigen Neurodegeneration im frontalen und temporalen Cortex und leiden unter einem fortschreitenden Wandel von Verhalten, Persönlichkeit und Sprache. Progranulin (GRN) spielt eine wichtige Rolle bei der Entstehung der Krankheit. In Patienten mit familiärer FTD wurden inaktivierende Mutationen im GRN-Gen gefunden, die eine Absenkung des GRN-Levels verursachen. GRN ist ein sekretiertes Glykoprotein mit Eigenschaften eines Wachstumsfaktors. Es setzt sich aus 7,5 Wiederholungen eines hochkonservierten und cysteinreichen Granulinmotivs zusammen und kann von verschiedenen Proteasen in Granulinpeptide gespalten werden. Zu Beginn dieser Arbeit waren die pathogenen Mechanismen weitgehend unbekannt, die durch reduzierte Expression von GRN den Verlust von Neuronen verursachen. Ziel dieser Arbeit war es einen funktionalen Bioassay zu entwickeln und neue Interaktionspartner von GRN zu identifizieren, um das Verständnis der physiologischen und pathologischen Funktionen von GRN zu verbessern.

Als Voraussetzung für das Etablieren eines Bioassays wurde ein Protokoll zur Expression von humanem GRN in HEK293T Zellen und dessen Aufreinigung via Affinitätschromatographie entwickelt. Das daraus resultierende hochreine Protein wurde in einem Assay für oxidative Glutamattoxizität auf zytoprotektive Eigenschaften getestet. In diesem Assay wird die murine hippokampale HT22 Zelllinie mit Glutamat behandelt, was zu einer Akkumulation von reaktiven Sauerstoffspezies führt, die den Zelltod verursachen. Rekombinantes GRN konnte die HT22 Zellen nicht vor der Glutamattoxizität schützen. Im Gegensatz dazu zeigten die Granuline, generiert durch *in vitro* Proteolyse des rekombinanten GRNs, eine starke neuroprotektive Wirkung. Bei einer Behandlung mit Glutamatkonzentrationen, die >50% der Kontrollzellen töteten, wurde die Viabilität der Zellen vollständig erhalten, die zusätzlich mit Granulinen behandelt wurden.

Um neue Interaktionspartner von GRN zu identifizieren wurde ein Yeast-2-Hybrid (Y2H) Screen wurde durchgeführt. Zuerst wurde die Methode in unserem Labor etabliert, indem der C-Terminus von APP gegen eine humane cDNA Bibliothek gescreent wurde. In diesem Kontroll-Screen wurde ein bekannter APP-Interaktionspartner, Fe65L1, wiederholt isoliert, was die erfolgreiche Implementierung der Methode zeigte. Das humane volle Länge GRN war nicht einsetzbar für einen Screen, da es eine ausgeprägte Autoaktivierung der Y2H-Reportergene verursachte. Eine extensive Deletionsanalyse zeigte jedoch, dass die Granulindomaine F dafür verantwortlich war. Folglich wurde Granulin F aus dem finalen Bait-Protein eliminiert. In diesem Screen wurde ein hoher Hintergrund von unspezifischen

Interaktionen beobachtet. Insgesamt 10 Proteine wurden als echte positive Hits klassifiziert, deren zelluläre Lokalisation eine Interaktion mit GRN im sekretorischen Weg oder im extrazellulären Raum zulässt. Drei dieser Kandidaten zeigten eine Rezeptor-ähnliche Struktur (TMEFF2, NRXN1, LRRN3).

Im Verlauf dieser Arbeit wurde die Expression und Aufreinigung von rekombinantem GRN in Säugetierzellen optimiert und für die Etablierung eines zellbasierten Bioaktivitätsassays für Granuline verwendet. Dieser Assay kann potentiell für ein genetisches Screening angepasst werden und könnte außerdem dafür verwendet werden spezifische Rezeptoren von Granulinen zu isolieren. Überdies kann eine Bestätigung der identifizierten GRN-Interaktionspartner zu einem besseren Verständnis von GRN führen und einen Ausgangspunkt für die Entwicklung von neuen therapeutischen Interventionen liefern.

1. Introduction

1.1. Frontotemporal Dementia (FTD)

By 2025 the number of people 65 years and older in both the developed and developing world will have doubled from 2000 levels. By drastically increasing the number of people living with dementia, a rapidly aging society presents unique burdens to society, to patients, to caregivers and also causes extreme financial stress on governmental health funds. Unfortunately, despite billions of euros spent and decades of research on various approaches, no therapy, even palliative, exists to help people suffering from dementia.

The most common form of dementia in the presenile age group (<60 years) is caused by neurodegeneration in the frontal and temporal lobes of the cortex (Knopman and Roberts, 2011). This disease is called frontotemporal dementia (FTD). Correlating with the affected brain regions the clinical outcome of FTD displays symptoms like abnormalities in personality, behavior and language while, unlike Alzheimer's disease (AD), memory functions are spared (Cruts and Van Broeckhoven, 2008).

However, the molecular pathology as well as the clinical symptoms and progression are strikingly heterogeneous, making differentiation between subtypes very difficult and thus the classification and terminology of the disease has changed as a result multiple times over the last decade. In addition, the clinical spectrum of FTD encompasses distinct canonical syndromes: the behavioral variant of FTD (bvFTD), and semantic dementia (SD) and progressive non-fluent aphasia (PNFA) as the language variants. Motor neuron disease similar to amyotrophic lateral sclerosis (ALS) is also frequently observed, particularly in bvFTD. Two other variants of FTD show an overlap with parkinsonian syndrome, progressive supranuclear palsy (PSP), and corticobasal syndrome (CBS) (Karageorgiou and Miller, 2014).

A positive family history has been found in approximately 40% of all cases. Similarly to the clinical development, the genetics of FTD also show a great heterogeneity, with mutations in the MAPT (Tau), GRN (Progranulin), VCP (valosin containing protein), CHMP2B (charged multivesicular body protein 2B), and C9orf72 (expanded hexanucleotide repeat in a noncoding region of chromosome 9 open reading frame 72) causing this disease (Baker et al., 2006; Cruts et al., 2006; DeJesus-Hernandez et al., 2011; Rademakers et al., 2004; Renton et al., 2011; Skibinski et al., 2005; Watts et al., 2004). Mutations that cause this disease are mostly passed on in an autosomal dominant pattern and in 50% of the familial

cases mutations in the MAPT or GRN gene have been identified (Chow et al., 1999; Goldman et al., 2005; Seelaar et al., 2008). To date, more than 70 GRN mutations have been found to cause FTD, spanning the entire gene (*www.molgen.vib-ua.be/FTDmutations*) (Cruts et al., 2012). The vast majority of these mutations introduce a premature termination codon in one allele. This leads to nonsense-mediated mRNA degradation resulting in a nonfunctional GRN allele. Consequently, this genetic variant of FTD is a disease of GRN haploinsufficiency (Rademakers and Rovelet-Lecrux, 2009). Interestingly, GRN levels in serum are decreased in mutation carriers by 70-80% compared to healthy controls, rather than the expected 50% (Finch et al., 2009). Recent studies suggest an influence of epigenetic mechanisms in mutation carriers as well as in a subset of familial FTD cases (Almeida et al., 2012; Banzhaf-Strathmann et al., 2013; Galimberti et al., 2013). The aberrant GRN levels can be detected in plasma, serum and cerebrospinal fluid (CSF) by ELISA and can reliably be used for diagnostics (Carecchio et al., 2009; Coppola et al., 2008; Finch et al., 2009; Ghidoni, 2008; Sleegers et al., 2009).

Table 1.1: Genetic and clinical classification of the molecular subtypes of FTD (adapted from (Rademakers et al., 2012) Abbreviations: ALS, amyotrophic lateral sclerosis; bvFTD, behavioral variant FTD; C9orf72, chromosome 9 open reading frame 72; CHMP2B, charged multivesicular body protein2B; FTLD, frontotemporal lobar degeneration; FUS, fused in sarcoma; MAPT, microtubule-associated protein tau; MND, motor neuron disease; PLS, primary lateral sclerosis; PNFA, progressive nonfluent aphasia; SD, semantic dementia; TARDBP and TDP, TAR DNA-binding protein; UPS, ubiquitin proteasome system; VCP, valosin-containing protein. The brackets indicate very rarely mutated genes (FUS, TARDBP) or unusual phenotypes.

Molecular classification	Associated genes	Associated clinical phenotypes				
		bvFTD	PNFA	SD	Parkinsonism	MND
FTLD-tau	MAPT	+	(+)	(+)	+	ALS, PLS
FTLD-TDP	GRN	+	+	(+)	+	ALS
	C9orf72	+	+	+	+	ALS
	VCP	+			(+)	
	(TARDBP)	+	(+)		+	ALS
FTLD-FUS	(FUS)	+				ALS/PLS
FTLD-UPS	CHMP2B	+			(+)	(ALS)

The neuropathological hallmarks of patients with GRN deficiency include inflammation, dystrophic neurites, ubiquitin-positive inclusions in microglia and neurons, and severe neurodegeneration in the frontal and temporal lobes. Other affected regions are striatum, thalamus, substantia nigra and hippocampus (Cruts and Van Broeckhoven, 2008; Eriksen and Mackenzie, 2008). The observed intracellular inclusions were identified as

hyperphosphorylated, ubiquitinylated and cleaved Tar DNA-binding protein 43 (TDP-43) (Mackenzie et al., 2006; Rademakers and Rovelet-Lecrux, 2009). TDP-43 is known as transcriptional repressor and inhibitor of exon splicing and was found to bind GRN mRNA (Sephton et al., 2012).

Behavioral changes are the most frequent clinical symptoms in FTD (70-80% of all patients) and include apathy, social withdrawal, disinhibition, poor judgment, and compulsive behaviors. Around twenty-five percent of patients present with early isolated language dysfunction and with relatively early single word comprehension impairment. Hallucinations and delusions are frequently reported. Episodic memory deficits occur in 10-30% and may lead to the clinical diagnosis of amnestic variant of mild cognitive impairment (MCI) or, together with parietal deficits (dyscalculia, visuospatial dysfunction, and limb apraxia), to AD (Benussi et al., 2008; Boeve et al., 2006; Josephs et al., 2007; Karageorgiou and Miller, 2014; Kelley et al., 2009; Le Ber et al., 2008; Mesulam et al., 2007; Rademakers et al., 2007).

1.2. Progranulin (GRN)

Progranulin (GRN) is a widely expressed precursor protein, which is cysteine-rich, secreted and highly glycosylated. Previously used synonymous names are proepithelin (Plowman et al., 1992), granulin-epthelin precursor (Bhandari, 1996), acrogranin (Baba et al., 1993), epithelial transforming growth factor (Parnell, 1992), and platelet cell derived growth factor (PCDGF) (Zhou et al., 1993). The 12 coding exons of the GRN gene are located on chromosome 17q21.32 and the protein is expressed predominantly in tissues with high turnover rate, like skin, gastrointestinal tract, adipocytes, cells of the immune system, and the reproductive tracts. In the adult central nervous system (CNS) the expression of GRN is restricted to microglia, which represent the immune system of the brain, and to neurons and motorneurons (Ahmed, 2007), after more widespread expression during early neural development (Daniel et al., 2003). Although GRN is expressed in various neuronal populations in the different brain regions (Chen-Plotkin et al., 2008; Ryan et al., 2009) like neocortex, hippocampus, hypothalamus and cerebellum, the neurons most sensitive to a lack of GRN are the neurons of the frontal and temporal cortex as they are affected primarily in FTD (Daniel et al., 2000; Matsuwaki et al., 2011; Moisse et al., 2009; Petkau et al., 2010; Ryan et al., 2009; Toh et al., 2011).

Human GRN is 593 amino acids long and it exists as a single copy in the genome located on chromosome 17q21.32. The protein is comprised of a secretory signal sequence and seven and a half repeats of a highly conserved 12-cysteine granulin motif separated by linker regions (Bhandari and Bateman, 1992). The protein-coding region of the GRN gene spans

3.7kB and consists of 12 exons. Each exon harbors the N-terminus and the C-terminus of one granulin motif, but in a way that each granulin domain is constructed from two exons. Following glycosylation GRN is secreted as a 90kDa protein. Several intracellular and extracellular enzymes have been shown to cleave the full-length protein releasing individual granulin peptides, including neutrophil elastase, proteinase 3, matrix metallopeptidase 12 and ADAMTS-7 (Gass et al., 2012b).

Cleavage can be inhibited by the secretory leukocyte protease inhibitor (SLPI), which binds to GRN (Zhu et al., 2002). No tertiary structure is established for the full-length protein, but some of the granulins (A, C and F) have been crystallized and the resulting diffraction pattern revealed four beta-hairpins stacked in a left-handed helix formation forming a globular structure through six disulfide bridges in the center (Hrabal et al., 1996; Tolkatchev et al., 2008).

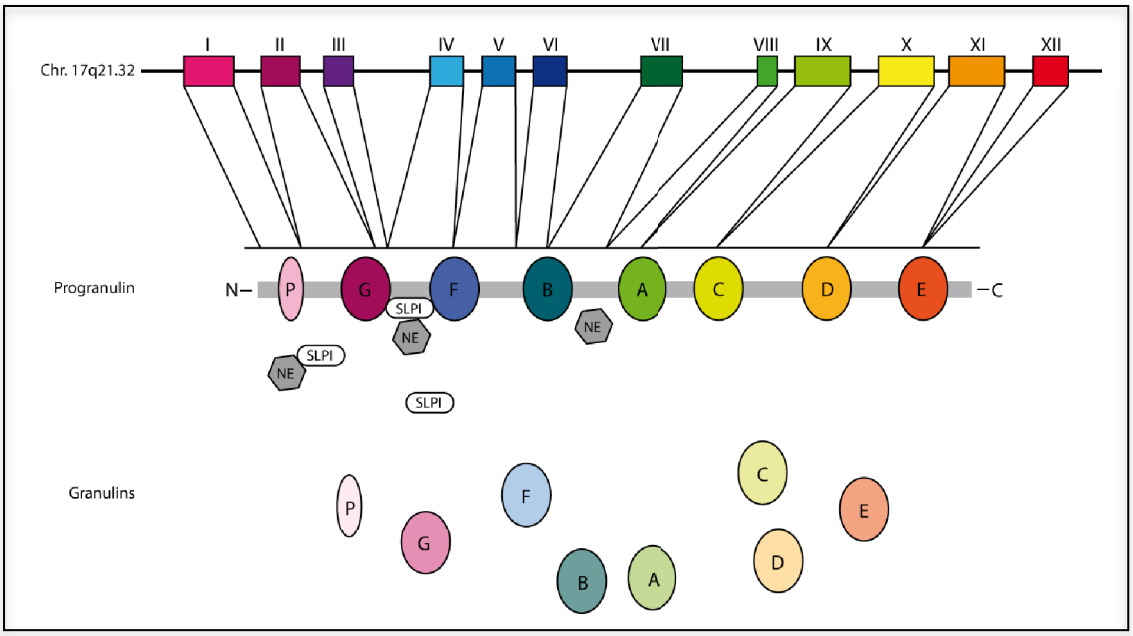

Figure 1.1: Structure of the progranulin gene and protein. A single copy of the GRN gene is located on Chr. 17q21.32 and shows a unique genetic organization. The full-length protein is encoded by 12 exons, with each exon carrying two hemigranulin subdomains. The first granulin motif is called paragranulin and represents the N-terminal half of the granulin domain (exon 1). The following seven domains were named in the order of their discovery and are each constructed from two sequential exons, one donating the N-terminus and the following donating the C-terminus of the granulin domain. The Progranulin protein can be cleaved in the short linker regions between the granulin domains by extracellular proteases, e.g. neutrophil elastase (NE). Cleavage can be prevented through the binding of the secretory leukocyte protease inhibitor (SLPI). The released granulin peptides (~6kDa) and the precursor have been shown to fulfill sometimes opposing physiological functions.

1.3. Functions of Progranulin

While various functions have been reported for GRN, not much is known about the mechanism(s) that lead to the specific neurodegeneration occurring in FTD. However, GRN is expressed in many cell types and diverse biological functions have been proposed. In the periphery the most obvious observation is the strong GRN expression in tissues with high proliferation rates, like epithelial cells or immunological tissues (spleen, lymph nodes) (Daniel et al., 2003; Daniel et al., 2000). Also the influence of GRN on growth capacities of certain cell types has been shown (He and Bateman, 1999; Monami et al., 2009). GRN is upregulated in skin cells after injury especially in wound fibroblasts and endothelial cells that show no GRN expression under normal conditions. Experiments administrating GRN *in vitro* showed the protein was able to stimulate proliferation and migration of fibroblasts and endothelial cells (Daniel et al., 2003; He et al., 2003).

GRN even counts as a tumor progression factor, as GRN expression is upregulated in numerous cancers supporting proliferation, angiogenesis, motility, invasion, and apoptosis inhibition (Cheung et al., 2004; He et al., 2002; He et al., 2003; Kong et al., 2007). GRN has been linked to cancers including carcinomas of the breast (Egland et al., 2003; Elkabets et al., 2011; Tangkeangsirisin and Serrero, 2004), ovary (Cuevas-Antonio et al., 2010; Jones et al., 2003; Liu et al., 2007), liver (Cheung et al., 2004; Ho et al., 2008), kidney (Donald et al., 2001), prostate (Monami et al., 2009), and bladder (Monami et al., 2006). GRN alone is not sufficient to fully transform healthy cells, but cells in a pre-cancerous state can be turned into a highly malignant cancer (He and Bateman, 1999; Lu and Serrero, 2001; Matsumura et al., 2006; Miyanishi et al., 2007). Additionally, GRN inhibits cell death induced by chemotherapeutics (Cheung et al., 2011; Monami et al., 2006; Pizarro et al., 2007). Further evidence showing GRN's role in supporting proliferation is derived from the observation that reduced levels of GRN protein in the periphery lead to impaired cell growth capacities in wound repair, reduced cartilage mass, increased susceptibility to collagen-induced arthritis, and contact dermatitis (Bateman and Bennett, 2009; Feng et al., 2010; Tang et al., 2011; Zhao et al., 2013).

The anti-inflammatory influence of GRN is evident in $GRN^{-/-}$ knockout mice showing exaggerated peripheral inflammatory responses with decreased secretion of anti-inflammatory interleukin-10 and increased secretion of the pro-inflammatory cytokines interleukin-6 and TNF-alpha by GRN-deficient macrophages (Yin et al., 2010a). GRN deficiency also caused a significantly worse course of experimentally induced inflammatory arthritis, while treatment with GRN rescued the phenotype (Tang et al., 2011). The influence of SLPI on inflammatory responses indicates opposing effects of full-length GRN and the granulins. $SLPI^{-/-}$ mice show symptoms of excessive inflammation (Ashcroft et al., 2000), which can be rescued by treatment with GRN (Zhu et al., 2002).

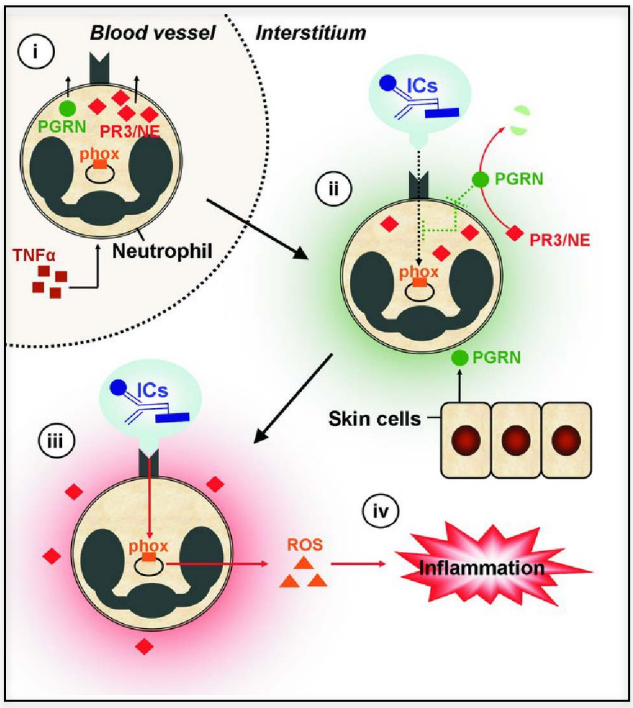

Figure 1.2: Proposed function of GRN in the innate immune response in the periphery (figure adapted from (Kessenbrock et al., 2008). TNF-α–primed neutrophils extravagate from blood vessels, translocate PR3/NE to the cellular surface, and discharge GRN to the pericellular environment (i). During transmigration of interstitial tissues (ii), neutrophil activation is inhibited by GRN (green shading) until IC depots are reached. Adherence of neutrophils to ICs (iii) further increases pericellular PR3 and NE activity. These proteases degrade GRN to facilitate optimal neutrophil activation (red shading), resulting in sustained integrin signaling (red arrow) and robust production of ROS by the phox system. Subsequently, neutrophils release ROS together with other pro-inflammatory mediators and chemotactic agents, thereby enhancing the recruitment of further neutrophils and establishing inflammation (iv). Abbreviations: PGRN, GRN; PR3, proteinase 3; NE, neutrophil elastase; ROS, reactive oxygen species, IC, immune complex; phox, phagocyte oxidase also called NADPH oxidase.

On the other hand, mice with a dual knockout of neutrophil elastase and proteinase 3 show a phenotype of decreased inflammatory responses due to prolonged lifetime of the full-length GRN protein (Kessenbrock et al., 2008). Taken together, an increase of inflammatory responses in GRN deficient mice shows the anti-inflammatory function of the full-length protein, in contrast to the pro-inflammatory effect of the granulins. However, without a pro-inflammatory stimulus, the phenotype in the peripheral immune system of $GRN^{-/-}$ knockout mice is mild (Yin et al., 2010a).

In the CNS, GRN is strongly expressed by microglia suggesting a role in neuroinflammation as these cells function as the brain's immune system (Czirr and Wyss-Coray, 2012; Ryan et al., 2009). Microglia become activated by ATP release, neurotransmitters, growth factors or cytokines, as well as ion changes in the local environment or loss of inhibitory molecules displayed by healthy neurons (Hanisch and Kettenmann, 2007). Activation also occurs upon contact to molecules not present in the healthy CNS, like intracellular components (e.g. RNA, DNA from necrotic cells), immunglobulin-antigen complexes, phosphatidylserine (apoptotic cells), abnormally folded proteins (e.g. protein aggregates), and more (Hanisch and Kettenmann, 2007). Following activation by specific stimuli, microglia cells respond in an appropriate and defined manner, ranging from the release of anti-inflammatory cytokines to the clearance of apoptotic or damaged cells. Even throughout normal aging of the brain an increased activation of microglia and infiltration of immune cells into the CNS is observed,

and neurodegenerative diseases (e.g. FTD, AD) exhibit extensive activation of microglia. Comparable to the up regulation of GRN expression in skin cells after injury with a role in the process of wound healing, an upregulation of GRN expression in microglia can be observed after physical trauma like axotomy or spinal cord contusion (Moisse et al., 2009; Naphade et al., 2010). Supporting the role of GRN as a suppressor of neuroinflammation, $GRN^{-/-}$ mice not only show abnormal inflammatory responses in the periphery, but also a significantly increased activation of microglia with increased expression of inflammatory cytokines in the CNS upon inflammatory stimulation (Yin et al., 2010a). Most recently, $GRN^{-/-}$ mice were shown to exhibit increased microgliosis and activation of the complement system in the brain, which caused enhanced pruning of inhibitory synapses and obsessive-compulsive behavioral phenotypes (Lui et al., 2016).

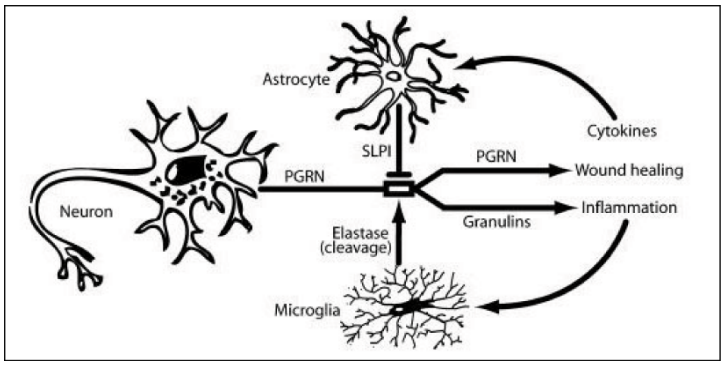

Figure 1.3: Proposed function of GRN expression in the CNS (figure adapted from (Eriksen and Mackenzie, 2008)). GRN expression in the adult CNS is restricted to neurons and microglia cells, and might play a role in wound healing and inflammation, similar to mechanisms in the periphery. In neurons, GRN might function as an autocrine, neuroprotective factor. In microglia cells, GRN appears to dampen inflammatory reactions including cytokine expression and complement activation. Under some circumstances, GRN and the granulins might have opposing functions. Certain cytokines can activate astrocytes. The astrocytes then secrete the protein SLPI, preventing the cleavage of GRN into pro-inflammatory granulins, and supporting wound healing pathways. In contrast, activated microglia secrete proteases that cleave the GRN into granulins and enhance the inflammatory response. Abbreviations: PGRN, Progranulin; SLPI, secretory leukocyte protease inhibitor.

Neurons are the second cell type expressing GRN in the brain. Several studies have observed a protective effect of GRN on neurons (Petkau and Leavitt, 2014). *In vitro*, GRN was found to support neuronal survival (Gao et al., 2010; Kleinberger et al., 2010; Ryan et al., 2009; Van Damme et al., 2008), even abolishing the requirement of trophic support from serum (Ryan et al., 2009). Furthermore, GRN can promote neurite outgrowth in stressed or GRN depleted neuronal cells (Gao et al., 2010; Ryan et al., 2009; Tapia et al., 2011; Van Damme et al., 2008), it can protect from excitotoxicity, and it also plays a role in synaptic transmission (Tapia et al., 2011). This suggests a function for GRN as an autocrine neuronal growth factor, also supported by an early study showing that low concentrations of GRN can

promote proliferation of PC12 cells (rat phenochromocytome-derived neuronal cell line) (Zhou et al., 1993).

Several groups found that the silencing of GRN expression in neuronal cell cultures or cell lines caused a sensitization to stimuli promoting caspase 3 activity. This mechanism led to the redistribution of TDP43 from the nucleus to the cytoplasm where the protein was cleaved into C-terminal fragments that are also seen in the brains of FTD patients with GRN mutations and sporadic FTD (Guo et al., 2010; Kleinberger et al., 2010; Zhang et al., 2007). However, these findings have remained controversial (Dormann et al., 2009). In $GRN^{-/-}$ knockout mice *in vivo*, insoluble TDP-43 aggregates and substantial neuronal loss as in FTD patients have not been observed. Nevertheless, GRN deficient mice showed signs of accelerated aging of the brain with premature microgliosis, neuronal lipofuscinosis and accumulation of ubiquitinated proteins (Ahmed et al., 2010). In hippocampal slices of $GRN^{-/-}$ mice neurons are more prone to undergo apoptosis under oxygen or glucose deprivation than in wild type brain slices (Yin et al., 2010a). Interestingly, GRN expression levels have been described to decrease or increase with age in different brain regions of wild type mice (Ahmed et al., 2010; Matsuwaki et al., 2011). In addition, an up regulation of GRN expression in microglia is evident in neurodegenerative diseases like FTD and AD (Pereson et al., 2009), although the causes and consequences of this up regulation are not clear.

1.4. Behavioral Phenotypes in Mouse Models of GRN Deficiency and Alternative FTD Animal Models

FTD caused by a mutation in the GRN gene is a disease of haploinsufficiency; consequently, GRN hemizygous or homozygous knockout mice are suitable disease models. Several $GRN^{-/-}$ knockout mouse lines have been established and tested for behavioral deficits. Changes in anxiety, activity levels, motor coordination, depressive and compulsive behaviors have been observed, and some lines also demonstrated memory problems at older age, partially resembling phenotypes in FTD patients (Ghoshal et al., 2012; Kayasuga et al., 2007; Lui et al., 2016; Petkau and Leavitt, 2014; Yin et al., 2010b). However, generally, behavioral phenotypes in $GRN^{-/-}$ knockout mouse lines have been inconsistent and appear to be mild, and are mostly completely absent in $GRN^{+/-}$ hemizygous mice (Petkau and Leavitt, 2014).

Further animal models that have been employed for FTD research include the nematode *Caenorhabditis elegans*, the fruit fly *Drosophila melanogaster* and the zebra fish *Danio rerio*. MAPT, GRN, VCP, and TDP-43 all have homologs in *C. elegans* proving this a suitable model organism to investigate FTD; especially as *C. elegans* development is characterized by an invariant pattern of cell division and cell death (Sulston et al., 1983). E.g. Studies on

C. elegans demonstrated that ectopic expression of TDP-43 can recapitulate many features of human FTD, including aggregate formation, synaptic and neuronal loss, motor defects, post-translational modification, nuclear localization of TDP-43 and age-associated decline (Ash et al., 2010; Liachko et al., 2010). In addition, it was discovered that GRN expression is initiated at the same time point like the first programmed cell deaths. The analysis of $GRN^{-/-}$ knockout worms revealed that the phagocytosis of apoptotic cells by macrophages was accelerated, giving damaged cells no time to recover (Kao et al., 2011). This might enhance disease progression under conditions where neurons are stressed.

1.5. Other Diseases of the Brain Linked to GRN

In terms of CNS pathology, GRN is not exclusively linked to FTD. Another important link is the connection between GRN and cancer. Growth promoting activities of GRN on cultured cell lines, promotion of anchorage-independent growth, and a correlation between secreted GRN and tumorigenicity of a teratoma cell line were already shown in early studies (Zhang and Serrero, 1998; Zhou et al., 1993). Cell lines with low tumor-forming capacity, like the SW13 cell line, have been found to form large tumors in mice when GRN overexpression was enforced (Figure 1.5.1) (He and Bateman, 1999). GRN expression is upregulated in numerous cancers including intracranial meningiomas and gliomas, supporting proliferation, angiogenesis, motility, invasion, chemo resistance, and apoptosis inhibition (Cheung et al., 2004; De Muynck and Van Damme, 2011; He et al., 2002; He et al., 2003; Kong et al., 2007; Toh et al., 2011). 3-30 folds higher expression levels of GRN in gliomas were detected with cDNA microarrays compared to normal brain tissue. A comparison of 21 samples via Northern blotting confirmed GRN expression in 18 of 21 gliomas, but was unable to detect GRN expression in 3 normal brain samples (Liau et al., 2000; Markert et al., 2001). An analysis of 210 astrocytic gliomas by immunohistochemistry found a positive correlation between GRN expression and the pathological grading of the tumors, as well as a negative correlation with survival times of glioblastoma patients (Wang et al., 2012). These and other findings indicate that GRN is not only able to increase the general growth capacities of cells, but is also an important regulator of tumorigenesis, significantly worsening progression and malignancy of cancers. Thus, the influence of GRN on brain tumors could be of critical importance when evaluating potential GRN-elevating therapeutics for the treatment of GRN deficiency in FTD. GRN therapeutics, especially in the brain, should not cause elevation of GRN protein expression above normal levels.

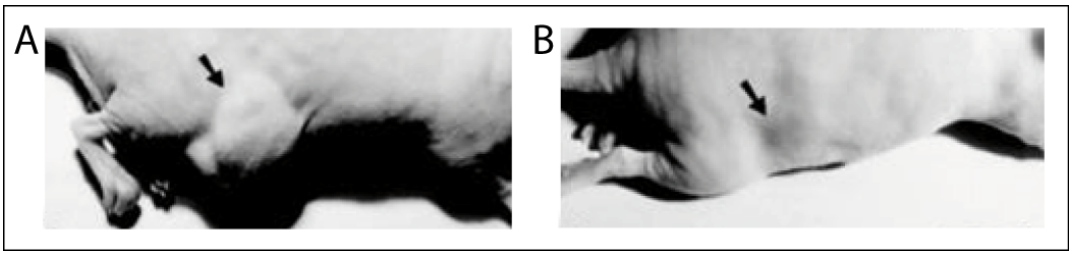

Figure 1.4: Influence of GRN expression on tumor growth (figure adapted from (He et al., 2003)). SW13 cells overexpressing GRN or carrying a control vector were injected subcutaneously into nude mice. A) After 8 weeks mice injected with GRN expressing cells showed large tumors. B) Mice injected with control cells have significantly smaller tumors. Arrows indicate the injection sites.

GRN might also play a role in AD and in mouse models of this most common neurodegenerative disease. Studies have noted that 9-17% of GRN mutation carriers present with an AD phenotype (Le Ber et al., 2008; Rademakers et al., 2007) and in > 30% of AD patients an abnormal TDP-43 staining is seen (Josephs et al., 2014). In addition, GRN was found to be one of the top ten up regulated genes in two mouse models of AD and the GRN levels positively correlated with amyloid plaque load, which is likely due to the up regulation of GRN expression in activated microglia cells (Pereson et al., 2009). In this study, the tight correlation between GRN levels and disease severity (amyloid plaque burden) suggested the utilization of GRN levels in the brain as an AD biomarker.

Importantly, a recent publication investigated the influence of microglial GRN expression on amyloid plaque formation in the 5xFAD mouse model of AD (Minami et al., 2014). Amyloid plaques are a neuropathological hallmark of AD and consist of aggregated amyloid-ß (Aß) peptides. In this very aggressive AD model severe plaque pathology and gliosis start to develop at an age of 2 months (Oakley et al., 2006). Similar to human AD patients, the animals develop amyloid plaques surrounded by activated GRN expressing microglia (microgliosis). The authors found that a reduction of microglial GRN expression resulted in an increased amyloid plaque burden due to decreased phagocytic uptake of Aß peptides, whereas an increase of GRN expression after injection of lentiviruses expressing GRN led to a reduced plaque burden in the 5xFAD mice. Furthermore, it was shown that viral GRN overexpression in cultured primary neurons of these mice protected the cells from Aß toxicity. This study strongly supports an important role for GRN in the development of AD pathology, with a deficiency of GRN protein reducing the phagocytic uptake and degradation of Aß peptides rendering the brain vulnerable to Aß toxicity (Minami et al., 2014).

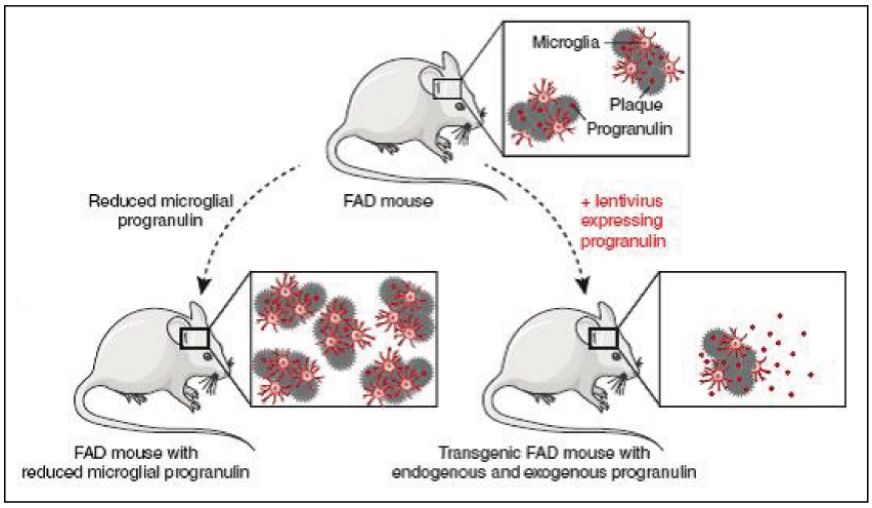

Figure 1.5: The role of GRN in amyloid plaque formation in AD (figure adapted from (Minami et al., 2014)). Transgenic mice develop an AD phenotype at 6-7 months of age with amyloid plaques surrounded by microglia cells expressing GRN similar to human AD patients. When GRN expression is reduced, mice showed impaired microglial phagocytosis and an increased plaque burden. On the contrary, lentivirus-mediated GRN expression in the brains of these AD mice reduced the plaque burden.

Patients carrying a GRN mutation also frequently develop mild Parkinsonism and even though the symptoms usually appear late in in the disease course of FTD, a subset of patients presents with Parkinsonism as predominant clinical manifestation (Benussi et al., 2009; Kelley et al., 2009; Puschmann, 2013). However, it is not clear whether Parkinsonism develops due to reduced GRN expression or whether it is a comorbidity that develops independently in these patients. One possibility is that the pro-inflammatory state of GRN deficient patients might be predisposing for neurodegenerative diseases in general, but this hypothesis needs further study.

Finally, very rare homozygous loss-of-function mutations in GRN have been shown to cause adult-onset neuronal ceroid lipofuscinosis (NCL) in humans (Smith et al., 2012). NCL is a lysosomal storage disease, in which abnormal lipopigments accumulate in lysosomes leading to neurodegeneration. This association of GRN deficiency with NCL and other findings from *in vitro* and animal studies strongly indicate that GRN might also be important for the proper function of and that lysosomal dysfunction might play a role in the pathogenesis of FTD (Gotzl et al., 2014; Holler et al., 2016; Tanaka et al., 2017).

1.6. GRN and Oxidative Stress

Kessenbrock et al. have described GRN as anti-inflammatory because it hampers neutrophils from initiating an oxidative burst. Phagocytes (e.g. neutrophils) represent the body's first line of antibacterial defense and they utilize the lethal effects of reactive oxygen

species and reactive nitrogen species to kill pathogens in a non-specific fashion (Kessenbrock et al., 2008; Nathan and Shiloh, 2000). The release of oxidizing species such as superoxide anions, hydrogen peroxide and hydroxyl radicals causes oxidative stress for any cell in close proximity and culminates in cellular damage and apoptosis (Brieger et al., 2012; Valko et al., 2005). Oxidative stress describes the situation of an imbalance between reactive oxygen species (ROS) and the availability of antioxidant defenses. This is a condition that can develop from normal cellular metabolism when defense mechanisms in the cell are overwhelmed or e.g. during inflammation, infection or exposure to radiation (Huang et al., 2012). However, at low and regulated concentrations ROS direct cell signaling cascades and take part in cell growth and apoptosis (D'Autreaux and Toledano, 2007). In neutrophils, reactive oxygen species are produced by the membrane-bound NADPH oxidase complex and the study by Kessenbrock et al. indicates that GRN somehow affects the activity of this enzyme although the molecular mechanism is unclear.

Importantly, oxidative stress might play a key role in the development of various neurodegenerative diseases like FTD (Gerst et al., 1999; Martin et al., 2001), but also including AD, Parkinson's disease, and amyotrophic lateral sclerosis (Andersen, 2004; Shukla et al., 2011). The most direct evidence that GRN can protect from oxidative stress is derived from a study using rat cortical neurons, which found that treatment with recombinant GRN protein rescues from cell death induced by oxidative stress (Xu et al., 2011). In this study, 35nM of recombinant GRN was able to protect neurons from MPP+ (1-methyl-4-phenylpyridinium) toxicity, H_2O_2 treatment as well as from glutamate excitotoxicity, all of which cause oxidative stress. In these experiments, neuroprotection was dependent on the activation of the phosphatidylinositol 3-kinase (PI3K/Akt) and the mitogen-activated protein kinases / extracellular-signal regulated kinases (MAPK/ERK) signaling pathways. These cell survival pathways are known to be activated by GRN (see below) and other growth factors (Cuevas-Antonio et al., 2010; He et al., 2002; He et al., 2003; Ho et al., 2008; Lu and Serrero, 2001; Monami et al., 2009; Monami et al., 2006; Youn et al., 2009; Zanocco-Marani et al., 1999). After an ischemic event leading to a shortage of oxygen in a tissue (hypoxia), reperfusion of the tissue can cause oxidative stress and further tissue damage. GRN expression is upregulated in rat fibroblasts and neuroblastoma cells as a response to hypoxia (Guerra et al., 2007; Piscopo et al., 2010). Furthermore, in rodent models of ischemic stroke, GRN has been demonstrated to be neuroprotective (Kanazawa et al., 2015).

Another very interesting study was conducted with induced pluripotent stem cells (iPSC) from a FTD patient carrying a heterozygous nonsense GRN mutation (S116X), being compared to cells from a healthy age matched control and an age matched sporadic FTD patient lacking mutations in GRN, MAPT, and C9orf72 to detect cellular phenotypes that are specific for

GRN deficiency (Almeida et al., 2012). Testing various cell stressors they discovered that the S116X cells are specifically sensitive to PI3K and MEK inhibition, suggesting that GRN deficiency leads to an impairment of the PI3K/Akt and MEK/MAPK signaling pathways. This phenotype could be rescued by GRN expression and a gene expression analysis revealed a down regulation of the S6K2 in the S116X cells, a serine/threonin kinase playing an important role in PI3K/Akt and MEK/MAPK signaling (Fenton and Gout, 2011). An involvement of GRN in the activation of the PI3K/Akt/S6K pathway was previously shown in cancer cells (Zanocco-Marani et al., 1999). These results argue, in contrast to the studies described above, for a GRN-independent increased sensitivity towards mitochondrial or oxidative stressors in later stages of FTD progression, as iPSCs from mutation carrier and sporadic FTD patient were equally sensitive.

1.7. GRN Receptors and Signaling Pathways

Because of the growth factor like structure and the biological functions of GRN it was assumed that the protein could act through a classical growth factor receptor. The mechanism of action of GRN in the CNS could be distinctive for neurons and for microglia cells, but it appears to involve typical growth factor signal transduction pathways. Both the GRN protein and the granulin peptides interact specifically with cell surface membrane proteins (Culouscou et al., 1993; Xia and Serrero, 1998). Competitive binding experiments have shown that only GRN itself but not a range of known growth factors and cytokines are able to hinder GRN from binding to its receptor (Culouscou et al., 1993). This supports the hypothesis of a unique GRN receptor. Cross-linking experiments with GRN identified binding sites on different GRN-responsive cell lines with a molecular weight of approximately 120-145 kDa (Culouscou et al., 1993; Xia and Serrero, 1998). Only a few proteins resembling receptors have been reported to bind GRN so far, and it has not been resolved whether these include a functional GRN receptor that explains the known biological and signaling functions of GRN in the brain. It is also unclear whether the full-length GRN and the granulin peptides interact with the same or different receptors.

The last three amino acids at the C-terminus of GRN were found to bind to sortilin (SORT1) (Hu et al., 2010; Zheng et al., 2011), which is a type-I receptor that regulates intracellular protein trafficking in the Golgi. This multi-ligand receptor is presented on the cell surface and internalizes upon binding of ligands, directing the binding partner to the lysosome (Canuel 2009). Sortilin is expressed in the endoplasmic reticulum (ER) and Golgi of microglia cells and was also detected in lysosomes of astrocytes. Sort1$^{-/-}$ deficient mice (Sort1$^{-/-}$) show fivefold more circulating GRN (Hu et al., 2010) and serum GRN levels of humans were shown to correlate with sortilin expression (Carrasquillo et al., 2010). This suggests a role of

sortilin in the intracellular transport and degradation of GRN, thereby regulating the levels of circulating GRN. However, even in the absence or after blocking of sortilin, GRN was found to promote neurite outgrowth (Gass et al., 2012b) and to enhance the survival of motor and cortical neurons (De Muynck et al., 2013) indicating that other receptors mediate these biological effects of GRN. Furthermore, GRN was shown to bind to Sort1$^{-/-}$ knock out neurons (Hu et al., 2010; Nykjaer and Willnow, 2012), suggesting the existence of additional neuronal receptors and limiting the function of sortilin to sorting and recycling of GRN.

Two recent publications showed the prosaposin protein (PSAP) as a binding partner of GRN (Nicholson et al., 2016; Zhou et al., 2015). The PSAP trafficking pathway complements the sortilin trafficking of GRN to the lysosome (Zhou et al., 2015). Both proteins are expressed strongly in cortical neurons and transport GRN from the cell surface to the lysosome. Absence of PSAP leads to defects in GRN trafficking and increases extracellular GRN protein levels (Nicholson et al., 2016; Zhou et al., 2015). PSAP is a secreted protein and the precursor of the saposin peptides that serve as activators of lysosomal sphingolipid metabolizing enzymes (Matsuda et al., 2007; O'Brien and Kishimoto, 1991; Qi and Grabowski, 2001; Zhou et al., 2015). Although these findings may provide a connection between GRN and lysosomal storage disorders such as NCL, the interaction between GRN and PSAP appears to mainly affect the lysosomal localization and degradation of GRN and no connection to the signaling functions of GRN has been reported up to now (Nicholson et al., 2016; Zhou et al., 2015).

Another possible GRN receptor, the tumor necrosis factor receptor (TNFR), was found in a yeast two-hybrid screen for GRN binding partners. TNFR is expressed predominantly by lymphocytes and binds the cytokine TNF-alpha, a major driver of rheumatoid arthritis and related inflammatory diseases. GRN was proposed to be antagonistic to the pro-inflammatory TNF-alpha by blocking its receptor (Tang et al., 2011). Although the interaction between GRN and TNFR could be highly relevant concerning the role of GRN in neuroinflammation, it is important to note that this interaction is discussed controversially. Another study was not able to reproduce the interaction between GRN and TNFR and the antagonistic effect of GRN on TNFR signaling (Chen et al., 2013). In response, Jian et al. showed that the binding between TNFR and GRN is abolished by treatment with DTT, in contrast to an increased binding between sortilin and GRN after this treatment (Jian et al., 2013). DTT affects the formation of disulfide bonds and thereby disturbs the proper folding and structure of the GRN protein. According to Jian et al., the proper conformation of GRN is essential for its binding to TNFR. The opposite effect of the DTT treatment on the GRN sortilin interaction might argue for a role of sortilin in removing circulating, maybe misfolded GRN proteins, channeling them into the lysosomal degradation pathway. Nevertheless, at present the biological relevance of the GRN-TNFR interaction and the possible role of TNFR

as a functional GRN receptor in the brain remain unresolved (Chen et al., 2013; Tang et al., 2011).

Finally, very recently, ephrin type-A receptor 2 (EphA2) has been proposed as a functional GRN receptor (Neill et al., 2016). EphA2 belongs to a family of receptor tyrosine kinases most well known for their role in cell motility and adhesion during development (Day et al., 2014). Binding of GRN to EphA2 stimulated its tyrosine kinase activity and downstream activation of the PI3K/Akt and MAPK/ERK signaling pathways. In addition, it was shown that GRN promoted the formation of capillaries from endothelial HUVEC cells and that this effect was dependent on EphA2 (Neill et al., 2016). Since EphA receptors are highly expressed in the CNS and binding of GRN to EphA2 stimulated signaling pathways known to be activated by GRN (see below), EphA2 would appear as a promising candidate for a functional GRN receptor. However, the relevance of EphA2 or other Eph receptors for GRN functions in the brain or in primary neurons or microglia cells has not been demonstrated yet.

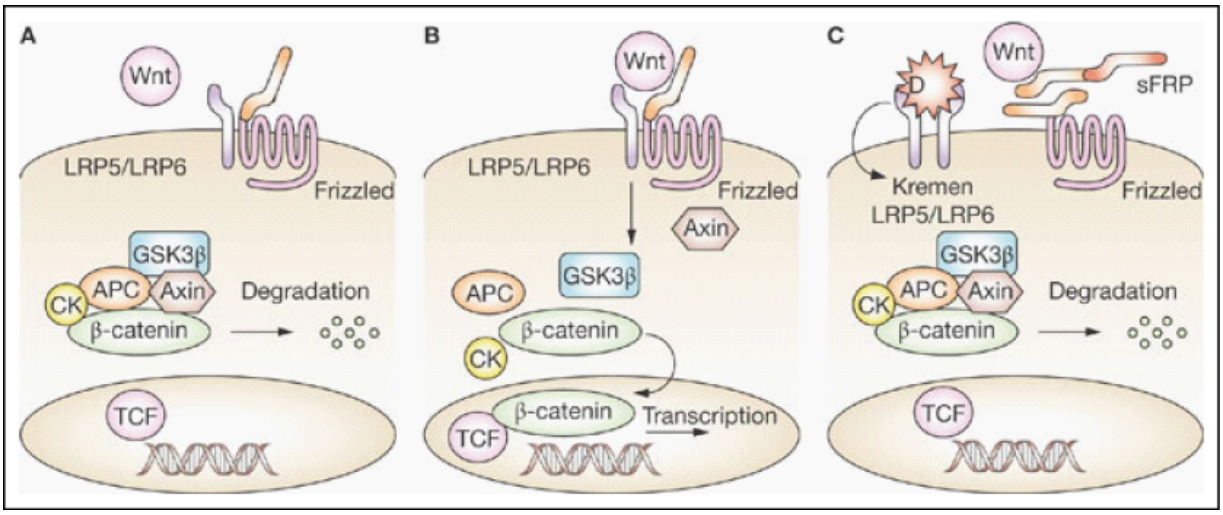

Figure 1.7: The canonical Wnt signaling pathway (Corr, 2008). Several lines of evidence connect GRN and FTD with the Wnt signaling pathway. **A)** In the absence of a Wnt ligand, cytoplasmic ß-catenin is bound to the multimeric CK-APC-GSK3ß-Axin complex, which facilitates its phosphorylation via GSK3ß and its subsequent degradation. **B)** When a Wnt ligand binds to a frizzled receptor (e.g. FZD2) and the co-receptors LRP5 or 6, Axin relocates to the plasma membrane and ß-catenin is released from the multimeric complex. The unphosphorylated ß-catenin then translocates into the nucleus and activates the expression of target genes. **C)** Wnt signaling can be inhibited through binding of DKK1 (D) to the co-receptors or sFRP to the frizzled receptor. Abbreviations: APC, adenomatous polyposis coli; CK, casein kinase; DKK1, Dickkopf 1; GSK3ß, glycogen synthase kinase 3ß; LRP, LDL-receptor-related protein; sFRP, secreted frizzled related protein; TCF, T-cell factor.

One signaling pathway that was reported to have a connection not only to GRN but also to FTD is the Wnt-signaling pathway (Rosen et al., 2011). In cultured cells, down regulation of GRN expression resulted in an up regulation of the Wnt-signaling pathway (Rosen et al., 2011). Mechanistically, this was explained by an up regulation of the Wnt receptor frizzled-2 (FZD2), which was detected in the brain of $GRN^{-/-}$ knockout mice and in human brain

samples from GRN mutation carriers. Upregulation of FZD2 was further shown to be neuroprotective in an *in vitro* neuronal cell culture model (Rosen et al., 2011). FZD2 is a seven-transmembrane G protein-coupled receptor, which is activated by secreted Wnt ligands. Activation of the canonical beta-catenin Wnt signaling pathway after loss of GRN expression might represent a compensatory neuroprotective response (Rosen et al., 2011).

The signal transduction pathways that have repeatedly been reported to be activated in response to GRN, particularly in cancer cells, are the PI3K/Akt and MAPK/ERK signaling pathways. Supposedly to enable increased proliferation, cell survival and invasion (Cuevas-Antonio et al., 2010; He et al., 2002; He et al., 2003; Ho et al., 2008; Lu and Serrero, 2001; Monami et al., 2009; Monami et al., 2006; Youn et al., 2009; Zanocco-Marani et al., 1999). However, in cortical neurons from $GRN^{-/-}$ mice, GRN treatment was only able to activate the PI3K pathway (Kleinberger et al., 2010), whereas in embryonic fibroblasts from $GRN^{-/-}$ mice both pathways were activated. An important downstream target of the PI3K/Akt pathway in neurons is the glycogen synthase kinase-3-beta (GSK3ß). An increase of phosphorylation indicating activation was detected in mouse cortical neurons for GSK3ß, Akt and ERK after treatment with GRN (Gao et al., 2010). Consistent with the finding that GSK3ß and Akt are important for neurite outgrowth and axon-dendrite polarity in neurons (Jiang et al., 2005), it was hypothesized that GRN regulates neurite outgrowth via GSK3ß.

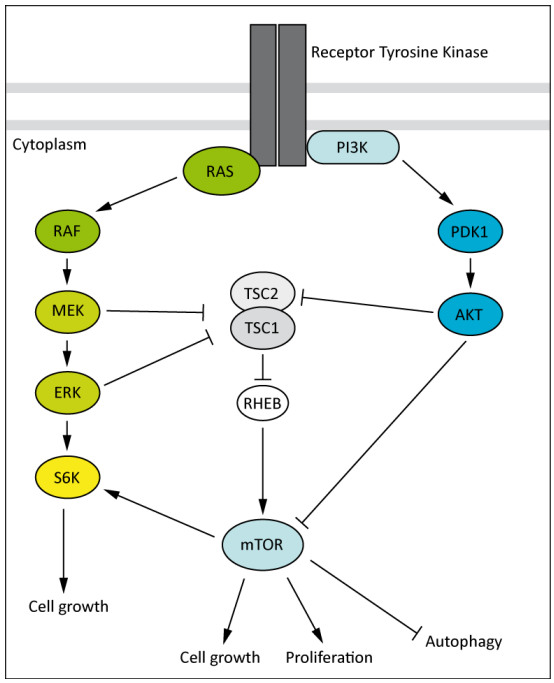

Figure 1.6: Simplified overview over the MAPK/ERK and PI3K/AKT signaling pathways. Both pathways are regulated by extracellular ligands (e.g. growth factors) that bind to a receptor tyrosine kinase on the cell surface (e.g. EGFR). This activates the cytoplasmic domain of the receptor and the intracellular cascade of kinases resulting in the translation of proteins that enhance biological processes like cell growth, proliferation or survival. Changes in these two pathways were detected when GRN expression was downregulated or after treatment with recombinant GRN. Cells from GRN mutation carriers were specifically sensitive to MEK and PI3K inhibition (Fenton and Gout, 2011).

1.8. Therapeutics for FTD

Most of the therapeutic approaches for FTD patients with GRN haploinsufficiency that have been proposed up to now aim at the up regulation of GRN protein levels in the brain. However, due to the suspected involvement of GRN in the progression of many cancers a very strict regulation of GRN levels would be crucial. Several ways to stimulate GRN expression have been suggested.

Table 1.2: Proposed therapeutic approaches for FTP patients with GRN mutations. Abbreviations: HDAC, histone deacetylase inhibitor; wt, wild type.

Approach	Known or proposed activity	targeted mechanism	effect
miRNA knockdown	miR-29b was shown to bind GRN mRNA. Reduction of miR-29b increased GRN mRNA levels in cultured cells.	decreased mRNA decay	increased GRN protein
GRN C-term peptide	exogenous peptide containing the sortilin-binding C-term could compete for sortilin binding	internalisation of GRN	extracellular GRN
Recombinant GRN	direct administration of purified GRN protein (by pump)	protein	increased total GRN protein
HDAC inhibitors	i.e. SAHA, a HDAC inhibitor, FDA approved for cancer treatment. Upregulates GRN expression in GRN+/-patient cells to nearly wt levels	expression	increased GRN protein
ATPase inhibitor	selective inhibition of vacuolar ATPase in cultured cells increased GRN independent of lysosomal degradation, autophagy or endocytosis	secretion	increased extracellular GRN
Viral gene replacement	introduction of exogenous transgene	expression	increased total GRN protein

An inhibitor of the vacuolar ATPase was shown to increase GRN protein levels without interfering with lysosomal degradation, autophagy or endocytosis. The mechanism remained unclear, but it was hypothesized that the change of the intracellular pH caused a translational upregulation of GRN expression. Consequently, FDA approved alkalizing compounds were tested and were also able to increase GRN expression in cortical neurons of $GRN^{+/-}$ mice and in lymphoblasts from patients with GRN mutation (Capell et al., 2011). Suberoylanilide hydroxamic acid (SAHA), an histone deacetylase (HDAC) inhibitor used for treatment of cutaneous T-cell lymphoma, was also found to restore GRN protein and mRNA levels in $GRN^{+/-}$ patient-derived lypmhoblasts back to wild type levels (Cenik et al., 2011). A different approach is to exploit microRNAs (miRNA) that regulate the expression of specific genes. Several miRNAs including MiR-29b have been shown to decrease GRN levels by preventing GRN mRNA translation. In human cells, a miR-29b knockdown increased GRN protein levels (Jiao et al., 2010). The protein sorting receptor sortilin has been shown to regulate

extracellular GRN levels. The last three amino acids at the GRN C-terminus bind to sortilin leading to endocytosis and sorting of GRN to the lysosome (Hu et al., 2010; Zheng et al., 2011). This led to the hypothesis that a C-terminal granulin peptide might compete with the intact GRN protein for the receptor binding-site. As a consequence, less GRN would be internalized and degraded, leading to a higher level of GRN in the extracellular space. Indeed, a five amino acid peptide corresponding to the GRN C-terminus was shown to interfere with GRN endocytosis in COS cells (Lee et al., 2014).

The U.S. National Institutes of Health (NIH) lists one clinical study in GRN mutation carriers that is underway as of this writing. This study investigates the HDAC inhibitor FRM-0334 (phase II). A second study, investigating the calcium channel blocker Nimopidine (phase I) was stopped recently.

Table 1.3: Potentially therapeutic compounds targeting GRN expression. Abbreviations: SAHA, Suberoyanilide hydroxamic acid (histone acetylase inhibitor); BBB, blood brain barrier.

Compound	Effect on target	Status	Limitations
Chloroquine	increased GRN secretion	Preclinical, clinical trial planned	Toxicity, BBB penetration
Amiodarone	increased GRN secretion	Preclinical	Toxicity, mechanism
SAHA	increased GRN expression	Preclinical	Toxicity, BBB penetration
Resveratrol	increased GRN expression	Preclinical	N/A

In conclusion, all the therapeutic approaches proposed to date aim at the increase of GRN protein levels. Likely limitations of these approaches are low blood brain barrier (BBB) penetration, toxicity and most importantly a narrow therapeutic window for the safe upregulation of GRN expression. High levels of GRN are not only supportive for tumor/cancer development, but might also cause problematic side effects in the periphery, like insulin resistance and obesity (Matsubara et al., 2012), artherosclerosis (Kojima et al., 2009; Yoo et al., 2013), and disturbances of the plasma lipoprotein metabolism (Hu et al., 2010; Okura et al., 2010) and the immune system through excessive monocyte recruitment (Youn et al., 2009). Moreover, all these mechanisms are not specific to GRN and will likely affect numerous other proteins with a high potential for clinical side effects, particularly if chronic treatment of patients over long periods of time is required. Therefore, it would appear much more promising to address a deficit in GRN signaling by targeting its dedicated receptor(s). As described in the following chapters, part of the objectives of this thesis was to discover novel functional GRN receptor candidates.

1.9. Objectives

Frontotemporal Dementia (FTD) is a severe and fatal disease of the brain affecting millions of people worldwide. Correlating with the degeneration of neurons in the frontal and temporal lobes of the cortex, patients suffer from progressive abnormalities in personality, behavior and language. The growth factor-like protein progranulin (GRN) is believed to play an important role in the pathogenesis of FTD as a subset of patients with familial forms of FTD harbor inactivating mutations in the GRN gene. In the CNS, the protein has been shown to modulate inflammatory processes and to provide trophic support for neurons. However, GRN might also increase the malignancy of tumors through its proliferative and pro-survival activities.

At the beginning of this thesis, no functional receptor(s) or other interaction partners of GRN had been described to explain the physiological functions and biological activities of GRN or the pathological mechanism(s) leading to FTD. Therefore, this thesis had the following objectives:

1) To generate highly purified and functional GRN protein by recombinant expression in mammalian cells. In addition, to validate described biological activities of GRN, like stimulation of proliferation or neurite outgrowth.

2) To develop a functional and robust biological assay for GRN activity. Available GRN bioassays are labor-intensive, time-consuming, and cannot be applied in high-throughput screenings. A robust bioassay suitable for compound and genetic screens could be used to identify novel GRN receptors and other proteins that mediate the biological functions of GRN.

3) To identify novel binding partners of GRN through a yeast-two-hybrid screen with GRN as the bait against a human brain cDNA library. This method was developed to detect novel protein-protein interactions on a genome-wide level in a cell-based system. Novel, potentially CNS-specific binding partners of GRN could aid in assigning additional molecular functions to GRN and in developing novel therapeutic approaches.

2. Materials

2.1. Yeast strains

Strain*	Function	Reporters
Y2H Gold	Mating partner	HIS3, ADE2, AUR1-C, MEL1
Y187	Library host strain	lacZ, MEL1

*Both yeast strains were bought from Takara Clontech, California.

2.2. Cell lines

Name	Celltype/origin	Company/Source/Ref.
293T	Human embryonic kidney	GenHunter
SW13	Human adrenal small cell carcinoma	Leibovitz et al., 1973
HT22	Mouse hippocampal cell line, cloned from HT4	AG Methner, HHU
THP-1	Human leukemic monocyte cell line	ATCC
GP2-293	Hek293 based retroviral packaging cell line	Clontech

2.3. Bacterial strains

DH5α	Competence	Manufacturer
Subcloning Efficiency	$>1x10^6$	Invitrogen
MaxEfficiency	$>1x10^9$	Invitrogen
Library Efficiency	$>1x10^8$	Invitrogen
Selfmade comp.cells	$<1x10^5$	

2.4. Plasmids and Primer

2.4.1. Plasmids

Name	Manufacturer
pCDNA3	Invitrogen
pLHCX	Clontech
pVSVG	Clontech
pGBKT7	Clontech
pGBT9	Clontech

2.4.2. Primer

Primer for Sequencing	
Name	Sequence 5'-3'
T7 Universal Primer	TAATACGACTCACTATAGGG
T7_Term_rev	GCT AGT TAT TGC TCA GCG G
Seq pGBKT7 PGRN_for	ATC ATG GAG GAG CAG AAG C
Seq pGBKT7 PGRN_rev	ACC TGA GAA AGC AAC CTG
seq_pGBKT7_for	GTT GAC TGT ATC GCC GGA
primer_seq_PGRN_rev	GAG TTG TTA CCT GAT CTT TG
Library_Seq_primer_rev	AGA TGG TGC ACG ATG CAC AG

Primer for Cloning	
Name	Sequence 5'-3'
Hind_GRN_for	TTTTaagcttATGtggaccctggtgagctgg
GRN_TEV_His_Cla_rev	TTTT atc gat TCA gtg atg gtg atg gtg atg gtg atg gtg atg gtg atg CTC ATT CAG ATA GAA CTG TCC cag cag ctg tct caa
TMEFF_Hind_for	TTT TAA GCT TAT GGT GCT GTG GGA GTC
TMEFF_Cla_V5_rev	TTT TAT CGA TTT ACG TAG AAT CGA GAC CGA GGA GAG GGT TAG GGA TAG GCT TAC CGA TTA ACC TCG TGG AC

Primer for Y2H Bait cloning	
Name	Sequence 5'-3'
EcoRI_APPcterm_for	TTT TGA ATT CAA GAA GAA ACA GTA CAC ATC
APPcterm_BamHI_rev	TTT TGG ATC CCT AGT TCT GCA TCT GCT C
pGBKT7_PGRN_for	CAT GGA GGC CGA ATT CAC GCG GTG CCC AGA TGG TCA GTT C
pGBKT7 PGRN Y2H rev	GCA GGT CGA CGG ATC CTC ACA GCA GCT GTC TCA AGG CTG G
primer 1 for	CTT CCA AAG ATC AGG TAA CAA CTC CTA AGT GGG TGC CAT

	CCA GTG CCC
primer 1 rev	TAT CAG GGC ACT GGA TGG CAC CCA CTT AGG AGT TGT TAC CTG ATC TTT
primer 2 for	CTG CAT CAC ACC CAC GGG CAC CCA CTA ACC CCT GGC AAA GAA GCT CCC
primer 2 rev	GGG CAG GGA GCT TCT TTG CCA GGG GTT AGT GGG TGC CCG TGG GTG TGA
primer 3 for	GGA GAA CGC TAC CAC GGA CCT CCT CTA AAC TAA GCT GCC TGC GCA CAC
primer 3 rev	CCA CTG TGT GCG CAG GCA GCT TAG TTT AGA GGA GGT CCG TGG TAG CGT
primer 4 for	GAA GGC CCC AGC TCA CCT CAG CCT GTA ACC AGA CCC ACA AGC CTT GAA
primer 4 rev	CTC TCT TCA AGG CTT GTG GGT CTG GTT ACA GGC TGA GGT GAG CTG GGG
primer 5 for	ACT GGA GAA GAT GCC TGC CCG CCG GTA AGC TTC CTT ATC CCA CCC CAG
primer 5 rev	TGT CTC TGG GGT GGG ATA AGG AAG CTT ACC GGC GGG CAG GCA TCT TCT
primer 6 for	CAC CTT CCT GGC CCG TAG CCC TCA CTA AGT GGG TGT GAA GGA CGT GGA
primer 6 rev	CAC ACT CCA CGT CCT TCA CAC CCA CTT AGT GAG GGC TAC GGG CCA GGA
primer 7 for_NEU	TTT TGA ATT CTC CTT ATC CCA CCC CAG AGA C
primer 8 for_NEU	TTT TGA ATT CTT GAA GAG AGA TGT CCC CTG T
primer 9 for_NEU	TTT TGA ATT CAC GGA CCT CCT CAC TAA GC
primer 10 for_NEU	TTT TGA ATT CGC CCA GAG GAC TAA CAG G

primer 11 for_NEU	TTT TGA ATT CGG TAA CAA CTC CGT GGG
primer 12 for_NEU	TTT TGA ATT CAC AAC ACT GAG CAG GCA
REV primer NEU	TTG AGA CAG CTG CTG TGA GGA TCC TTT T
deltaF GRN for	TCA GGT AAC AAC TCC CCC CTG GCA AAG AAG
deltaF GRN rev	CTT CTT TGC CAG GGG GGA GTT GTT ACC TGA

2.5. Antibodies

2.5.1. Primary antibodies

Name	Antigen	Species	Type	Company/ Reference
α-PCDGF	Progranulin (human), C-terminal region	Rabbit	Polyclonal	Invitrogen (#40-3400)
N-19	Progranulin (human), N-terminal region	Goat	Polyclonal	Santa Cruz (#sc-11342)
α-Flag	Flag tag	Mouse	Monoclonal	Sigma-Aldrich (#F 9291)
α-Myc	c-myc (human)	Mouse	Monoclonal	Calbiochem (#OP10)
α-V5	V5 tag	Mouse	Monoclonal	Life technologies (#37-7500)
α-actin	Actin, C11	Rabbit	Polyclonal	Sigma-Aldrich (#A 2066)
α-tubulin	alpha-tubulin	Mouse	Monoclonal	Sigma-Aldrich (#K 4777)
NTR3	Sortilin (human), aa300-422	Mouse	Monoclonal	BD Biosciences (#612100)
α-HA	HA tag, aa90-115	Mouse	Monoclonal	Santa Cruz (#sc-7392)
α-His	polyhistidine	Rabbit	Polyclonal	Santa Cruz (#sc-803)
α-p53	p53 (human)	Mouse	Monoclonal	Dako (#M 7001)
α-β-catenin	β-catenin	Mouse	Monoclonal	BD Biosciences (#610153)

2.5.2. Secondary antibodies

Name	Conjugate	Company
α-mouse	HRP	Dianova
α-rabbit	HRP	Dianova
α-goat	HRP	Santa Cruz
α-mouse	IR Dye 800nm	Licor
α-rabbit	IR Dye 800nm	Licor
α-goat	IR Dye 800nm	Licor
α-mouse	IR Dye 680nm	Licor
α-rabbit	IR Dye 680nm	Licor

2.6. Reagents

2.6.1. Chemicals

30 % Acrylamide 37.5 :1, Bis-Acrylamide	*National Diagnostics, USA*
Agar	*Carl Roth, Karlsruhe*
Agarose	*BioBudget, Krefeld*
Alamar Blue	*Invitrogen, Carlsbad, CA*
Albumin Standard (BSA)	*Thermo Scientific, Rockford, IL*
Ammoniumpersulfate (APS)	*Sigma-Aldrich, Steinheim*
BCA Reagent A	*Thermo Scientific, Rockford, IL*
BCA Reagent B	*Thermo Scientific, Rockford, IL*
BisTris	*Calbiochem, Darmstadt*
Bromphenolblue	*Carl Roth, Karlsruhe*
ClearMount™ mounting solution	*Invitrogen, Carlsbad, CA*
Desoxynucleotide-tri-phosphate (dNTP)	*New England Biolabs, Ipswich*
Dimethylsulfoxide (DMSO)	*Carl Roth, Karlsruhe*
Dithiothreiotol (DTT)	*Sigma-Aldrich, Steinheim*
DMEM	*Invitrogen, Carlsbad, CA*
Dry-milk (fat-free)	*Oxoid, Hampshire, UK*
Ethanol	*Carl Roth, Karlsruhe*
Ethidiumbromide	*Sigma-Aldrich, Steinheim*
Fetal Calf Serum (FCS)	*Invitrogen, Carlsbad, CA*
GeneJuice Transfection Reagent	*Merck, Darmstadt*
Glacial Acetic Acid	*Merck, Darmstadt*
Glycerine	*Carl Roth, Karlsruhe*
Hydrochloric acid (HCl)	*Sigma-Aldrich, Steinheim*

Igepal (NP40)	*Sigma-Aldrich, Steinheim*
Immobilion™ Western HRP Substrate Luminol Reagent	*Millipore, Schwalbach*
Immobilion™ Western HRP Substrate Peroxidase	*Millipore, Schwalbach*
Isopropanol	*Carl Roth, Karlsruhe*
Lipofectamine 2000	*Invitrogen, Carlsbad, CA*
Magnesium-chloride ($MgCl_2$)	*Carl Roth, Karlsruhe*
Midori Green Advance	*Biozym, Oldendorf*
Methanol	*Carl Roth, Karlsruhe*
Opti-MEM	*Invitrogen, Carlsbad, CA*
Paraformaldehyde	*Sigma-Aldrich, Steinheim*
PBS	*Invitrogen, Carlsbad, CA*
Polybrene	*Sigma-Aldrich, Steinheim*
Ponceau S	*Sigma-Aldrich, Steinheim*
Potassium chloride (KCl)	*Sigma-Aldrich, Steinheim*
Potassium dihydrogen phosphate (KH_2PO_4)	*Carl Roth, Karlsruhe*
Protease inhibitor cocktail tablets, EDTA-free	*Roche, Basel*
Random Hexamers	*Roche, Basel*
Sodium azide (NaN_3)	*Merck, Darmstadt*
Sodium chloride (NaCl)	*Carl Roth, Karlsruhe*
Sodium dihydrogen phosphate (NaH_2PO_4)	*Merck, Darmstadt*
Sodium dodecyl sulfate (SDS)	*Carl Roth, Karlsruhe*
Sodium hydroxide (NaOH)	*Merck, Darmstadt*
Sodium pyruvate	*Invitrogen, Carlsbad, CA*
TEMED (N,N,N+,N+-Tetramethylendiamine)	*Sigma-Aldrich, Steinheim*
Tris hydrochloride (HCL)	*Carl Roth, Karlsruhe*
Tris-Base	*Carl Roth, Karlsruhe*
TRIzol	*Invitrogen, Carlsbad, CA*
Trypan blue	*Invitrogen, Carlsbad, CA*
Trypsin/EDTA	*Gibco/Invitrogen, Carlsbad,CA*
Tryptone	*Carl Roth, Karlsruhe*
Tween-20	*Carl Roth, Karlsruhe*
Xylol	*Carl Roth, Karlsruhe*
Yeast Extract	*Carl Roth, Karlsruhe*

2.6.2. Antibiotics

Ampicillin	*Sigma-Aldrich, Steinheim*
Blasticidin	*Invitrogen, Carlsbad, CA*
G418	*Sigma-Aldrich, Steinheim*
Kanamycin	*Sigma-Aldrich, Steinheim*
Penicillin/Streptomycin	*Invitrogen, Carlsbad, CA*
Hygromycin B	*Carl Roth, Karlsruhe*

2.6.3. Size Standards

Biotinylated Protein Ladder	*Cell signalling, Boston, MA*
2-log DNA Ladder	*New England Biolabs, Ipswich*
peqGOLD Prestained Protein Ladder IV	*Peqlab, Erlangen*
Novex Sharp	Invitrogen, Carlsbad, CA

2.7. Enzymes

2.7.1. General Enzymes

Name	Buffer	Company
Antarctic Phosphatase	10x Antarctic phosph. buffer	New England Biolabs
Pfu Ultra High-Fidelity Polymerase	10x Reaction buffer	Stratagene
Phusion High-Fidelity Polymerase	5x Phusion HF buffer	Finnzymes
T4 DNA Ligase	10x Ligase buffer	New England Biolabs

2.7.2. Restrictionendonucleases

Name	Sequence	Company
ClaI	5´-AT↓CGAT-3´	New England Biolabs
EcoRI	5´-G↓AATTC-3´	New England Biolabs
HindIII	5´-A↓AGCTT-3´	New England Biolabs
BamHI	5´-G↓GATCC-3´	New England Biolabs
AluI	5´-AG↓CT-3´	New England Biolabs
HaeIII	5´-GG↓CC-3´	New England Biolabs

2.7.3. Endopeptidases

Name	Company
Neutrophil Elastase	Sigma

2.8. Kits

BCA Protein Assay Kit	*Pierce, Bonn*
DC Protein Assay	*Biorad, München*
Jet Star Plasmid Maxi-Prep Kit	*Genomed, Löhne*
QIAquick Gel Extraction Kit	*Qiagen, Hilden*
PCR purification Kit	*Qiagen, Hilden*

Yeast Kits:

Matchmaker™ Gold Yeast Two-Hybrid System	*Clontech, California*
Yeastmaker™ Yeast Transformation System 2	*Clontech, California*
Easy Yeast Plasmid Isolation Kit	*Clontech, California*
Matchmaker™ Insert Check PCR Mix 2	*Clontech, California*

2.9. Consumables

Cell culture dishes / flasks	*Nunc, Wiesbaden*
Cover Slips	*Engelbrecht, Engermünde*
Cryotubes	*Nunc, Wiesbaden*
Disposable gloves	*Semperit, Wien*
High performance chemiluminescence film	*Amersham Biosciences,UK*
Immobilion®-P Transfer Membrane	*Millipore, Schwalbach*
Immobilion®-FL Transfer Membrane	*Millipore, Schwalbach*
Microscope slides	*Thermo Scientific, Waltham*
Multiwell plates (cell culture)	*Nunc, Wiesbaden*
Novex Gel Cassettes	*Invitrogen, Carlsbad, CA*
Pasteur pipettes	*Carl Roth, Karlsruhe*
PCR reaction tubes	*Thermo Scientific, Waltham*
Reaction tubes	*Sarstedt, Nümbrecht*
Petri dishes (bacteria/yeast)	*Sarstedt, Nümbrecht*
Pipet tips	*Starlab, Ahrensburg*
Pipettes (5 ml – 25 ml)	*Corning Inc., Corning, NY*
Whatman paper	*Whatman, Dassel*

2.10. Laboratory hardware and appliances

Autoclaves	*Systec, Wettenberg*
Block Thermostat	*HLC BioTech, Bovenden*
Centrifuges	*Eppendorf, Hamburg*
	Hettich, Tuttingen
Fluorescence microscope IX 50/ U-RFL-T	*Olympus GmbH, Münster*
Freezers and fridges	*-80°C Heraeus*
	-20°C Liebherr
	4°C Liebherr
Glassware	*Schott, Mainz*
Incubator	*Binder, Tuttlingen*
Laminar flow (Typ EF/S)	*CleanAir Technik, Woerden*
Luminescent Image Analyzer LAS-3000 mini	*FUJIFILM, Düsseldorf*
Microscope	*Nikon Instr., Düsseldorf*
Microwave pressure cooker ‚multi gourmet'	*Braun, Kronberg /Ts.*
Nanodrop ND1000	*Peqlab, Erlangen*
Paradigm Detection Platform	*Beckman Coulter, Krefeld*
pH-Meter	*WTW, Weilheim*
Photomicroscope	*Leica Microsystems, Wetzlar*
Pipettes	*Gilson, Middleton, WI*
Pipettors	*BRAND, Wertheim*
Power supplies	*Consort, Turnhout*
RunOne Electrophoresis Cell System	*EmbiTec, San Diego*
Scales	*Sartorius, Göttingen*
StepONE Plus Real Time PCR System	*Applied Biosystems, CA*
T3 Thermocycler	*Biometra, Göttingen*
Tank Blotter	*CBS Scientific, USA*
ViCell^{TM} XR Cell Viability Analyzer	*Beckman Coulter, Krefeld*

2.11. Software

Adobe Design Standard CS3
CLC DNA Workbench 6
Fuji Imaging Software
Microsoft Office 2010/2011
National Center for Biotechnology Information - BLAST / PubMed
Prism GraphPad 5.0

3. Methods

3.1. Tissue Culture

Routine cell culture was performed under sterile working conditions in S1 or S2 qualified laboratories. Pipettes, dishes, plates, filter tips, tubes, syringes and sterile filters were single-use plastic items and cell culture qualified. All solutions and media were stored at 4°C unless otherwise indicated by the manufacturer. Cells were cultured in the appropriate medium supplemented with selection antibiotics as necessary and incubated at 37°C in 5% CO_2. Growth and morphology were checked on a daily basis and mycoplasm tests were performed regularly.

Cell culture media:

DMEM complete: DMEM (high glucose, + L-glutamine)
10 % FCS
1 mM Na-Pyruvate
2 % Penicillin/Streptomycin (10000 U/ml Penicillin / 10000 µg/ml Streptomycin)

Serum-free treatment media were made as listed above, without FCS supplementation.

3.1.1. Passaging of adherent cell lines

In general, adherent cell lines were cultured in 10 cm cell culture dishes. If cells were cultured in smaller or larger vessels the volumes were adjusted accordingly.

- Remove cell culture medium from dish.
- Add 5 ml 1 x PBS (Gibco, Invitrogen), sway dish, and remove buffer.
- Add 1 ml 1 x trypsin/EDTA (Gibco, Invitrogen) and sway dish, incubate for 1 min to 5 min at 37°C.
- Add 9 ml of the appropriate culture medium containing FCS and pipet up and down to achieve a single cell suspension.
- Transfer the desired amount of cell suspension into a fresh 10 cm dish, adjust volume to 10 ml with complete growth medium and add the appropriate selection antibiotic.

3.1.2. Cryopreservation of cells

For long-term storage and preservation cell lines were frozen and stored in liquid nitrogen. Trypsinize and resuspend cells as for passaging (see item 3.1.1).

- Transfer cell suspension to a 15 ml tube and centrifuge at 1000xg for 5 min.
- Resuspend pellet in freezing media (90% FCS/10% DMSO), 1 ml per 10 cm dish.
- Aliquot cell suspension (1 ml) into 1.8 ml screw cap cryo-vials and place on ice.
- Transfer vials to -80°C quickly. For long-term storage transfer vials into liquid nitrogen tank.

3.1.3. Thawing of frozen cell stocks

- Prepare 15 ml tube with 10 ml pre-warmed complete growth medium.
- Place cryo-vial in 37°C water bath and thaw cells.
- Transfer cells into the medium and spin down at 1000 x g for 5 min.
- Remove supernatant and resuspend cells in complete growth medium.
- Transfer cells onto a 10 cm dish and place in incubator.

3.1.4. Transient transfection

- The day before transfection, seed target cells in 6-well dishes. Cell density should be adjusted for each cell line so that cells reach 80-90% confluency 24 h later.
- Change medium on cells to 2 ml OptiMEM.
- For each well, pipet 250 µl OptiMEM to a sterile 1.5 ml tube and add 10 µl Lipofectamine 2000.
- In a separate tube dilute 4 µg DNA in 250 µl OptiMEM.
- Incubate for 5 min at RT.
- Transfer DNA dilution to the transfection reagent mixture and incubate for additional 20 min at RT.
- Add transfection mixture to cells.
- Change medium after 4-6 hours and assay for transgene expression after 24-72 hours.

3.1.5. Generation of retroviral particles

When working with retroviral particles, adhere to biosafety level 2 (S2) rules, these include (but are not limited to):

- Work only in S2 qualified rooms and at S2 qualified cell culture benches.
- Wear lab-coat at all times.
- Double-glove with nitril gloves.
- Wear arm protection.

- Keep disinfectant ready at hand.
- Use plastic pipettes and filtered pipette tips; no glassware!
- Inactivate liquid waste by incubation with 70% ethanol or disinfectant before autoclaving.
- Double-bag solid waste and autoclave on a regular basis.

Day 1:

- Split a confluent plate of GP2-293 cells 1:4 into T75 flasks.

Day 2:

- Cell density should be 70 – 80%.
- Prepare transfection mixture for each plate:
- Add 800 µl Optimem (Invitrogen) to a sterile 1.5 ml tube.
- Add 45 µl Gene Juice and incubate for 5 min at RT.
- Add 7.5 µg retroviral shuttle plasmid (e.g. pLPCX, pLHCX, etc.), containing gene of interest, and 7.5 µg pVSVG plasmid to the transfection mixture. The total volume of the DNA should not exceed 100 µl.
- Incubate for 15 – 20 min at RT.
- Carefully change medium on the GP2-293 cells.
- Add the transfection mix in a drop wise manner onto the cells and carefully sway the plate.
- Place in incubator.

Day 4:

- Take off supernatant and inactivate with disinfectant.
- Carefully add 5 ml fresh medium and place cells in incubator.

Day 5:

- Draw supernatant containing the retroviral particles into a 10 ml syringe.
- Place a sterile filter (0.45 µm) on the syringe and filter supernatant into a 50 ml tube to remove cells and debris.
- Aliquot filtered supernatant into screw cap cryovials (1 ml per vial).
- Store virus particles at -80°C.
- Inactivate and discard cells.

3.1.6. Infection with viral particles

To produce cell lines with stable expression of transgenes, cells were infected with retroviral particles and then subjected to selection with the appropriate antibiotic depending on the resistance gene encoded on the plasmid.

Day 1:

- Seed target cells in T25 flasks. Cell density should be adjusted so that cell lines reach confluence about 48 – 72 h later, approximately 500 000 cells/T25 flask.

Day 2:

- Aspirate medium, replace by 1 ml fresh complete growth medium and add 2 µl polybrene stock solution (5 mg/ml).
- Thaw viral particles quickly in a 37°C water bath.
- Add 1 ml viral particles to cells and incubate for 24 h.

Day 3:

- Remove medium containing viral particles and inactivate.
- Wash cells with 1 x PBS and add fresh medium.
- Incubate for 24 h.

Day 4:

- Trypsinize the infected cells and resuspend in 10 ml medium containing the appropriate concentration of selection antibiotic.
- Plate cells on a 10 cm dish. For fast growing cells split cells 1:10.

Change media every 2 – 3 days and add selection antibiotic until stable cell clones appear. Make sure the control cells are all dead.
Check expression of transgene by Western Blot analysis.
Do not remove selection antibiotic until stable clones are frozen for long-term storage.

3.1.7. Killing curves

To evaluate the concentration of selection antibiotic needed to select for transfected cells, cell lines without expression of the transgene were subjected to treatment with different concentrations of the selection antibiotic. The concentration range was dependent on the cell line and the antibiotic used:

Hygromycin 100 µg/ml to 800 µg/ml
Puromycin 0.25 µg/ml to 6 µg/ml
Geneticin 100 µg/ml to 800 µg/ml
Blasticidin 1 µg/ml to 8 µg/ml

- Seed cells at low density in 12-well plates.
- After 24 h change medium to medium containing the selection antibiotic and keep 1 well in regular medium.
- Exchange medium every 2 – 3 days and add fresh selection antibiotic.

Depending on the cell line selection takes 1 – 2 weeks. Check cells regularly and note at which concentration all cells are dead.

For selection of cell lines with transgenes use the concentration at which all cells were dead and in addition one lower concentration at which approximately 80% of all cells were dead or dying. Sometimes selection at lower concentrations yields higher expression levels.

3.1.8. Proliferation assay

To investigate differences in proliferation rates of cell lines or differently treated cells, percentages of growth were evaluated by counting cell numbers.

- Seed cells at low density in 12-well plates.
- The following day, wash cells once with PBS and change to serum-free medium and add treatment.
- Trypsinize cells after an appropriate time of growth (3-7 days) and count cell numbers using the automated cell counter (Vi-Cell).

3.1.9. Toxicity Assay

HT22 cells were used as the indicator cell line for endogenous oxidative stress and alamarBlue® was used to measure cell viability. This blue compound, resazurin, is membrane permeable and will be reduced to red resofurin by viable cells.

- Seed cells at low density in 96-well plates (5000 c/well).
- The following day, starve cells in serum-free medium for four hours, followed by treatment with GRN or granulin peptides.
- After an incubation of 24 hours, change medium to serum-free medium containing GRN/grn plus glutamate.
- After additional 24 hours incubation add alamarBlue® and wait for the colour change.
- Measure absorbance at 560 nm and use 600 nm as reference wavelength.

3.1.10. β-Catenin Assay

The monocytic cell line THP-1 was used for the detection of changes in the intracellular β-catenin levels after stimulation of the Wnt signaling pathway. Upon activation of the pathway an increase ofβ-catenin in the cytosol can be detected via Western blot analysis. To detect a possible effect of GRN on the canonical Wnt pathway THP-1, cells were also treated for 24 hours with different combinations of GRN, grn, and Wnt-agonizing or -antagonizing molecules.

- Seed THP-1 cells in 24-well plates in 500 µl RPMI medium at a density of 2.5 x 10^5 per well.
- After 24 h treat cells with Wnt3a (250 ng/µL), Dkk1 (1 µg/µL), GRN (1 µM), or grn (1 µM), and combinations thereof. Incubate 24 h.
- Harvest the cells and lyse in 40 µL RIPA buffer.
- Load 8 µg of total protein onto a 12 % BisTris-SDS-Gel.
- β-catenin is then detected on the Western blot membrane with an anti- β-catenin antibody (BD Biosciences).

RPMI medium:		RPMI 1604
	10%	FCS
	1mM	Pyruvate
	2mM	L-Glutamine
	50uM	beta-Mercaptoethanol
	10nM	PMA
	2%	Penicillin/Streptomycin (10000 U/ml Penicillin / 10000 µg/ml Streptomycin)

3.2. Proteinbiochemistry

3.2.1. Harvesting of secreted proteins

To investigate secreted proteins, cell culture supernatants were harvested.

- Prepare 1.5 ml tubes by adding 20 µl 25x complete protease inhibitor stock solution per 500 µl of supernatant.
- Place cell culture dish or plate on ice and transfer 500 µl of supernatant into the prepared tubes.
- Centrifuge samples for 3 min at 13000 x g at 4°C.
- Transfer supernatant to fresh tubes and store at -80°C.

25 x Complete Protease Inhibitor: dissolve one tablet in 2 ml Milli-Q water (EDTA-free; Roche).

3.2.2. Harvesting of cellular lysates

To investigate intracellular or membrane proteins, cells were lysed in NP40-buffer.

- Place cell culture dishes or plates on ice.
- Remove supernatant and wash cells once with cold 1 x PBS.
- Add 1 ml 1 x PBS onto the cells and scrape them off the plate.
- Transfer cells into 1.5 ml tube and centrifuge for 3 min at 13 000 x g.
- Discard supernatant and add appropriate amount of cold NP40 lysis-buffer with protease inhibitor. Resuspend pellet by pipetting.
- Incubate for 20 min on ice and vortex every 5 min.
- Centrifuge for 20 min at 13000 x g at 4°C.
- Transfer supernatant into fresh tube. Store at -20°C.

NP40 Lysis Buffer:	50 mM	Tris-HCl, pH 7.8
	150 mM	NaCl
	2 %	NP40
	Store at 4°C.	
NP40 Lysis Buffer+PI:	50 mM Tris-HCl, pH 7.8	
	150 mM	NaCl
	2 %	NP40
	1x	Complete Protease Inhibitor
	Store at 4°C.	
10 x PBS, pH 7.4:	137 mM	NaCl
	2.7 mM	KCl
	10 mM	Na_2HPO_4
	10 mM	KH_2PO_4
	Store at RT.	
25 x Complete Protease Inhibitor:	Dissolve one tablet in 2 ml Milli-Q water.	
	Store at -20°C.	

3.2.3. Bicinchonic acid protein assay (BCA)

Determination of the protein concentration of cell lysates was achieved using the bicinchonic acid protein assay (Pierce). This detection method is a two step colorimetric method starting with the chelation of copper (biuret reaction: reduction of Cu2+ to Cu1+ by protein) followed by the reaction of bicinchonic acid with the cuprous cation that was formed in step one. The purple coloured reaction product exhibits strong linear absorbance at 562nm.

Pipetting procedure for BSA standards:

Final concentration [µg/ml]	Volume NP40 buffer [µl]	Volume BSA standard [µl]
0	50	-
100	45	5
200	40	10
300	35	15
400	30	20
500	25	25
600	20	30

- Add 45 µl NP40 buffer into 1.5 ml tubes and add 5 µl samples.
- Mix BCA Reagent A and B in a 50:1 ratio.
- Add 1 ml of BCA reagent mix to each sample and standard.
- Incubate for 30 min at 60 °C.
- Load samples and standard in duplicates onto a clear 96-well microtiter-plate, 200 µl per well.
- Measure OD at 540 nm and calculate sample concentration.

NP40 Lysis Buffer:
50 mM Tris-HCl, pH 7.8
150 mM NaCl
1 % NP40
Store at 4 °C.

BSA Standard, 1mg/ml:
Albumin Standard, 2mg/ml 1 ml
NP40 Lysis Buffer 1 ml
Store at 4°C

3.2.4. Detergent compatible (DC) protein assay

To determine the protein concentration of the purified Progranulin the DC protein assay from Biorad was used because this assay is compatible with certain amounts of Tris and Imidazole. This colorimetric assay is adapted from Lowry *et al.* 1951 and consists of a first step where copper reacts with protein at an alkaline pH, and a second step where the Folin reagent is reduced by the cuprous ions from step one. The characteristic blue colour is stable for one hour and absorbance is measured at 750 nm.

Pipetting procedure for BSA standards:

Final concentration [µg/ml]	Volume PBS [µl]	Volume BSA standard [µl]
0	50	-
200	40	10 - 1 mg/ml
500	20	20 – 1 mg/ml
750	10	30 – 1 mg/ml
1000	50	50 – 2 mg/ml
1250	12	20 – 2 mg/ml
1500	10	30 – 2 mg/ml
2000	-	15 – 2 mg/ml

- Transfer 5 µl sample or standard per well on a clear 96-well plate. Always load duplicates for the standard and triplicates for the samples.
- Add 25 µl Reagent A per well
- Add 200 µl Reagent B per well, carefully mixing the samples by pipetting up and down.
- Incubate for 10 min at RT
- Measure OD at 750 nm and calculate sample concentration.

3.2.5. SDS-Polyacrylamide gel electrophoresis (SDS-PAGE)

SDS-Polyacrylamide gel electrophoresis allows the separation of denatured proteins according to their molecular weight. The loading buffer for the proteins contains SDS, which results in an overall negative charge of the proteins; therefore their separation is not influenced by any intrinsic charges.

- Prepare resolving gel mixture:

	10 % Acrylamide 1x	10 % Acrylamide 2x	12 % Acrylamide 1x
30% Acrylamide 37,5:1	2.2 ml	4.4 ml	2.64 ml
1.6 M Bis-Tris pH 6.4	1.65 ml	3.3 ml	1.65 ml
ddH2O	2.7 ml	5.4 ml	2.26 ml
10 % APS	33 µl	66 µl	33 µl
Temed	11 µl	22 µl	11 µl

- Gently mix the resolving gel mixture and fill 3/4 of the Novex gel cassette.
- Carefully overlay the gel mixture with isopropanol and wait until the polymerization is complete (~ 15 min).
- Pour off the isopropanol and wash the gel surface with MilliQ water. Carefully drain all the water out of the gel cassette

- Prepare the stacking gel mixture:

	4 % Acrylamide 1x	2x
30 % Acrylamide 37.5 :1	260 µl	520 µl
1.6 M Bis-Tris buffer	500 µl	1 ml
MilliQ-water	1.23 ml	2.46 ml
10 % APS stock solution	20 µl	40 µl
Temed	5 µl	10 µl

- Gently mix the stacking gel mixture and pour it onto the gel cassette up to the top.
- Add the comb and wait until the gel is polymerized.
- Gels can be used immediately or stored at 4 °C if wrapped in wet paper towels and cling wrap.
- Remove comb and wash each slot with MilliQ water to remove unpolymerized acrylamide.
- Place gel in running chamber and fill with 1 x MES running buffer.
- Load samples and run gel at 150 V for approximately 60 min.

Bis-Tris gel-buffer:	1.6 M Bis-Tris, pH 6.4 Sterile filter and store at RT.
10 % APS:	10 % Ammoniumpersulfate in MilliQ water Store at -20°C.
20 x MES:	1 M MES 1 M Tris-Base 69.3 mM SDS 20.5 mM EDTA Store at RT.
4 x SDS sample buffer:	1.44 M Bis-Tris 0.64 M Bicine 4 % SDS 100 mM DTT 0.05 % Bromphenoleblue Store at -20°C.

3.2.6. Western-Blot

To enable the specific investigation of proteins previously separated on a SDS gel, proteins were transferred on a PVDF membrane by application of an electric field that pulls the proteins towards the cathode. After blotting, the samples can be further investigated by immunostaining with specific antibodies.

- Fill blotting tank with 1x transfer buffer and soak two pieces of 1 mm Whatman paper and two blotting sponges in the buffer.
- Soak respective membrane in Methanol.
- Build blotting stack starting on the Anode (black side of the cassette):
  - Sponge
  - Paper
  - SDS gel
  - Membrane
  - Paper
  - Sponge

  While building the stack make sure to avoid bubbles of air between the layers.
- Close the cassette and place stack in the tank.
- Blot for 1-2 h at 200 mA or overnight at 30 V and 4°C.

10x Transfer buffer:	250 mM Tris-Base
	1920 mM Glycin
	Store at RT.
1x Transfer buffer:	25 mM Tris-Base
	192 mM Glycin
	20 % Methanol
	Store at 4°C.

3.2.7. PonceauS staining of membranes

PonceauS solution may be used to reversibly stain proteins on PVDF membranes after Western blotting. This method was used to confirm the transfer of the proteins from the SDS gel onto the membrane before continuing with immunostaining.

- Take the membrane out of the blotting tank and incubate in PonceauS solution for ~ 1 min.
- Transfer membrane into MilliQ water and gently swirl until bands are clearly visible.
- Wash membrane with TBST to completely destain proteins.

Ponceau S solution:	0.2 % PonceauS
	3 % Glacial acetic acid
10x TBS, pH 7,4:	1.37 M NaCl
	27 mM KCl
	0.25 M Tris-Base
1x TBST:	137 mM NaCl
	2.7 mM KCl
	25 mM Tris-Base
	0.1 % Tween-20

3.2.8. Immunostaining of membranes

Specific proteins were visualized by immunostaining of the membranes with the respective antibodies:

- Block membrane in 5 % dry-milk/TBST, 3 % BSA/ TBST, or TBST alone, for 1 h at RT with gentle shaking. Blocking conditions depend on the antibody used.
- Wash membrane once with TBST for 5 min at RT with shaking.
- Dilute primary antibody in TBST with 0.02 % NaN_3.
- Incubate for 2 h at RT or 4°C overnight with gentle shaking. Dilution and optimal incubation time depends on the antibody.
- Wash the membrane at least 3 x 10 min or longer with TBST with shaking.
- Incubate membrane with secondary antibody for 1 h at RT with gentle shaking. Antibody is diluted in TBST or blocking solution.
- Wash the membrane at least 3 x 10 min or longer with TBST with shaking.
- Wash the membrane once with TBS.

Proteins were visualized using either fluorescence or enhanced chemiluminescence, depending on the sample and the first antibody.

- Choose respective secondary antibody for each technique, coupled to either a fluorescent molecule or HRP.
- For detection via fluorescence take the membrane and place it upside down on the glass surface of the Licor Unit.
- For detection via enhanced chemiluminescence take membrane out of the TBS and shake excess liquid carefully off the membrane. Then add HRP substrate and incubate for 1-2 min. Expose membrane to film or CCD camera.

10 x TBS, pH 7.4:	1.37 M NaCl 27 mM KCl 0.25 M Tris-Base
TBS:	1:10 dilution of 10 x TBS
TBST:	1:10 dilution of 10 x TBS 0.1 % Tween-20

3.2.9. Co-Immunoprecipitation

To investigate specific protein-protein interactions, one binding partner can be employed to pull the second binding partner from a supernatant or lysate. Therefore, the first protein is coupled via specific antibodies to bead material, followed by incubation with the putative binding partner. This complex can be pulled from the solution via the bead material. An interaction can be detected in the samples that are eluted from the beads and analysed with Western blotting. The membrane is probed with an antibody specific for the putative binding partner, which will only be present in the elution if the two proteins interacted.

- Transiently transfect a 10 cm dish of murine hippocampal HT22 cells with Lipofectamine/pLHCX-TMEFF-V5.
- After 24 hours prepare NP40 cell lysates.
- Pre-incubate the lysates with protein NHS-activated sepharose (GE Healthcare Life Sciences) to capture non-specifically binding proteins.
- Subsequently, couple anti-V5 antibody to fresh NHS-Sepharose according to manufacturer's instructions and add the cleared HT22 lysates.
- Add the recombinant full-length GRN and incubate the mixture at 4°C on rotator overnight to enable binding of GRN to TMEFF2.
- Discard the supernatant and wash three times with 500 µL NP40 buffer for 20 min at 4°C on rotator.
- Elute the immunoprecipitated material by boiling the NHS-activated sepharose and analyze samples by Western blotting with anti-V5 and anti-GRN antibodies.

3.3. Molecular Biology

3.3.1. DNA preparation

Plasmid DNA from bacteria was isolated using a combination of alkaline lysis and ion exchange columns that are the basis for almost all commercially available DNA extraction kits. For large scale DNA extraction from 250 ml bacterial cultures the JETstar plasmid purification system from Genomed, for small scale DNA extraction from 4 ml of bacterial culture the Plasmid Mini kit from e.z.n.a. was used. Both kits contained all the necessary buffers and solutions and the DNA extraction was performed according to the manufacturer’s protocol.

3.3.2. Agarose gel electrophoresis

To analyse DNA fragments they were separated depending on their size in an electric field on an agarose-gel matrix. The percentage of agarose (w/v) depends on the size of the DNA fragments that are analyzed. Usually 1 % agarose in 1 x TAE is used for fragments ranging from 1 kb to 8 kb.

DNA detection with Ethidiumbromide:

- Boil agarose in 1 x TAE buffer.
- Swirl the dissolved agarose and let it cool down to approximately 65°C.
- Pour agarose in gel cassette and place comb in the gel.
- Wait until the gel is solid.
- Remove comb and place gel in running chamber filled with 1 x TAE.
- Load samples and size standard and run at 100 V.
- Place gel in ethidiumbromide bath to stain DNA and incubate for 15 min.
- Wash gel once in 1 x TAE and place on UV table to take picture or excise fragments.

DNA detection with Midori Green:

- Boil agarose in 1 x TAE buffer.
- Swirl the dissolved agarose and let it cool down to approximately 65°C.
- Pour appropriate amount of dissolved agarose in a small glass (~20ml/~50ml) and add Midori Green (1.5 µl/ 3 µl). Stir for 2 min then pour in cassette.
- Continue as explained above. When the run is finished, place gel directly on UV table to take a picture or excise fragments.

10 x TAE:	0.80 M Tris-Base 20 mM EDTA 1 % Glacial acetic acid
1 x TAE:	1:10 dilution of 10 x TAE in MilliQ water.
Ethidiumbromide bath:	1 x TAE 10 µl Ethidiumbromide solution (10 mg/ml)
Midori Green:	Biozym

3.3.3. Gelelution

To purify PCR products from the plasmid template DNA or to remove the vector backbone after restriction digests, the DNA was loaded onto an agarose gel and the respective band was excised with a razor blade. The DNA was then eluted from the gel slice using the Qiagen Gel Extraction Kit according to the manufacturer's protocol. DNA was eluted in 30 µl sterile filtered MilliQ water pH 8.0.

3.3.4. Restriction enzyme digest

Digestion of DNA with restriction enzymes lead to formation of either sticky or blunt ended DNA. Sticky ends have single stranded base overlaps that can anneal to sticky ends of another DNA fragment, which was digested with the same enzyme. The recognition sequences of restriction enzymes are palindromic stretches of DNA of four, six, or eight base pairs length.

For an analytic digest approximately 1 µg DNA was digested in a final volume of 20 µl with either one or two different enzymes at the same time. The analytic digests were incubated at 37°C or the respective optimal temperature for the enzyme, for 1-3 h. For preparative digests the volume was increased due to the larger amounts of enzyme and DNA used. Preparative digests were incubated for at least 6 h at 37°C or, in the case of e.g. PCR-product double-digests, overnight at 37°C.

Analytic digest:

DNA	1 µg	
Enzyme	0.5 µl	(at least 1 U)
100 x BSA stock	0.2 µl	
10 x Enzyme buffer	2 µl	
Water	x µl	(adjust total volume to 20 µl)

Preparative digest:

DNA	10-20 µg	
Enzyme	2 µl	
100 x BSA stock	0.5 µl	
10 x Enzyme buffer	5 µl	
Water	x µl	(adjust total volume to 50 µl)

3.3.5. Dephosphorylation of DNA

To avoid re-ligation of a vector after digestion with restriction enzymes it was treated with Antarctic phosphatase. This treatment removes the 5'phosphate from the DNA strand thereby preventing a ligation of the two ends of the vector with each other as for this process the existence of the 5'phosphate group is essential. In the desired ligation reaction the insert DNA will provide the phosphate for the new bond.

Digest	50 µl
10 x Antarctic phosph. buffer	6 µl
Antarctic phosphatase	2 µl
Water	2 µl

- Incubate reaction for 2 h at 37°C.
- Heat inactivate enzyme for 20 min at 65°C.
- Purify reaction via agarose gel elution.

3.3.6. Ligation of DNA

The ligation of cohesive ended DNA was performed in a total volume of 10 µl. Plasmid and insert were usually mixed in a 1:3 molar ratio. The concentration of the fragments was measured with a NanoDrop spectrophotometer (peqlab) and confirmed on an agarose gel. The enzyme used for the ligation was the T4 DNA ligase that catalyses the formation of a phosphodiester-bond between two juxtaposed 5' phosphate and 3' hydroxyl termini in duplex DNA.

- Thaw 10 x ligase buffer on ice.
- Prepare ligation mixture in a small volume, preferably 10 µl:

Plasmid DNA	100 ng
Insert DNA	x µl
10 x buffer	1 µl
Ligase	1 µl
Water	x µl to a final volume of 10 µl

- Also prepare a ligation control containing water instead of the insert DNA to assess possible religation of the vector.

- Incubate ligation mixture in the Thermo Cycler for several hours or overnight:

  37°C – 1min
  22°C – 1min
  16°C – 1min 99 cycles
  65°C – 10min
  4°C – Pause

- Transform into bacteria immediately.

3.3.7. Transformation

Plasmids were transformed into bacteria to propagate the amount of DNA. Positive clones were confirmed and then used for DNA preparation. Small variability in the protocol occur depending on the specific cells that were used. For the transformation of a ligated construct the complete ligation reaction was transformed into cells purchased from Invitrogen (Max efficiency DH5α for difficult constructs, subcloning efficiency DH5α for normal ligations). Concerning retransformations of already existing constructs a maximum of 0.5 µl vector DNA was transformed into self-made competent DH5α.

- Thaw competent bacteria on ice.
- Add DNA (plasmid or ligation) and incubate for 30 min on ice.
- Heat shock for 90 sec in a 42 °C water bath.
- Place on ice for 2 min.
- Add 1 ml pre-warmed (37°C) SOC medium.
- Incubate at 37°C for 1 h, shaking.
- Pellet bacteria by centrifugation at 1000 x g for 2 min.
- Resuspend pellet in 100 µl SOC and spread on agar plate with appropriate selection antibiotic.
- Incubate overnight at 37 °C, upside down.

SOB medium:
8 g Tryptone
2 g Yeast extract
0.2 g NaCl
400 ml de-ionized water
Autoclave and store at 4°C.

SOC medium:
10 ml SOB medium
200 µl 2 M Glucose (sterile filtered)
Store at 4°C.

LB medium:	1 % Trypton
	0.5 % Yeast extract
	1 % NaCl
	Autoclave and store at 4°C.
LB-agar:	1 % Trypton
	0.5 % Yeast extract
	1 % NaCl
	1.5 % Agar
	Autoclave, pour plates, and store at 4°C.
Ampicillin Stock:	50 mg/ml Ampicillin
	Sterile filter and store at -20°C.
Kanamycin Stock:	50mg/ml Kanamycin
	Sterile filter and store at -20°C.

3.3.8. Polymerase Chain Reaction (PCR)

PCR allows in vitro amplification of specific DNA sequences using a thermostable DNA polymerase. During a PCR cycle the DNA becomes thermally denatured and hybridizes with short oligonucleotides (primer) that are subsequently elongated by the polymerase. This denaturation, hybridization/annealing and elongation are repeated approximately 30 times resulting in the amplification of the DNA sequence that is flanked by the forward and reverse primer.

The details of the PCR protocol vary depending on annealing temperatures of the primers, the polymerase and the length of DNA fragment that needs to be amplified.

3.4. Yeast experiments

First described in 1989 by Fields and Song, the Yeast-2-Hybrid system today is a well-established system for the detection of new protein-protein interactions. The system that was utilized here, the “Matchmaker Gold” Y2H system from Clontech, still uses the principle of the two domains of the Gal4 transcription factor that were separated from each other and fused to either bait or prey protein. Brought into close proximity through the binding of bait and prey, the two domains activate the transcription of reporter genes thereby showing the interaction in an easily monitored fashion like a change of color or independence of certain nutrients.

The huge advantage of this system is the change from using a co-transformation to introduce the library prey plasmids into the yeast cells together with the bait plasmid, to using the ability of different yeast strains to mate with each other. The library for this screen was already pre-transformed into the Y187 yeast strain whereas the bait plasmid was transformed into the Y2H Gold strain. Consequently for the screen the two strains were combined and mated with each other. A process that fuses two yeast cells and combines their DNA content. With this method the cDNA library is combined with the bait protein (1:1) avoiding numerous difficulties of a co-transformation.

3.4.1. Cryopreservation of yeast cells

For long-term storage and preservation yeast strains were frozen and stored at -80°C.

- Scoop one large healthy colony and dissolve completely in 500 µl freezing medium.
- Freeze immediately by placing vial in -80°C freezer.

Yeast freezing medium:	1x YPDA medium (Clontech)
	+ 25 % Glycerol

3.4.2. Thawing yeast cells

- Thaw cells quickly in 37°C water bath.
- Prepare adequate dropout agar plate by placing 100 µl ddH_2O on the agar.
- Transfer 0.2-0.5 µl thawed cells in the drop of water and spread on the plate with a sterile plastic rod.
- Incubate upside down at 30°C for 3 days.

3.4.3. Starter cultures

- Dissolve 1-3 large colonies in 3 ml 2x YPDA by vortexing rigorously.
- Incubate at 30°C and 260 rpm overnight.
- Pellet cells at 700 x g for 5 min.

3.4.4. Generating competent yeast cells

For the transformation of plasmids into the yeast cells the "Yeastmaker Yeast Transformation System 2" from Clontech was used. This transformation procedure starts with the highly efficient preparation of the yeast cells with a polyethylene glycol (PEG)/LiAc-based method. The manufacturer's protocol was slightly changed after experiencing various problems.

- Prepare a starter culture ideally inoculated with one colony. Incubate at 30°C and 260 rpm for 8-12 h.
- Pellet cells at 700 x g for 5 min. Resuspend in 50 ml 2x YPDA in a 500 ml flask and incubate shaking at 250 rpm until OD600 reaches 0.4-0.5 (2-4 h).
- Divide culture into two 50 ml sterile Falcon tubes and centrifuge at 700 x g for 5 min at RT.
- Discard supernatant and resuspend pellets in 30 ml sterile ddH_2O each. Centrifuge again.
- Discard supernatant and resuspend each pellet in 1.5 ml 1.1x TE/LiAc. Transfer suspension in two 1.5 ml micro centrifuge tubes and centrifuge for 15 sec at max. speed.
- Discard supernatant and resuspend each pellet in 600 µl 1.1x TE/LiAc. The cells are now ready to be transformed with plasmid DNA.

1.1x TE/LiAc:	1.1ml	10x Tris-EDTA
	1.1ml	1 M Lithium Acetate
	Ad 10ml	H_2O

3.4.5. Transformation of yeast cells

- Pre-chill respective number of 1.5 ml micro centrifuge tubes on ice.
- Dilute plasmid DNA to a concentration of 100 ng/µl and transfer 1 µl in the tube.
- Denature Yeastmaker Carrier DNA at 95°C for 5 min and cool rapidly in ice bath. Add 5 µl of carrier DNA in each tube.
- Now add 50 µl competent cells and mix gently.
- Add 500 µl PEG/LiAc and mix gently. Incubate at 30°C for 30 min. Mix cells every 10 min.

- Add 20 µl DMSO, mix gently and incubate tube in a 42°C water bath for 15 min. Mix cells every 5 min.
- Pellet cells by centrifugation at max speed for 15 sec and remove supernatant.
- Resuspend cells in 1 ml YPD Plus Medium and incubate with shaking for 30-60 min.
- Centrifuge again at max speed for 15 sec.
- Discard supernatant and resuspend cells in 1 ml ddH_2O or 0.5x YPDA.
  Vortex 30-60 sec.
- Dilute cells and spread 100 µl of each dilution on the respective selection agar plates. Use 1/10, 1/100 and 1/1000.
- Incubate upside down at 30°C for 3 days.
- Calculate transformation efficiency:

$$\text{Transformation efficiency} = \frac{\text{cfu}\times\text{suspension volume[ml]}}{\text{volume plated [ml]}\times\text{amount of DNA [}\mu g\text{]}}$$

PEG/LiAc:	8 ml	PEG 50%
	1 ml	10x Tris-EDTA
	1 ml	10x Lithium Acetate

3.4.6. Co-Transformation of yeast cells

A Co-Transformation was performed to confirm positive interactions found in the screen and to reveal false positive results.

For the co-transformation stick to the protocol above with the following changes:

- The amount of plasmid DNA required is 200 ng each.
- The dilutions for plating should include 1/1 and 1/10.
- Plate on DDO and QDO-X-A (Clontech)

3.4.7. Mating

This method is used for the actual screening process hence it is essential to perform control experiments to ensure that the technique is handled well and works perfectly. The Matchmaker^{TM}Kit from Clontech provides the adequate control plasmids as well as a small-scale protocol for the initial control experiment and a library scale protocol for the screen. The latter was also used for a control experiment before performing the real screen.

The positive control bait is the murine p53 fused to the Gal4 DNA binding domain. P53 is known to interact with the large T-antigen in the yeast-two-hybrid assay, which is here used as the prey protein, fused to the Gal4 activation domain assay (Li & Fields, 1993; Iwabuchi *et al.*, 1993). Transformed into the respective yeast strains Y2H Gold and Y187 a mating will

result in the activation of all four reporter genes. The negative control bait is lamin fused to the Gal4 DNA binding domain. Lamin does not interact with large T-antigen. Therefore a mating will not activate the reporter genes and the yeast will be unable to grow on the DDO-X-A agar. However both mated cultures will be able to grow on the single and DDO plates as they only select for the presence of the plasmids.

Small scale (control experiments):

- Transfer 500 µl 2x YPDA in two respective 1.5 ml micro centrifuge tubes.
- Inoculate one tube with 1 Y2H Gold colony containing the **positive control bait** (pGBKT7-p53).
- Inoculate the second tube with 1 Y2H Gold colony containing the **negative control bait** (pGBKT7-Lam).
- Now inoculate each tube with 1 Y187 colony containing the **control prey** (pGADT7-T).
- Vortex thoroughly and incubate shaking at 200 rpm and 30°C overnight (20-24 h).
- The next day spread the mated cultures as follows and incubate upside down at 30°C for 3 days:

Dilutions: Selection markers:	1/10	1/100	1/1000
-Trp			
-Leu			
DDO			
DDO-X-A			

Expected results after 3-5 days:

	Positive control plasmids			Negative control plasmids		
Dilutions: Selection markers:	1/10	1/100	1/1000	1/10	1/100	1/1000
-Trp	xxx	xx	x	xxx	xx	x
-Leu	xxx	xx	x	xxx	xx	x
DDO	xxx	xx	x	xxx	xx	x
DDO-X-A	xxx blue	xx blue	x blue			

Library scale (Screen):

- Prepare a concentrated overnight culture of the bait strain:
- Inoculate 1 fresh colony of the bait strain into 50 ml –Trp Medium (2x)
- Incubate shaking at 30°C and 260 rpm until OD_{600} reaches 0.8 (20-24 h)
- Pellet cells at 1000 x g for 5 min at RT and discard supernatant.
- Resuspend cells in –Trp Medium (2x) to a density of >$1x10^8$ cells/ml (4-5 ml).
- Combine the library strain with the bait strain:
- Thaw an aliquot of the library strain in a RT water bath and remove 10 µl for titering on –Leu Agar plates.
- Combine the library with the bait strain in a sterile 2 L flask.
- Add 45 ml of 2x YPDA. Rinse library vial twice with 2x YPDA and add to flask.
- Incubate at 30°C for 20-24 h, slowly shaking (30-50 rpm). Use the slowest shaking speed possible without allowing cells to settle at the base of the flask.
- Check for Zygotes:
- After 20 h check a drop of the mating culture under a phase contrast microscope.
- If no zygotes are present incubate for an additional 4 h.
- If zygotes are present pellet cells at 1000 x g for 10 min at RT in 50 ml falcon tubes.
- Meanwhile rinse the 2 L flask twice with 50 ml 0,5x YPDA, combine the rinses and use this to resuspend the cells.
- Centrifuge again at 1000 x g for 10 min at RT and discard supernatant.
- Resuspend the cells in 10 ml 0.5x YPDA and **measure the total volume** (e.g. in a 10ml pipette)
- Spread 100 µl of the mated culture in the following dilutions and on respective selection plates. This will allow to calculate the number of clones screened as the number of cfu on the different selection agars shows the efficiency of the mating procedure (SD vs. DDO) and the titering on the DDO agar tells the total number of mated clones in the screen when connected to the total volume of mated culture.

Dilutions: Selection marker:	1/10	1/100	1/1000	$1/1x10^4$	$1/1x10^5$	$1/1x10^6$	$1/1x10^7$	$1/1x10^8$
-Trp								
-Leu								
DDO								

Plating the Screen:

Plate the remainder of the mated culture on 150 mm DDO-X-A agar plates. Use 200 µl per plate. This will result in ca. 60 plates.

Incubate all plates upside down at 30°C for 3 days.

3.4.8. Library titering

The library titering is very important for the accurate calculation of all the parameters that provide information about the quality of the performed screen.

- Transfer the 10 µl aliquot from the freshly thawed library (see library scale mating protocol above) into 1 ml YPDA in a 1.5 ml micro centrifuge tube. Mix by gentle vortexing (dilution 1/100).
- Spread 100 µl of each dilution on –Leu Agar plates and incubate upside down at 30°C for 3 days:

Dilutions: Selection marker:	1/100	1/1000	$1/1x10^4$	$1/1x10^5$
-Leu				

- Calculate the titer as follows: $$\frac{\text{Number of colonies}}{\text{plating volume [ml]} \times \text{dilution factor}} = \text{cfu/ml}$$

Clontech, Matchmaker™ Gold Yeast Two-Hybrid System User Manual:

"If your titer is $2x10^7$ cells/ml, you will obtain 200 colonies on the 1/1x10.000 dilution plate."

"Due to slight variability in pipettes and pipetting techniques, a 2-5-fold range in titer calculation is not unusual."

3.4.9. Calculate mating efficiency

A successful screen should include at least 1 million diploids. Therefore, reaching a mating efficiency of 2 % is essential.

- Check the viabilities:
  No. of cfu/ml on –Leu agar plates = viability of prey library
  No. of cfu/ml on –Trp agar plates = viability of bait
  No. of cfu/ml on DDO = viability of diploids

- Calculate efficiency: $$\frac{\text{No. of cfu/ml of diploids} \times 100}{\text{No. of cfu/ml of limiting partner}} = \%\ \text{diploids}$$

- Limiting partner: Either bait or prey strain that has the lower viability.

3.4.10. Calculate the number of screened clones

By counting the colonies on the DDO plates the number of cDNA clones that were actually screened can be determined. It is essential that a certain number of clones is screened to ensure statistically that every clone from the library was present in the experiment.

cfu/ml of diploids × resuspension volume = No. of screened clones

3.5. Analysis of the Screen

3.5.1. Segregation of clones

Blue colonies were picked from the 15 mm DDO-X-A plates and streaked onto QDO-X-A agar, together with positive and negative control diploids on each plate. After an incubation at 30°C for 5 days the clones were further analysed.

3.5.2. Colony PCR

The first step of analysis was a colony PCR with primers that bind in the prey plasmid (pGADT7) and amplify the insert. This technique shows if more than one prey plasmid is in the respective clone and what size the insert has. Therefore the “Matchmaker Insert Check PCR Mix 2” was used, followed by analysis of the PCR products on 1% Agarose/Midori Green gels.

In some cases a digest with AluI or HaeIII of PCR products that show the same size was performed to recognize identical inserts. Again followed by analysis of the digestion products on 1% Agarose/Midori Green gels.

The majority of the PCR products was column purified with the PCR Purification-Kit from Qiagen and sequenced with the T7 primer.

3.5.3. Plasmid DNA Isolation from yeast cells

To enable an analysis and/or identification of a specific prey plasmid, the plasmid has to be rescued from the yeast clone and amplified in bacteria. The isolation of plasmids from yeast cells is highly dependent on the efficient disruption of the yeast cell walls. In the “Easy yeast Plasmid Isolation Kit” from Clontech a lytic enzyme called Zymolyase is utilized for this procedure followed by alkaline lysis of the resulting spheroblasts.

- Use a sterile pipette tip to scrape colonies of the plate and weigh them on the special accuracy scales. Do not use more than 10mg. Resuspend cells in 500 µl 10 mM EDTA.
- Centrifuge at 11.000 x g for 1 min. Discard supernatant.

- Resuspend pellet in 200 µl ZYM Buffer, vortex.
- Add 20 µl Zymolyase suspension and vortex gently.
- Incubate with gentle shaking at 30°C for 1 h (place tubes in 250 ml flask).
- Pellet spheroblasts at 2000 x g for 10 min. Discard supernatant.
- Resuspend in 250 µl Y1 Buffer/RNase A.
- Add 250 µl Y2 Lysis Buffer and mix gently by inverting the tube 6-8 times. Incubate at RT for a maximum of 5 min.
- Add 300 µl of Y3 Neutralization Buffer. Mix gently by inverting the tube 6-8 times.
- Clarify the lysate by centrifuging at 11.000 x g for 5 min at RT. Transfer the supernatant to clean microfuge tube and repeat centrifugation.
- Load supernatant onto Yeast Plasmid Spin Column ant centrifuge at 11.000 x g for 1 min. Discard flow through.
- Add 450 µl of Y4 Wash Buffer and centrifuge at 11.000 x g for 3 min. Discard flow through and repeat centrifugation.
- Place column in a 1.5 ml microfuge tube and add 50 µl YE Elution Buffer. Incubate at RT for 1 min then centrifuge at 11.000xg for 1 min.

3.5.4. DNA Amplification

To amplify the plasmids rescued from the yeast clones, the eluted DNA was transformed into MaxEfficiency DH5alpha and plated on LBampicillin plates. By using Ampicillin as selection marker only cells containing the library plasmid were propagated as the bait plasmid carries the Kanamycin resistance. With the mini prep Kit (e.z.n.a.) the amplified DNA was extracted and the concentration of the elution was measured using a Nanodrop1000.

3.5.5. Sequencing / BLAST

Clones that showed no autoactivation in the retransformation experiment were sequenced with the appropriate sequencing primers by StarSeq (Mainz). The obtained nucleotide sequences were then analyzed in the NCBI database BLAST.

4. Results

4.1. Expression and Purification of the Recombinant Progranulin Protein

Not much known is known about the physiological functions of GRN, and even less about potential pathological mechanisms. Various studies have demonstrated GRN to influence cells with respect to survival (Ryan et al., 2009; Van Damme et al., 2008; Van Kampen et al., 2014), proliferation (He and Bateman, 1999; Monami et al., 2009), cytokine production (Yin et al., 2010a), and motility (Cheung et al., 2004; He et al., 2002; He et al., 2003; Kong et al., 2007). Unfortunately, these studies did not reveal much about GRN functions in the central nervous system. To confirm previous reports about biological activities of GRN and to discover novel physiological functions, our first goal was to establish a protocol for the expression and purification of biologically active human GRN protein.

GRN is a secreted and highly glycosylated protein (Songsrirote et al., 2010) and therefore, a mammalian cell line was chosen for the expression. This ensures proper glycosylation, which would not be present in a bacterial expression system. The secretion of the GRN protein should allow the purification from conditioned medium. The recombinant GRN was translated from the human full-length GRN cDNA with C-terminally attached GB1 tag, V5 tag and 6xHis tag inserted into a pCDNA3 expression plasmid. This construct was transiently transfected into COS1 cells, and after confirmation of proper expression and secretion of the recombinant GRN, the protein was purified from cell culture supernatants (Figure 4.1).

COS1 cells originated from a monkey kidney cell line (CV-1; african green monkey) and were immortalized by the introduction of the defective SV40 virus producing the large T-antigen. This enables the cells to replicate plasmids containing an SV40 origin of replication rapidly to high copy numbers, resulting in high-level expression of the encoded protein (Hancock, 1992). The B1 domain of streptococcal protein G (GB1) has two important features making this tag very popular for protein expression and purification. First, protein G is one of several immunoglobulin-binding bacterial proteins (e.g. protein A, protein L) that are commonly used for detection or purification of immunoglobulins (Ig). Each of these proteins has a specific profile of antibody parts and types that are recognized. The recombinant GB1 tag only presents the IgG-binding domain of protein G (Sjobring et al., 1991). Second, fusing the GB1 domain to a protein improves the solubility of the target protein keeping it in solution during purification and experimental procedures (Cheng and Patel, 2004). Consequently, despite of its rather big size of 56 amino acid residues, the GB1 tag is widely used for protein purification as it allows simple and efficient protein purification via the IgG affinity and the additional benefit of keeping proteins in solution (Gronenborn et al., 1991; Sommer et al.,

2012; Tapaneeyakorn et al., 2010). The immune precipitation (IP) of GRN-His-V5-GB1 was first tested with conditioned supernatants from transiently transfected COS1 cells (Figure 4.1 A, B). The secreted recombinant protein was collected in complete medium with 10% FCS for two days. The harvested supernatants were cleared from cell debris and incubated overnight with IgG coupled beads at 4°C on an overhead shaker. Washes and elution were done with low speed centrifugation and resuspension cycles, using TBSE to wash the beads and glycine to elute GRN protein. Resolving the binding between tag and IgG with low pH did not disturb the binding of the antibody to the beads, therefore no IgG was found in the eluted GRN protein fraction. Subsequently, pH was neutralized with Tris buffer. Samples were subjected to SDS gel electrophoresis and stained with Coomassie blue (Figure 4.1 B).

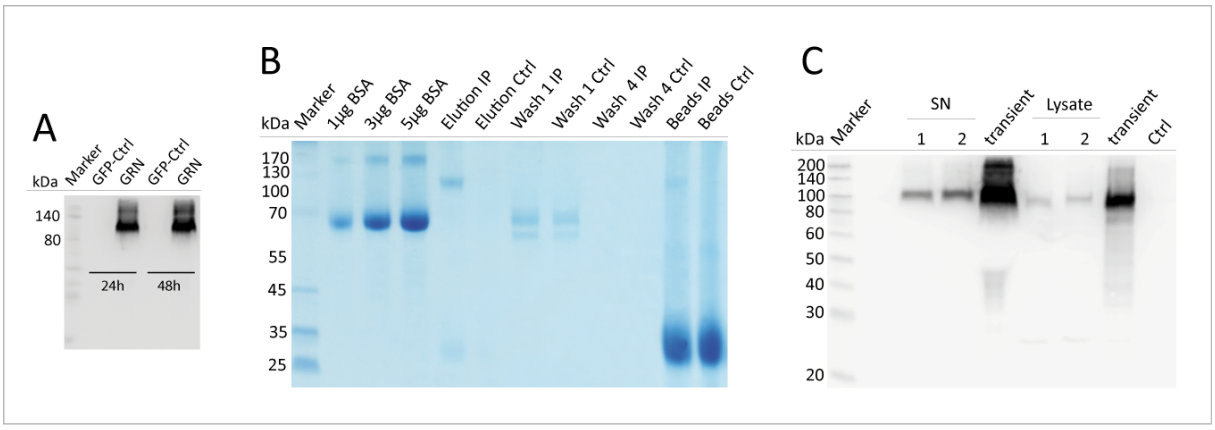

Figure 4.1: A) Transient transfection of COS1 cells with pCDNA3-GRN-His-V5-GB1. Supernatants (SN) were collected after 24 and 48 hours and analyzed by Western blotting. The membrane was probed with anti-PCDGF antibody (human-specific, polyclonal anti-GRN antibody, Zymed) and signals recorded with a CCD camera (Fuji). No signal was detected for the pLPCX-GFP transfected controls, while supernatants from GRN-GB1 transfected cells generated strong bands, with supernatant collected after 48hours generating a slightly more intense signal. **B) Test IP of GRN-His-V5-GB1 with supernatants from transient transfection.** GRN was precipitated from COS1 supernatants, using IgG coupled beads. The protein was eluted with glycine and the pH was neutralized with Tris buffer. The Coomassie staining detected a clearly visible GRN signal in the elution fraction with minor impurities at 30kDa. The control IP was performed with COS1-pLPCX-GFP supernatant. **C) Stable COS1-His-V5-GRN cell line.** COS1 cells were transfected with the pCDNA3-GRN-His-V5-GB1 plasmid and selected with Neomycin (600µg/ml). Expression in cell lysates and secreted levels of the recombinant protein from two separate mass cultures were analyzed via Western blotting. The membrane was probed with anti-PCDGF antibody (Zymed) and signals recorded with a CCD camera (Fuji). Both mass cultures show expression and efficient secretion of the recombinant GRN. No GRN is detectable in the non-transfected control.

In the first three lanes, one, three, and five microgram BSA were loaded as quantity controls. Only the first wash fraction (Wash 1) showed unspecific bands, and the last wash (Wash 4) contained no detectable protein anymore. The boiled beads were loaded as well (Beads) and showed unspecific bands at a small size (ca. 30kD). A difference between IP and control IP was detectable in the elution, where a distinct band at the expected size of approximately 100kDa appeared in the IP elution (IP) and no signal was visible in the elution of the control

IP (Ctrl IP). The control IP was performed with supernatant from pLPCX-GFP control transfected COS1 cells (Figure 4.1 A).

Based on these results, a stably expressing COS1 cell line was selected to allow the production of larger volumes of supernatant containing the secreted GRN protein. Different mass cultures were analyzed by Western blotting and compared to the transient transfection (Figure 4.1 C). Although both mass cultures showed less expression than the transiently transfected cells, the amount of protein secreted by this cell line was deemed sufficient to pursue GRN purification. 50ml of conditioned supernatant were collected from the stable cell line, centrifuged and incubated with 0,5ml IgG Sepharose at 4°C overnight on an overhead shaker. The following day, the IP was centrifuged at low speed and the supernatant was discarded. TBSE was used as washing buffer and the GRN protein elution was done with glycine. The pictures shown in Figure 4.2 are representative of six independent purifications.

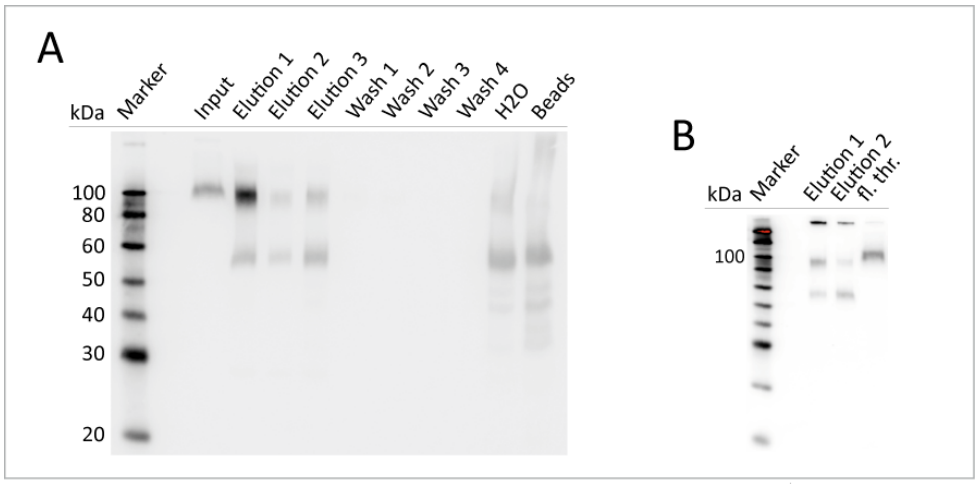

Figure 4.2: A) GRN-His-V5-GB1 purification from stable COS-1 cells and 50ml of cell culture supernatant. The conditioned complete medium was incubated with a batch of 0.5ml IgG Sepharose (GE Healthcare) overnight. The Western blot analysis of the purification showed GRN in the input and elution fractions, but also an additional band at approximately 55kDa. **B) Subsequent analysis of flow through.** Compared to elution 1 and 2, the amount of GRN detected in the flow through was markedly higher than in the elution fractions showing the inefficiency of this purification protocol. Both membranes were probed with the anti-PCDGF antibody (Zymed) and signals recorded with a CCD camera (Fuji). This experiment is representative of six independent purifications. Fl.thr., flow through.

Analysis of the elution fractions by Western blotting detected a small amount of purified GRN that was contaminated with a non-specific protein of approximately 55 kDa. No protein was detectable in the wash fractions, neither with the anti-PCDGF antibody, nor with Coomassie blue staining (data not shown). Furthermore, the purified GRN seen by Western blotting was also not detectable with Coomassie blue staining, indicating low protein levels (data not shown). This poor purification efficiency made it necessary to change the GRN purification strategy. As the purification of GRN was better with the highly expressing transiently transfected COS1 cells (Figure 4.1), Hek293T cells were transfected with the pCDNA3-GRN-

His-V5-GB1 construct to generate an alternative stably expressing cell line. As Hek293T cells are resistant to the antibiotic G418 due to the introduction of the large T-antigen with a neomycin-geneticin resistance gene, these cells had to be co-transfected with an empty pLHCX plasmid to facilitate the selection with hygromycin.

The Hek293T cell line is a derivative of the human embryonic kidney cell line (HEK293) expressing the large T antigen from a defective SV40 virus. This epithelial cell line is highly transfectable and able to replicate plasmids with SV40 origin of replication to high copy numbers (Hancock, 1992). The large T antigen can also bind to SV40 enhancers of expression vectors to markedly increase protein expression (Hancock, 1992). Because of these properties, Hek293T cells are widely used in industry for the production of therapeutic proteins or viruses used for gene therapy.

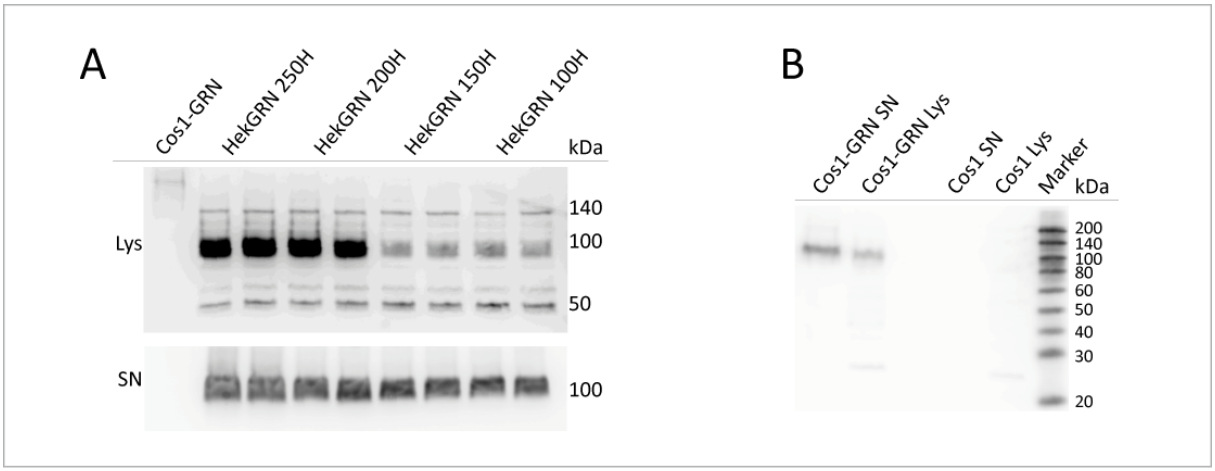

Figure 4.3: A) GRN-His-V5-GB1 overexpressing Hek293T cells. The pCDNA3-GRN-His-V5-GB1 construct was transfected into Hek293T cells together with pLHCX plasmid and stable mass culture were selected with hygromycin. The Hek293T cells showed considerably stronger expression than the previously generated COS1-GRN cells (A). The samples were probed with anti-V5 antibody (Invitrogen) and the signals were recorded with a CCD camera (Fuji). Lys, lysate; SN, supernatant; H, Hygromycin; 250H, 250µg/mL Hygromycin. **B) GRN-His-V5-GB1 expressing COS1 cell lines.** Supernatants and lysates were analyzed by Western blotting with the anti-PCDGF antibody (Zymed), and signals were recorded with a CCD camera (Fuji). The stable COS-1 GRN-His-V5-GB1 cell line showed a GRN signal in lysate and supernatant while no signal was detected in the samples from the non-transfected control.

Western blot analysis of lysates and supernatants of several Hek293T cell lines selected with increasing concentrations of hygromycin (100-250 ug/ml) revealed high overexpression of GRN. Probed with anti-V5 antibody, all new cell lines showed markedly stronger expression of the recombinant GRN compared to the previously used COS1-GRN cell line, which did not generate a signal with the time of development that was used for the Hek293T cell lines (Figure 4.3 A). To confirm expression in the COS1-GRN cell line, lysate and supernatant were again loaded on a different gel and compared to the non-transfected COS1 cells

(Figure 4.3 B). In these experiments, the expression of recombinant GRN in the selected COS1 cell line was observed (see also Figure 4.1 C).

Since HEK cells can be cultured under serum free conditions, the new Hek293T-GRN cell line was used in serum-free medium to avoid BSA that might contaminate purifications. In addition, it was decided not only to use a new cell line but also to try a different purification method, which was successfully used by previous authors (Gass et al., 2012a; He et al., 2003; Monami et al., 2006). In Figure 4.4, test purifications are shown. NiNtA (Qiagen) was used to capture the His-tag in the recombinant GRN protein. The recombinant GRN protein was harvested in serum-free medium, therefore no harsh washing condition was needed to get rid of non-specifically bound proteins. 50mM Tris, pH8 was used as a washing buffer and different imidazole concentrations were used for the elution of GRN. Subjected to Western blot analysis, the wash fractions showed no signal, in stark contrast to the signals in the elution fractions that increased with increasing imidazole concentration. In the input lane a strong signal for GRN was visible, while there was no detectable GRN in the flow through (Figure 4.4 A).

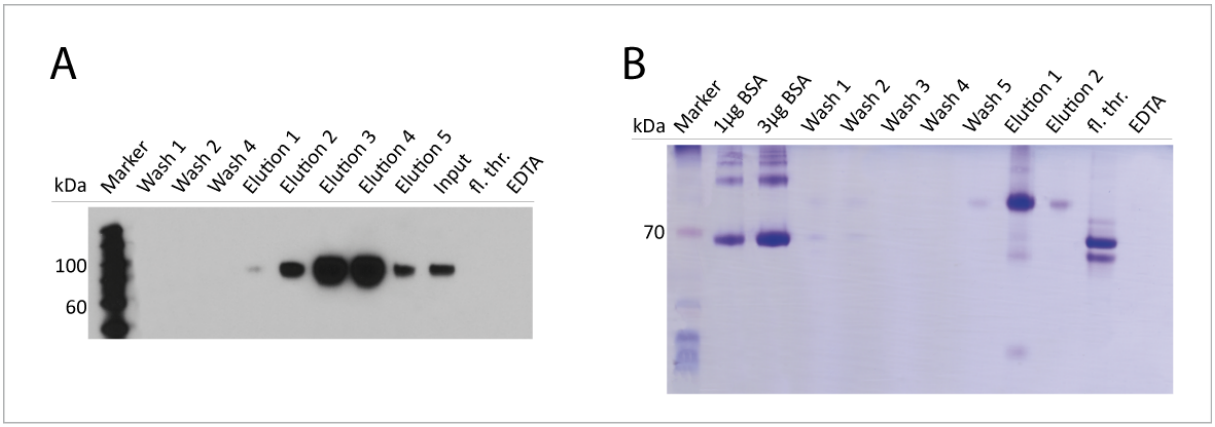

Figure 4.4: A) GRN test purification using His-tag and NiNtA, from supernatants of Hek293T-GRN-His-V5-GB1 **cells cultured under serum-free conditions.** Supernatant was harvested from the Hek293T cell line, which had been co-transfected with pCDNA3-GRN-His-V5-GB1 and pLHCX and stably selected with hygromycin. NiNtA was used for capturing the protein and different imidazole concentrations were applied for elution. Washing buffer was 50mM Tris, pH8. Samples were analyzed by Western blotting with the anti-V5 antibody (Invitrogen) and chemiluminescence was detected on film. Even after long exposure no signal appeared in the flow through lane. Elution 1-5: 50/100/150/200/250mM imidazole. EDTA was used to strip the beads after elution. **B) Larger scale His-tag purification of GRN from Hek293T-GRN**-His-V5-GB1 **supernatants.** GRN was purified from 50ml conditioned, serum-free medium. The medium was incubated with a batch of NiNtA. Elution buffer contained 250mM imidazole. All fractions were collected, loaded on a SDS-gel and stained with Coomassie blue. Washes 1-4 were done with 50mM Tris, wash 5 also contained 10mM imidazole. Fl.thr., Flow through.

However, although the test purification produced decent signals in the Western blot analysis, Coomassie staining detected no protein in these samples. To increase the quantity of recombinant protein in the elution fraction, the total volume of supernatant was increased,

which led to an elution signal that was detectable on a Coomassie stained gel (Figure 4.4 B). For this purification, 50ml of serum-free conditioned media were incubated with 200µl NiNtA material, which was then centrifuged at low speed and washed, first with 50mM Tris followed by a wash with 10mM imidazole in 50mM Tris. The elution buffer was 50mM Tris containing 250mM imidazole. On the Coomassie stained gel additional signals in the elution fraction were detected, either degradation products or contaminants. However, a strong signal was detected for the purified GRN protein. Subsequently, batches of purified GRN were dialyzed against PBS overnight, using a Slide-A-Lyzer™ dialysis cassette (Thermo Scientific™) with a 10kDa cut off to ensure efficient removal of imidazole while retaining recombinant GRN with its approximate molecular weight of 100kDa.

Small additional changes were made for subsequent purifications. As observed in the experiment shown in Figure 4.4 B, even 10mM imidazole in the last wash step was sufficient to elute GRN from the column. Therefore, imidazole was eliminated from the washing buffers and instead the total volume of the wash was increased. To increase the total amount of purified GRN, a larger volume of conditioned supernatant from Hek293T-GRN cells was applied onto a NiNtA column by a peristaltic pump drive (Heidolph). With this device, it was possible to apply medium onto the connected column at very low speed, which significantly increased binding of GRN to the column material. First, the column was washed with water, then loaded with $NiSO_4$, and afterwards equilibrated with washing buffer (50mM Tris, pH8). Finally, the conditioned serum-free medium was loaded at very low speed (100 mL in 24 hours) (Figure 4.1.5). The column was then washed with 12ml washing buffer before eluting with 250mM imidazole in 50mM Tris buffer (4ml). Fractions were then loaded on a SDS gel and stained with Coomassie blue. The result showed that almost the complete background was removed during the washing step, and in the elution fraction a signal for the full-length recombinant GRN protein with minor contaminants was visible.

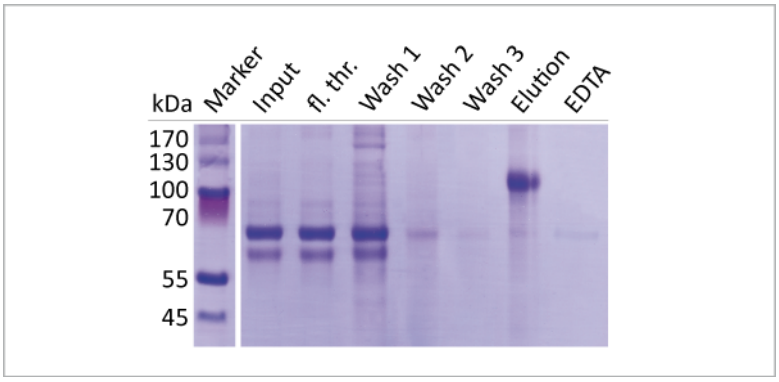

Figure 4.5: His-tag purification of GRN with peristaltic pump drive. 100ml of conditioned, serum-free medium were applied on a NiNtA column over 24 hours. The different fractions of the purification were subjected to SDS gel electrophoresis and stained with Coomassie blue. In the elution fraction a signal for the full-length GRN wss detected. The purity of the eluted recombinant GRN was about 95%. Fl.thr., flow through.

Hence, the purification using the peristaltic pump drive resulted in a sample of GRN protein of high purity (>95%) and sufficient protein concentration. As this method did not require permanent care, the handling of larger volumes was easily possible. Therefore, the total volume of applied supernatant was increased to over 200ml resulting in estimated 190µg GRN at a concentration of 1,85mg/ml (28µM) without visible contaminants.

Comparing different GRN supernatants the observation was made that GRN produced under serum-free conditions (sf) resulted in a slightly smaller size of the protein, than GRN expressed in complete medium (c). The size shift was not identical for all samples.

The size shift was not identical for all samples. But even though some displayed only a minor difference in size, others showed a pronounced shift, and the difference between expression in serum-free or complete medium was detectable in all samples (Figure 4.6 A). The most abundant posttranslational protein modification is glycosylation. As described in the introduction, GRN is known to be a highly glycosylated protein (Songsrirote et al., 2010). Its multiple N-glycosylations are important for the secretion and probably also for other functions (Jia, 2009). To test the possibility of an altered glycosylation due to serum deprivation, supernatants and purified GRN were subjected to a de-glycosylation experiment. Removing all glycosylation from the proteins should lead to an identical size of GRN, in contrast to the untreated samples. Shown in Figure 6 are the Western blots of the GRN samples and the de-glycosylation experiment.

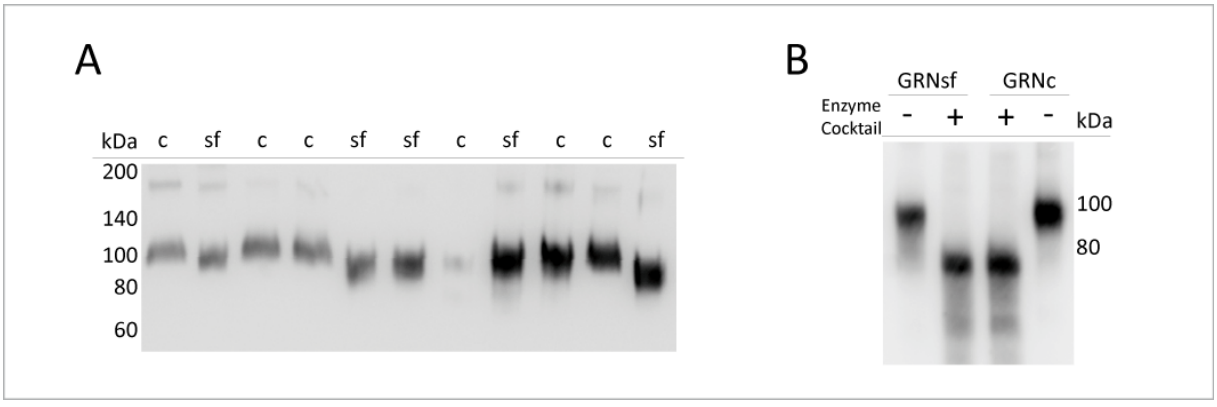

Figure 4.6: A) Western blot analysis of different GRN samples. 11 different GRN samples were subjected to Western blotting. The membrane was probed with anti-PCDGF antibody (Zymed) and signals were recorded with a CCD camera (Fuji). The blot shows a consistent difference in size between GRN expressed in serum-free medium (sf) and GRN expressed in complete medium (c). **B) GRN deglycosylation.** Two batches of purified GRN were subjected to deglycosylation under denaturing conditions following the manufacturer's instructions (NEB). Samples were analyzed via Western blotting and the membrane was probed with anti-PCDGF antibody (Zymed). Signals were recorded with a CCD camera (Fuji). The untreated samples (-) run at a significantly higher size than the deglycosylated samples (+).

The size shift between GRN purified from serum-free medium and GRN purified from complete medium is not very pronounced on the blot shown in Figure 4.6 B. However, this

effect had been observed with great consistency before (Figure 4.6 A). As expected, the samples treated with the de-glycosylation enzyme cocktail ran at a smaller size than the untreated control samples. However, only treatment under denaturing conditions resulted in the same running size of the two samples (Figure 4.6 B). It is possible that sugars are masked under non-denaturing conditions by the secondary protein structure of GRN due to its high content of cysteine, and therefore cannot be removed. These results supported the hypothesis of an altered GRN protein glycosylation depending on the availability of FCS. Based on these experiments, it was concluded that GRN should be purified from complete medium, as only incubating the overexpressing cells in medium containing FCS allowed more complex glycosylation that could be essential for the full bioactivity of GRN.

Considering the initial GRN purification results, serum-free medium appeared superior in obtaining highly purified GRN and switching to complete medium might lead to considerable impurities in the elution. Using NiNtA slurry instead of pre-packed columns and allowing the protein of interest to bind in batch mode to the chromatography material for an increased time period is not only a widely recommended method for secreted proteins, but could also reduce the amount of non-specifically captured serum proteins to a minimum. Therefore, GRN was purified by directly comparing purification with and without serum, and purification using the peristaltic pump drive (NiNtA column) or the batch method.

Table 4.1: Comparison of GRN purification strategies. The purification of GRN using these three protocols in parallel allowed a comparison of the influence of FCS and the applied purification method. 200ml of conditioned medium and 1mL NiNtA were used on all three protocols and purified GRN was dialyzed against PBS using a 10kDa cut-off membrane (Thermo Scientific). PPD, peristaltic pump drive.

complete	serum-free	complete	200ml
PPD	PPD	batch	NiNtA
Dialysis	Dialysis	Dialysis	PBS, 10kDa MWCO
Elution 1	**Elution 2**	**Elution 3**	

Analyzed by Coomassie blue staining the three protocols (Table 4.1) led to three different results (Figure 4.7). Purifying conditioned complete medium with the peristaltic pump drive and a NiNtA column resulted in purified GRN with substantial non-specific background signals. Also, overall binding of GRN to the column was rather low. Hence, purification with the peristaltic pump drive was not suitable for complete medium (Figure 4.7 A). Using serum free medium in the purification worked well with the peristaltic pump drive, as described before. Coomassie staining showed a higher amount of purified full-length GRN compared to purification from complete medium and the impurities in the elution fraction were markedly

lower (Figure 4.7 B). For the third purification, a volume of 1ml NiNtA was added to 200 mL conditioned supernatant containing FCS and incubated overnight at 4°C on an overhead shaker. The medium was then centrifuged at low speed, the supernatant discarded and the purified protein eluted after washing the NiNtA slurry with 50mM Tris buffer. Subsequent analysis by Coomassie staining detected even more full-length GRN protein and less non-specific background signal compared to the purification from serum free medium (Figure 4.7 C). Consequently, the batch purification method of GRN from complete medium was used for further experiments.

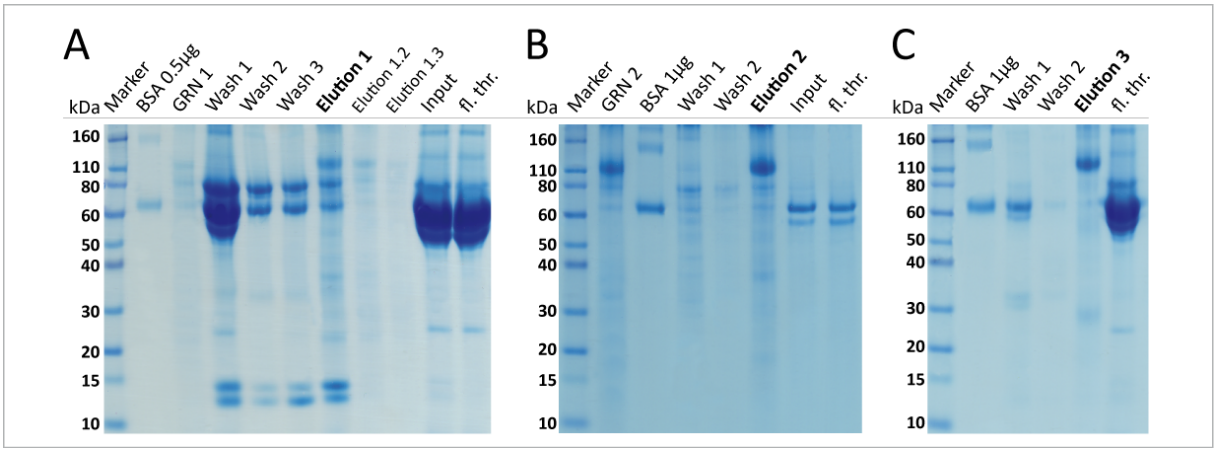

Figure 4.7: Direct comparison of three different GRN purification protocols. Coomassie staining for the different purification protocols. 200 mL conditioned medium were used for each experiment, washes were done with 50mM Tris buffer, and elution with 250mM imidazole in 50mM Tris. Elution fractions were dialyzed and are labeled GRN1 and GRN2. **A) Coomassie staining of peristaltic pump drive purification from complete medium.** The elution contained several unspecific protein bands, each of them as strong as the band corresponding to the purified full-length GRN. **B) Coomassie staining of peristaltic pump drive purification from serum-free medium.** The elution contained minor impurities and a strong band for purified full-length GRN. **C) Coomasie staining of batch purification from complete medium.** The elution from the NiNtA batch has less background than the elution from serum-free medium shown in B and also a strong GRN signal.

However, the problem of weak affinity between the recombinant GRN and the NiNtA material, as observed during the optimization process (Figure 4.4 B), still remained leading to loss of protein during the washing steps. To improve the strength of binding, a new GRN construct was designed, fusing a 12x His tag with a TEV (Tobacco etch virus protease) cleavage site to the C-terminus of human GRN, thereby decreasing the size of the tag from 250bp to 57bp. This was assumed to increase the binding of GRN to the NiNtA material by increasing the number of histidine residues. In addition, the inserted cleavage site would allow removal of the His tag after purification. As a vector backbone the retroviral pLHCX plasmid was used to allow the production of retroviruses for infection of cells instead of transfection. Retroviral particles were generated as described in 3.1.5 and used to infect Hek293T cells. Subsequently, new stable cell lines were selected with 150, 200 and

250µg/ml hygromycin respectively. Lysates and supernatants were analyzed for GRN expression and secretion (Figure 4.8 A).

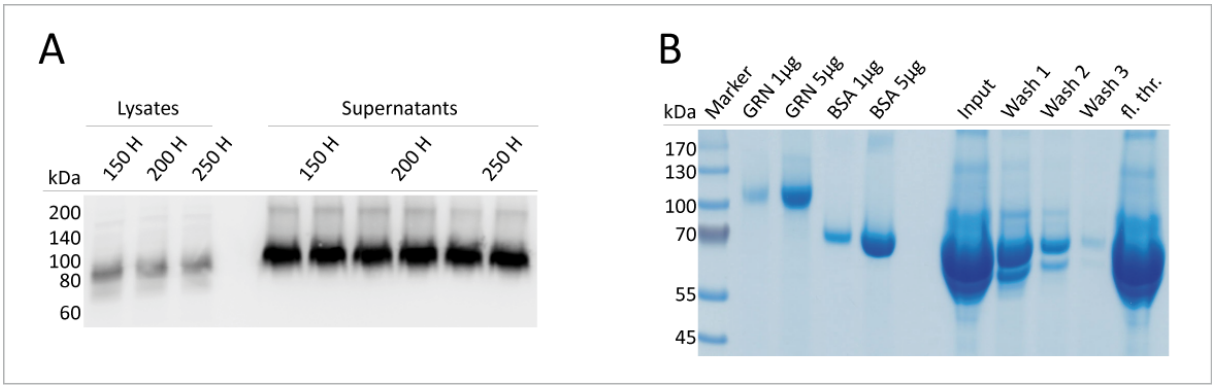

Figure 4.8: A) GRN-12xHis overexpressing cell lines. Hek293T cells were infected with a retroviral vector encoding the GRN-12xHis protein. Mass cultures were selected with three increasing hygromycin concentrations. Western blot analysis showed expression and efficient secretion of the recombinant protein. Blots were probed with the anti-PCDGF antibody (Zymed) and signals were recorded with a CCD camera (Fuji). H, Hygromycin. **B) Purification of GRN-12xHis.** 200 mL conditioned serum-containing medium were used to purify GRN-12xHis using 1ml NiNtA in batch mode. GRN was eluted with 500 mM imidazole in 50 mM Tris buffer, washes were performed without imidazole. The eluted GRN was dialyzed against PBS and protein concentrations were determined with the DC protein detection Kit (BioRad). Comparing the band intensities of GRN to the BSA controls confirmed the results of the protein detection assay. GRN, dialyzed elution; fl.thr., flow through.

The Hek293T-GRN-12xHis cell lines showed good expression and efficient secretion of the recombinant GRN protein from the new expression construct with no obvious differences between cell lines selected with different stringencies. Therefore, the mass culture selected with the lowest hygromycin concentration was chosen for further protein expression and purification (Figure 4.8 A). Supernatants were harvested from the Hek293T-GRN-12xHis cell line and purified in batch mode as described above. SDS-gel analysis and Coomassie blue staining showed that the purification of GRN-12xHis was very efficient, resulting in high concentrations of GRN without any visible impurities (Figure 4.8 B). This optimized protocol to purify the GRN-12xHis protein yielded final protein concentrations between 2 and 3,5mg/ml. Calculated molarities were in a range of 25 to 40µM.

In summary, through testing different cell lines and culture conditions, purification modes and materials, the production of GRN could be markedly improved resulting in highly pure and concentrated recombinant protein. Key steps in the optimization were the generation of HEK293T cells with high and stable expression of His-tagged GRN, the use of cell culture medium containing 10% FCS, the use of NiNtA instead of IgG as a purification material, and the purification in batch mode instead of a purification column.

4.2. Progranulin Bioactivity Assays

Artificial overexpression, the addition of tags, and harsh purification methods can affect the biological activity of recombinant proteins. Therefore, the next goal was to confirm the bioactivity of the purified GRN protein in previously published GRN bioactivity assays. For these experiments, the SW13 cell line was chosen, which originated from human adrenal gland cancer cells and which has previously been shown to respond with increased proliferation to treatment with recombinant GRN (He and Bateman, 1999). The cells were seeded in 12-well plates at a density of $5x10^5$ cells/well in 500µl complete medium containing 10% FCS. The day following the seeding procedure, the medium was changed to serum-free DMEM to starve the cells for 24 hours. On the third day, cells were washed with PBS and then treated with purified GRN in serum-free medium, followed by incubation for five days. Afterwards, cells were trypsinized and counted in a cell counter (Vi-Cell) (He and Bateman, 1999). The purity and the concentration of the applied GRN protein were confirmed via SDS-gel and Coomassie staining (Figure 4.9 A). Three independent assays were performed, including a BSA control treatment to confirm the specificity of any potential effect. However, no increase in cell proliferation could be detected (Figure 4.9 B).

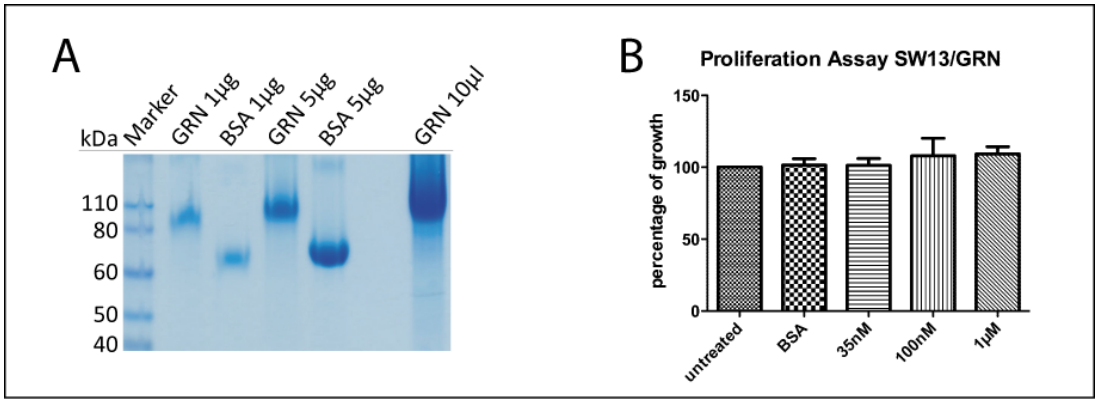

Figure 4.9: A) Purified recombinant GRN protein. Using the optimized purification protocol, recombinant GRN was purified from 200ml conditioned complete medium. Protein concentrations were determined with the DC protein assay (BioRad) and samples were subjected to SDS gel electrophoresis and stained with Coomassie Blue. This batch of GRN protein had a concentration of 2,3mg/ml and showed a high grade of purity. Protein concentrations were confirmed through comparison with BSA quantity controls. **B) SW13 proliferation assay.** SW13 cells were seeded at a density of $5x10^5$cells in 12-well plates and treated with 35nM, 100nM or 1µM purified GRN in serum-free medium. After incubation for 5 days, cells were trypsinized and counted with an automated cell counter (Vi-Cell, Beckmann-Coulter). Cell numbers were normalized to the untreated control condition, which was set to 100%, and expressed as percentage of growth. Three independent biological experiments were performed (n=3), with three technical replicates per condition. The data was analyzed by one-way ANOVA with Bonferroni post tests. The GRN treatment had no significant effect on the growth of the cells ($p<0,05$).

SW13 cells have been shown to respond to GRN treatment (He and Bateman, 1999), and the purification via C-terminal His-tag using NiNtA has been previously used to generate bioactive GRN protein (Gao et al., 2010; Monami et al., 2006). Therefore, a different GRN bioactivity assay was investigated. Stimulating SW13 cells with recombinant GRN protein models the paracrine influence of extracellular GRN on neighboring cells and tissues However, GRN has also been proposed to support cells, in particular neurons, in an autocrine fashion. This could be mimicked in a survival assay, in which the proliferation of cells overexpressing GRN is compared to the proliferation of cells that do not overexpress the protein (He et al., 2002). We used Hek293T cells with stable expression of GRN-12xHis compared to the parental Hek293T cells. The two cell lines were seeded at identical cell numbers, and the increase of cell numbers over time was monitored, either growing under serum-free conditions or in serum-containing medium.

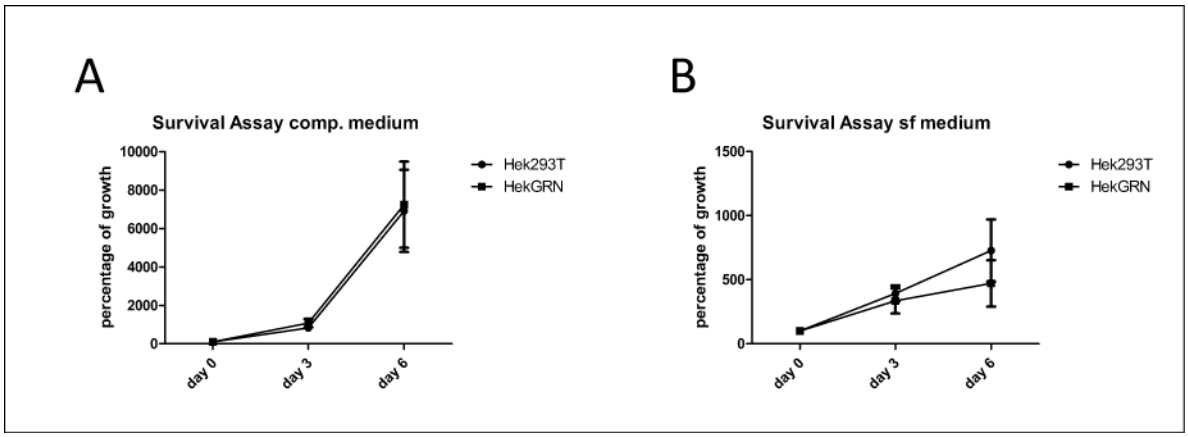

Figure 4.10: Survival assay with GRN expressing cells. The GRN-12xHis overexpressing Hek293T cell line (HekGRN) and the parental Hek293T cell line were seeded at a density of $1x10^5$ cells/well in poly-L-lysin coated 6-well plates. The following morning, medium was changed to complete (A) or serum-free (B) medium for each cell line. One well each was trypsinized and counted on day 0, day 3, and day 6. Cell numbers were normalized to the numbers at day 0, which were set to 100%, and expressed as percentage of growth. No significant differences in proliferation were observed between the GRN overexpressing and the parental Hek293T cells (n=3).

Similar to the treatment of SW13 cells with recombinant GRN as shown in Figure 4.9, no significant influence of GRN overexpression on the proliferation rate of Hek293T cells could be observed. The experimental conditions with complete medium resulted in nearly identical cell numbers for both cell lines (Figure 4.10 A). Under serum-free conditions, overall cell numbers were much lower with a tendency for reduced growth by the GRN-overexpressing cells. However, changes were also not significant (Figure 4.10 B).

GRN has also been suspected to play a key role in the protection of neurons against oxidative stress and in the generation of ROS by neutrophils (Xu et al., 2011) (Kessenbrock et al., 2008). Oxidative stress is a condition that might promote various neurodegenerative diseases including FTD (Bishop et al., 2010; Gerst et al., 1999; Martin et al., 2001).

Furthermore, changes in the oxidation of proteins, DNA, and other cell components have been shown to be associated with aging (Lopez-Otin et al., 2013). Levels of the small-molecule antioxidant glutathione (GSH) have been shown to be decreased repeatedly in tissues of aged humans or animals (Liu et al., 2004; Sekhar et al., 2011; Zhu et al., 2006). GSH is an important antioxidant consisting of the three amino acids glutamate, glycine, and cysteine. The reduced state of the molecule (GSH) is able to donate a reducing equivalent to reactive oxygen species (ROS). Thereby, the molecule itself becomes reactive and forms the dimeric glutathione disulfide (GSSG) with another reactive GSH monomer. The enzyme glutathione reductase (GSR) can regenerate GSH or the dimer is exported from the cell by multi-drug resistance proteins (Minich et al., 2006; Noble et al., 2005). GSH is synthesized in all mammalian tissues (Kaplowitz et al., 1985) and 90% of the cellular GSH is located in the cytosol (Hwang et al., 1992; Meredith and Reed, 1982). An important function of GSH is the storage of cysteine, an essential amino acid for protein synthesis, which is otherwise unstable and auto-oxidizes to cystine. One key factor that determines the cellular level of cysteine is the X_c^- system, which is an amino acid antiporter of cystine and glutamate in the cell membrane (Bannai and Kitamura, 1981; Gochenauer and Robinson, 2001; Patel et al., 2004). This transporter is able to transport in both directions, however, system X_c^- usually imports cystine while exporting glutamate in a 1:1 ratio (Bannai, 1986). Within the cell, cystine can be reduced to cysteine by thioredoxin reductase and incorporated into GSH or be used for protein synthesis. Excess of extracellular glutamate inhibits the cystine uptake via X_c^- system (Makowske and Christensen, 1982). This fact has been exploited to establish an in vitro model for oxidative stress (Lewerenz et al., 2013). Inhibition of cystine import by extracellular glutamate leads to a time-dependent GSH depletion resulting in oxidative stress through an exponential increase of ROS in the cell (Tan et al., 1998). This activates cell-signaling pathways that cause cell death. This cell death paradigm has been called oxidative glutamate toxicity and has been extensively studied in the mouse hippocampal cell line HT22 (Lewerenz et al., 2013; Murphy et al., 1989; Tan et al., 2001).

We used this cell line (a kind gift of A. Methner, University of Mainz) to investigate potential protective effects of recombinant GRN protein against oxidative glutamate toxicity. First, a killing curve was recorded for the treatment of the HT22 cells with glutamate to find an appropriate glutamate concentration that would induce oxidative stress and kill around 50% of the cultured cells (Figure 4.11 A). The cells were seeded at a density of $5x10^4$cells/well in a 96-well plate and after 48 h treated with increasing concentrations of glutamate. Control cells were not treated at all (100% cell viability control). After additional 24 h of incubation, the cell viability was measured with the alamarBlue® assay. In this assay, the non-fluorescent dye resazurin is converted to the red–fluorescent compound resorufin by metabolically active cells. The change in absorption can then be measured at 570/600nm. Treatment with 1-

1.5 mM glutamate induced sufficient toxicity with around 50 % of the cells still being alive. Therefore, this concentration was picked for the induction of glutamate toxicity in the subsequent experiments with GRN.

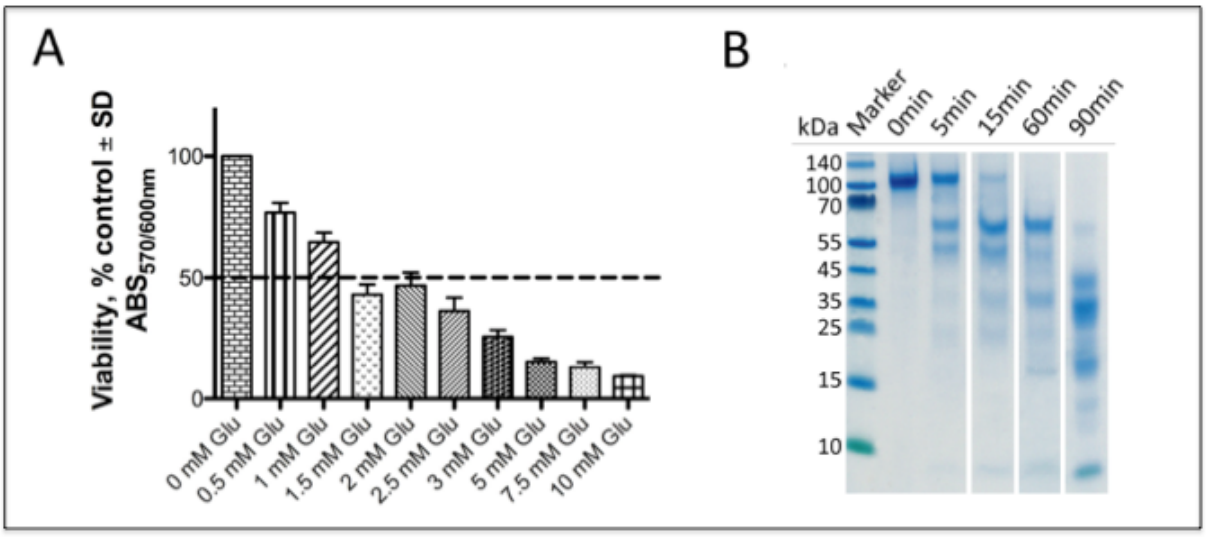

Figure 4.11: A) HT22 glutamate killing curve. HT22 cells were seeded at a density of $5x10^4$cells/well in a 96-well plate. After 48 h of cultivation, increasing concentrations of glutamate were added to the cell culture media. After additional 24 h, the cell viability was determined with the alamarBlue® assay (n=3). **B**) **GRN digest.** Recombinant full-length GRN was incubated with NE at 37° for the indicated time periods. The cleavage of the full-length GRN was monitored over time on a Coomassie stained SDS-gel. With increasing incubation time the signal from the full-length GRN disappeared in favor of smaller bands protein bands. Glu, glutamate; NE, neutrophil elastase.

After failing to detect any bioactivity of the full-length recombinant GRN in the assays performed earlier, it was decided to also investigate the activity of the granulin peptides. Some biological activities have been described for the granulins, and these activities in some cases appear to oppose the activities reported for the full-length GRN (Zhu et al., 2002). Gass et al. even reported that only the granulins have biological activities in contrast to the inactive full-length precursor protein (Gass et al., 2012a). Although several research groups have described biological effects after the treatment of cells with the precursor protein, it is possible that certain cell lines have the ability to cleave the protein into the granulin peptides. Neutrophil elastase (NE) is a serine protease secreted by neutrophils and macrophages that is able to cleave the full-length GRN protein into the small granulin peptides (grn) (Kessenbrock et al., 2008, Zhu et al., 2002). This was confirmed by co-incubation of recombinant GRN with NE *in vitro* and analysis of the samples by SDS-gel and Coomassie staining (Figure 4.12A). With increasing incubation time, the signal for the full-length GRN protein above 100 kDa was reduced and smaller protein fragments between 5-70 kDa appeared. These fragments likely corresponded to single or multiple granulin domains released from the full-length precursor protein (Figure 4.11 B). Subsequently, both full-length recombinant GRN and NE-treated GRN (grn) were evaluated for protective effects in the

HT22 assay. For these experiments, the cells were seeded at a density of $5x10^4$cells/well in a 96-well plate. The cells were pretreated with GRN or grn in medium containing 1% FCS for 24 hours. Then fresh medium was added containing 1mM glutamate and either GRN or grn. Control cells were not treated at all (100% cell viability control) or treated only with 1 mM glutamate (maximal toxicity control). To detect any possible effects of the neutrophil elastase (NE) used to cleave the full-length GRN into granulins (grn), additional control cells were treated with glutamate and only heat-inactivated NE. Concerning the enzyme concentration, this treatment was equivalent to treatment with 2µM grn. After another 24 hours of incubation, the cell viability was measured using the alamarBlue® assay.

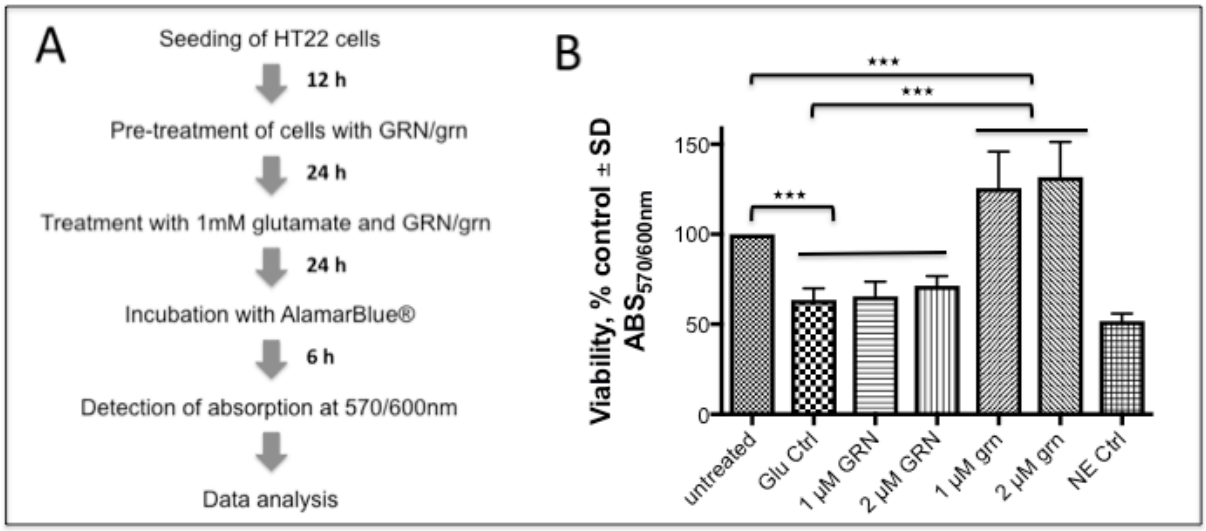

Figure 4.12: A) Time course of the HT22 glutamate toxicity assay. B) Protective effect of grn in the oxidative glutamate toxicity assay. HT22 cells were seeded at a density of $5x10^4$cells/well in 96-well plates. Following a pretreatment with full-length recombinant GRN or NE-cleaved GRN (grn) for 24 hours, the medium was changed and 1mM glutamate was added in the presence of GRN or grn. After another 24h of incubation, the viability of the cells was measured with the alamarBlue® assay. The relative metabolic activity as compared to the untreated control cells was calculated and statistically analyzed via one-way ANOVA with Tukey post-tests. Treatment with glutamate caused a significant reduction in the viability of the HT22 cells as compared to the untreated control cells. The results further showed a protective effect of the granulin peptides ($p<0.05$). However, no difference in viability was observed between cells treated with only glutamate and cells treated with glutamate in combination with 1-2 µM full-length GRN. N=2, 6 technical replicates each. Glu, glutamate; GRN, full-length progranulin; grn, granulin peptides.

As shown in Figure 4.12 B, glutamate treatment reduced the viability of the HT22 cells significantly (Glu Ctrl) compared to the untreated control condition. Treatment with increasing concentrations of full-length GRN did not affect the viability and did not rescue the cells from glutamate toxicity. In contrast, the cells treated with grn were rescued from the glutamate toxicity and showed a significant increase in viability compared to the untreated control cells. The NE control condition did not differ from the cells treated only with glutamate, which proved that the enzyme did neither have a protective nor a detrimental effect on the viability

of the HT22 cells. These results showed a strong protective effect of granulin peptides against glutamate induced oxidative stress in HT22 cells.

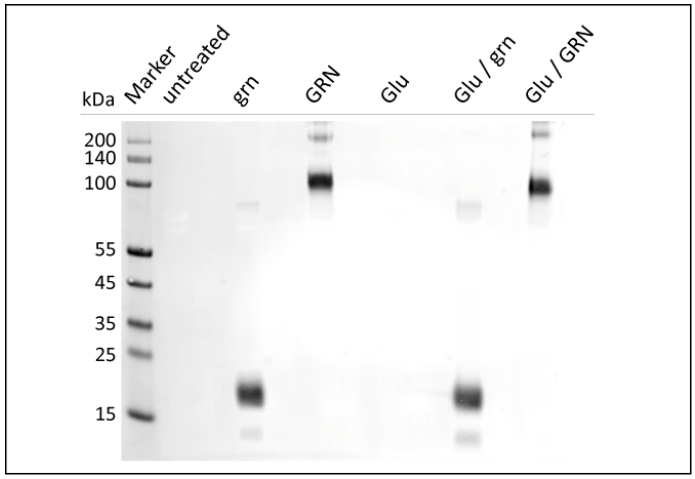

Figure 4.13: Post experimental analysis of cell culture supernatants. After the completed experiment supernatants were collected and subjected to Western blot analysis. Detection with anti-PCDGF antibody (Invitrogen) showed no degradation in the tissue culture supernatants to which the full-length GRN was added (lanes GRN and Glu/GRN). In contrast, the supernatants to which NE-treated GRN was added showed no full-length GRN and only a protein fragment with a size of approximately 20 kDa (lanes grn and Glu/grn). Additionally, no difference was observed between cells treated with or without glutamate.

Figure 4.13 shows a post experimental Western blot analysis of tissue culture supernatants that were collected from cells at the end of the 36h incubation period. Probed with the anti-PCDGF antibody, it was observed that the added full-length GRN was not cleaved, nor degraded during the experiment. No protein fragments were detected. In contrast, the supernatants to which NE-treated GRN was added showed no remaining full-length GRN and mainly one protein band with a size of approximately 20 kDa. In conclusion, these experiments indicated that GRN can potently protect HT22 cells from oxidative glutamate toxicity. However, in this assay only granulin fragments that are released from the recombinant full-length GRN protein conferred protection while the precursor protein showed no biological activity. Hence, the assay can be regarded as a bioassay for granulins.

4.3. Yeast-2-Hybrid Screening for Novel GRN Interaction Partners

The yeast-2-hybrid (Y2H) system is a powerful technique to investigate protein-protein interactions. This transcription-based method allows the investigation of two individual proteins and the discovery of new interaction partners by screening a protein or a single domain (a bait) against a library of proteins. This method was chosen to identify unknown interaction partners of GRN.

The Matchmaker® Gold Yeast Two-Hybrid System distributed by Takara Clontech is a GAL4-based Y2H assay using four different reporter genes. The GAL4 DNA-binding domain (DNA-BD) of the GAL4 transcription factor is fused to the bait protein, while the prey library is expressed fused to the GAL4 DNA-activation domain (DNA-AD). Brought into close proximity through the interaction of bait and prey, the two domains activate transcription from the GAL4-responsive promoters controlling the reporter genes. In addition to two different metabolic reporter genes that confer the ability to grow on media lacking adenine and histidine, the Matchmaker® Gold Yeast Two-Hybrid System also uses the dominant mutant version of the AUR1 gene that confers resistance against Aureobasidin A. The resistance against the highly toxic drug Aureobasidin A markedly reduces the background due to false-positive interactions as compared to the use of only metabolic reporter genes, and is considered a superior marker for screening purposes (MatchmakerManual).

Table 4.1: Reporter genes used to detect interaction of bait and prey proteins. The two yeast strains carry different reporter genes that are used to identify interactions between bait and prey proteins. His3 and Ade2 are nutritional markers that allow yeast to grow on media lacking adenine and histidine, while the expression of alpha- or beta-galactosidase (MEL1) allows the hydrolysis of a chromogenic substrate to an insoluble blue product. The most stringent reporter is Aur1. This reporter was introduced to reduce the background due to false-positive interactions. Upon activation of this reporter the cells become resistant against the antibiotic Aureobasidin A (AbA^r).

Strain	Gene	Function	Promoter
Y2H Gold	HIS3	biosynthesis of histidine	G1
	ADE2	biosynthesis of adenine	G2
	AUR1-C	resistance against AbA^r	M1
	MEL1	expression of alpha-galactosidase	M1
Y187	lacZ	expression of beta-galactosidase	G1
	MEL1	expression of alpha-galactosidase	M1

Vectors encoding control proteins for validated positive and negative interactions are included with the Matchmaker™ Gold Yeast Two-Hybrid System to ensure that the multi-step procedure is working properly. The p53 protein is used as the positive control bait (pGBKT7-p53). Together with the SV40 large T-antigen as a prey protein (pGADT7-T), it can activate all four reporters. The intermediate filament protein lamin is used as negative control bait (pGBKT7-lam) that is not able to interact with the T-antigen prey. This pair is not able to activate any reporter genes. To perform a control experiment, all three vectors have to be transformed separately into a yeast strain; Y2H Gold cells are used for the two bait plasmids and Y187 for the prey plasmid. The transformed yeast cells are plated on agar plates lacking either leucine (-leu, selects for the prey plasmid) or tryptophane (-trp, selects for the bait plasmid). Positive clones can be picked and the respective pairs are mated. In the mating process two yeast cells with opposite mating types (sexual reproduction) fuse with each other and a diploid daughter cell is generated (here Y2H Gold and Y187). This cell contains the complete genetic information of both parental cells, including the bait and prey plasmids. A diploid cell that contains the bait and prey plasmid is able to grow on double drop out plates (-Trp, -Leu). In addition, when two proteins interact (positive control) the reporter genes are activated and the cells acquire the ability to grow on media lacking adenine (-ade) and histidine (-his), they become resistant against Aureobasidin A, and they turn blue in the presence of X-alpha-Gal. If there is no interaction between bait and prey (negative control), no colonies will appear on agar plates containing Aureobasidin A because the reporter genes are not activated and the toxicity of Aureobasidin A prevents cell growth. Screening a library of bait proteins follows the same principle only with the components scaled up to enable mating of the whole library. Comparing the results from the screen to the positive/negative controls will identify yeast cells showing an interaction of bait and prey proteins.

Table 4.2: Bait and prey expression plasmids. The plasmids carry nutritional reporters that are expressed in yeast as well as an antibiotic resistance gene for selection in *E.coli*. Each plasmid fuses a GAL4-TF domain to the N-terminus of the respective insert.

Plasmid	Features	Function	Inserts
pGBKT7	DNA-BD	fuses a DNA-binding domain to the insert	p53
	Kan^r	Kanamycin resistance in *E. coli*	lam
	TRP1	tryptophane synthesis in yeast	bait
pGADT7	DNA-AD	fuses a DNA-activation domain to the insert	T-antigene
	Amp^r	Ampicillin resistance in *E. coli*	
	LEU2	leucin synthesis in yeast	

Even though the theoretical background of the Y2H assay is straightforward, performing a Y2H screen is a multi-step process that requires a high degree of diligence and consistency to generate reliable results. In addition, prior to the studies in this thesis, our research group had no experience with yeast as an experimental system and had never performed a Y2H screen. Therefore, prior to the GRN Y2H screen and to establish the Y2H method in our laboratory, a test screen was performed in which a bait protein with known strong interaction partners was screened against the prey library of interest. For this test screen, we chose the cytosolic C-terminus of the amyloid precursor protein (APP) as the bait. APP is a type-I transmembrane protein strongly implicated in the pathogenesis of AD and its cytosolic C-terminus, which consists of 46 amino acids, has been shown to interact with numerous adapter proteins (Zheng and Koo, 2011). The APP C-terminus has previously been used as the bait in numerous Y2H screens to isolate new APP interaction partners. For example, in a study conducted by Hao *et al*. the APP C-terminus was screened against a human brain cDNA library. They were able to detect novel interaction partners of APP and verified interaction with already known binding partners of the APP C-terminus like Fe65, X11 and JIP-1 (Hao et al., 2011). Fe65 was the first protein shown to interact with the C-terminus of APP (Fiore et al., 1995). It belongs to a highly conserved protein family whose members share high sequence and domain homology. The three Fe65 proteins (Fe65, Fe65L1, Fe65L2) have an identical multi-modular structure comprised of three different protein-protein interaction domains: a WW ligand interaction domain followed by two phosphotyrosine binding (PTB) domains called PTB1 and PTB2 (Duilio et al., 1998; Guenette et al., 1996; Zambrano et al., 1997). The APP C-terminus contains an Asn-Pro-X-Tyr motif that binds with high affinity to the PTB2 domain of the Fe65 proteins when the tyrosine residue is phosphorylated (Borg et al., 1996; McLoughlin and Miller, 1996). This interaction between APP and FE65 is very strong and can be easily demonstrated by co-immunoprecipitation.

In accordance with Hao *et al*. (Hao et al., 2011), the C-terminal amino acids 649-695 of the brain specific APP695 transcript were cloned into the pGBKT7 yeast bait expression vector, using the EcoRI and BamHI restriction sites. The construct was then transformed into the Y2H Gold strain and expression of the bait protein was confirmed by Western blotting (Figure 4.13 A). Subsequently, the Y2H Gold strain expressing the bait was used for yeast mating with the Y187 strain pre-transformed with a normalized human brain cDNA library (Mate&Plate^{TM} library, Clontech, see below for more information on the library). The mated yeast strains were plated on DDO/X/A_{125} agar plates (-Trp, -Leu double dropout agar with X-alpha-gal and Aureobasidin A, 125ng/ml) and fast growing blue colonies were picked and transferred onto QDO/X/A_{125} agar plates (-Trp, -Leu, -His, -Ade quadruple dropout agar with X-alpha-gal and Aureobasidin A, 125ng/ml). In contrast to the DDO agar plates, the QDO agar plates do not only select for the presence of both plasmids, but also for the expression

of two additional reporter genes carried by the Y2H Gold yeast strain, which allow the yeast to grow on plates lacking histidine and adenine (-His, -Ade). Colonies growing under this increased selection stringency were classified as positive and further analyzed by colony PCR using primers flanking the insert of the prey plasmid. After visualization on agarose gels, the PCR products revealed the size of the putatively interacting prey cDNA clones as well as the number of prey plasmids present in each yeast clone (Figure 4.14 B). In the majority of diploids, only one prey plasmid was present. However, some diploids carried two prey plasmids (these clones produced two PCR products, which appeared as two distinct bands on the agarose gel, see Figure 4.14, clone #74). In this case, it was possible to separate the plasmids by repeated re-streaking on fresh agar plates. After several rounds of re-streaking, the yeast were found to only contain the plasmid encoding the putative interacting prey plasmid, while the plasmid encoding the additional non-interacting prey protein was lost.

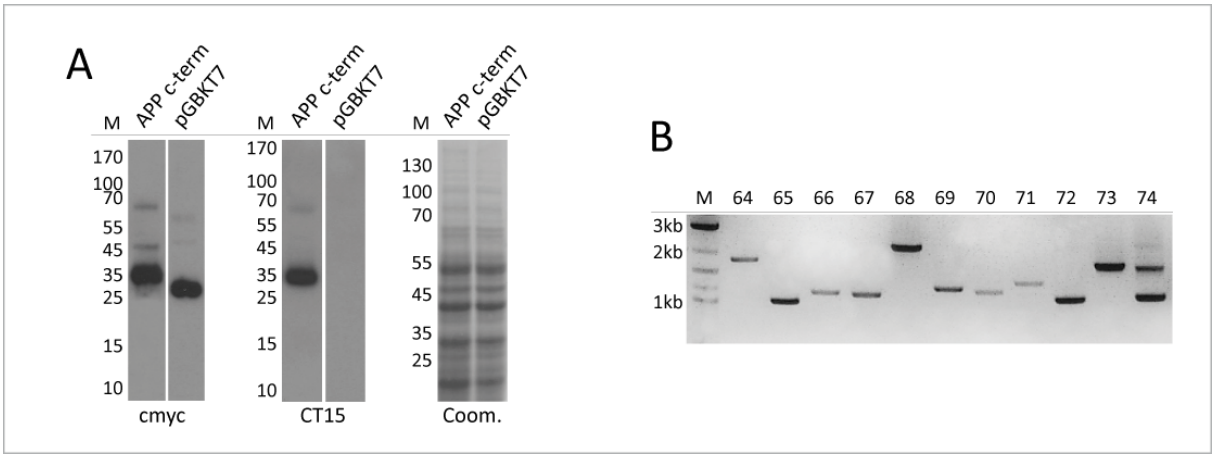

Figure 4.14: Y2H test screen with the APP C-terminus. **A) Bait protein expression.** Y2H Gold cells were transformed with the APP C-terminus bait vector or the empty pGBKT7 vector and lysates of an overnight culture were analyzed by Western blotting. The first two lanes show the detection with an anti-Myc antibody (Calbiochem). The myc-epitope is fused to the N-terminus of the bait protein. The APP C-terminus bait protein was detected at approximately 35kDa. In yeast transformed with the empty vector pGBKT7 a smaller protein of approximately 26 kDa was detected, which represented the Gal4 DNA-binding domain, a myc-epitope and linker sequences without the fused APP C-terminus. The following two lanes show the detection with an antibody directed against the last 15 C-terminal amino acids of APP (CT15, Sisodia *et al.*, 1993) This antibody only detected the APP C-terminus bait protein with the same size as the anti-Myc antibody (35kDa). No signal was detected in the empty-vector control. The last two lanes show a Coomassie staining as a loading control. **B) Colony PCR analysis of positive diploids.** The positive diploids from the APP C-terminus Y2H screen were analyzed by colony PCR using primers targeting the prey plasmid insert. Loaded on agarose gels the amplified DNA revealed the size of the respective prey insert. Shown here are the samples # 64 to 74. The PCR of clone # 74 clearly showed the presence of two prey plasmids. (Coom.: Coomassie, M: marker)

In the next step, the PCR samples were purified and sequenced to identify the candidate interacting prey proteins. Plasmids were then isolated from the respective yeast clones and

transformed into DH5α bacteria. As the pGADT7-RecAB library prey plasmid conferred resistance to ampicillin while the pGBKT7 bait plasmid conferred resistance to kanamycin, the transformed bacteria were plated on ampicillin agar plates to prevent contamination of the DNA preparations with bait plasmid. A total of 105 individual clones were sequenced after excluding diploids containing more than one plasmid via colony PCR. The most informative clones for the validation of the Y2H screening method encoded the proteins Fe65L1, phosphoglutamase 1 (PGM1), and COP9 (COPS5). The cDNA sequences encoding Fe65L1 were present in 5 of the 105 sequenced clones. All five cDNA clones were confirmed to be cloned in frame with the activation domain of the prey plasmid and had substantial sequence overlap. All cDNA clones covered the complete sequence of the PTB2 domain of Fe65 that had been found to interact with the NPXY motif of the APP C-terminus (McLoughlin and Miller, 2008) (Duilio et al., 1998; Guenette et al., 1996; Zambrano et al., 1997). The cDNA clones were amplified in DH5α bacteria and subsequently retransformed into Y2H Gold cells. Plated on selection agar plates, these clones were not able to activate the reporter genes indicating that they had no auto-activating activity and that they were encoding a true interaction partner of the APP C-terminus (Figure 4.3.2c).

Seven of the 105 clones were found to contain parts of the PGM1 cDNA. Further analysis showed that all clones were not cloned in frame with the activation domain in the prey plasmid. In addition, a retransformation into Y2H Gold cells and plating on selection agar revealed their capability to auto-activate the reporter genes. Since the PGM1 cDNA was not in frame, these prey clones encoded non-natural proteins, which are likely unfolded and often display high, non-specific affinity to the bait protein. Hence, these PGM1 clones were false-positive hits in the screen. Six of the 105 clones encoded parts of the COP9 protein. This protein was chosen for further testing because it is a known member of the "top ten sticky preys" occurring in Y2H assays (*http://www.dkfz.de/gpcf/251.html*). These proteins appear frequently and with high redundancy in Y2H screens but generate an interaction signal in a non-specific way. They bind directly to the GAL4 part of the bait protein or auto-activate the reporter genes independently. All six COP9 clones were found to be in frame, and upon retransformation into Y2H Gold cells COP9 showed strong auto-activation of the reporter genes. Consequently, the COP9 prey protein was also a false-positive hit in our screen.

Taken together, the results of the test screen with the APP C-terminus strongly supported that the Y2H system was successfully established in the laboratory. With FE65L1 a known interaction partner of APP was isolated that had been previously identified with the exact same methodology and is now one of the best-characterized, functionally important APP adapter proteins (Duilio et al., 1998; Guenette et al., 1996; Zambrano et al., 1997; Zheng and Koo, 2011). Furthermore, the isolated prey clones all encoded the FE65L binding domain known to interact with the APP C-terminus further indicating that this is a genuine protein-

protein interaction (Figure 4.15 A and B) (Duilio et al., 1998; Guenette et al., 1996; Zambrano et al., 1997). Importantly, this screen also showed that a careful analysis of positive clones is essential, as the reporter genes can be non-specifically auto-activated by prey proteins through various mechanisms. This can occur through the translation of non-natural prey proteins as exemplified by the PGM1 clones not in frame with the GAL4 DNA-activation domain, or through particularly sticky prey proteins as exemplified by the COP9 clones. In both cases, retransformation experiments with Y2H Gold cells were sufficient to reveal the auto-activating capabilities of the PGM1 and COP9 clones. These control experiments clearly showed that the two prey proteins activate the reporters independently of the bait protein (Figure 4.15C).

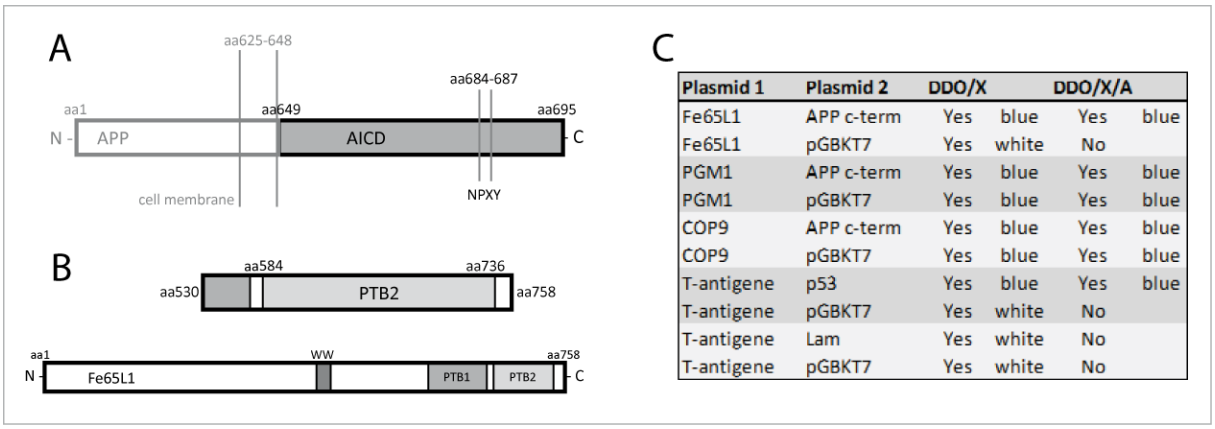

C

Plasmid 1	Plasmid 2	DDO/X		DDO/X/A	
Fe65L1	APP c-term	Yes	blue	Yes	blue
Fe65L1	pGBKT7	Yes	white	No	
PGM1	APP c-term	Yes	blue	Yes	blue
PGM1	pGBKT7	Yes	blue	Yes	blue
COP9	APP c-term	Yes	blue	Yes	blue
COP9	pGBKT7	Yes	blue	Yes	blue
T-antigene	p53	Yes	blue	Yes	blue
T-antigene	pGBKT7	Yes	white	No	
T-antigene	Lam	Yes	white	No	
T-antigene	pGBKT7	Yes	white	No	

Figure 4.15: A) Schematic representation of the amyloid precursor protein (APP). The C-terminus of APP was cloned into the pGBKT7 bait plasmid and used for the test screen (grey). Amino acids 649-695 constitute the cytosolic C-terminus of APP, and contain the NPXY motif, which is known to interact with the PTB2 domain of the Fe65 proteins. The different protein parts are not drawn to scale with respect to their sizes. **B) Fe65L1.** Schematic representation of the captured Fe65L1 prey proteins (average size of a total of five different clones) and the full-length Fe65L1 below. All captured clones were in frame with the start codon of the library expression plasmid and covered the APP-interacting PTB2 domain. As in A the different protein parts are not drawn to scale with respect to their sizes. **C) Retransformation experiments.** To assess possible auto-activating properties of the captured prey proteins, the prey plasmids of interest were co-transformed into the Y2H Gold cells with the APP C-terminus bait plasmid or the empty bait plasmid (pGBKT7). Fe65L1 was confirmed as a real positive hit, as no colonies appeared on DDO/X/A plates without the APP C-terminus bait. In addition, DDO/X plates showed colonies but they did not turn blue. Consequently, the prey alone was not able to activate the reporter. These result were identical to the positive control plasmids (T-antigen/p53). In contrast, the PGM1 and COP9 prey proteins activated the reporter genes in the absence of the APP C-terminus bait protein and blue colonies grew on DDO/X/A agar plates. The negative control plasmids (T-antigen/lamin) showed no activation of the reporters.

Based on these successful, preliminary experiments, a Y2H screen with GRN as the bait protein was performed. First, the GRN bait construct was cloned and tested for expression and auto-activation. The Y2H assay is based on the interaction of two proteins inside a yeast cell. However, GRN is a secreted glycoprotein. Therefore, the N-terminal signal sequence (17 amino acids following the initial methionine) was deleted that might otherwise direct GRN

into the secretory pathway. The human full-length GRN sequence lacking the signal sequence was cloned into the pGBKT7 bait expression vector using the EcoRI and BamHI restriction sites. Thereby, the GAL4 DNA-binding domain was fused to the N-terminus of GRN. This construct (GRN-FL) was transformed into Y2H Gold yeast cells and plated on agar plates selecting for the bait plasmid (-Trp agar plates). Individual colonies were picked and yeast cell lysates were prepared and analyzed by Western blotting. The pGBKT7 yeast expression vector is a high-copy plasmid with constitutive high protein expression, which usually allows detection of the bait protein by Western blotting. Successful bait protein expression with a size > 80 kDa was confirmed as shown in Figure 4.18 A.

The next important step was to test if the GRN-FL bait construct might have auto-activating activity, which would preclude the use of the full-length bait in the Y2H assay. Therefore, the GRN bait plasmid was transformed into the Y2H Gold yeast cells, which were then plated on SD/X and SD/X/A agar plates with the following selection markers: SD are single dropout plates lacking tryptophane (-Trp), which selected for the bait plasmid. X indicates the presence of the chromogenic substrate X-α-Gal, which upon activation of the MEL1 reporter gene encoding alpha-galactosidase reporter leads to blue colored colonies. A indicates the presence of the antibiotic Aureobasidin A, which suppressed the growth of yeast cells without expression of the AUR1 resistance gene. Both the MEL1 and the AUR1 reporter genes were expressed under control of a GAL4-responsive promoter and should only be activated in yeast cell with a productive bait and prey interaction.

Unfortunately, strong auto-activation of the reporter genes including AUR1 was detected with the GRN-FL bait (Figure 4.16). Compared to the positive control (p53/T-antigen) plated on SD/X/A agar, the number of colonies and their respective sizes were comparable for the GRN-FL bait (Figure 4.16 A and C). Furthermore, no difference was detected between plating cells on SD/X or SD/X/A agar with or without Aureobasidin A, although AUR1 is a highly stringent selection marker (Figure 4.16 B and C). Following instructions in the Matchmaker^{TM} Gold Yeast Two-Hybrid System manual, an Aureobasidin A gradient was tested, ranging from 125ng/ml to 500ng/ml. However, even at the highest Aureobasidin A concentration the number of yeast colonies that appeared on the agar plates was not reduced indicating very high expression of the AUR1 resistence gene in yeast transformed with the GRN-FL bait. Consequently, the GRN-FL bait construct could not be used for a Y2H screen. The strong auto-activation of the reporter genes would have masked any genuine bait-prey interaction.

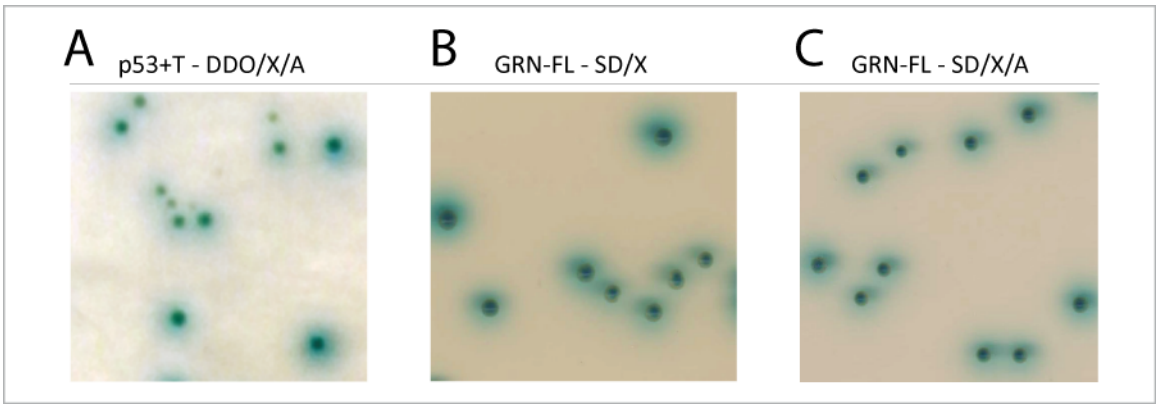

Figure 4.16: Test for auto-activation of the GRN full-length bait (GRN-FL). The GRN-FL bait plasmid was transformed into Y2H Gold cells and plated on selection agar plates in comparison with the positive control diploids (p53/T-antigen). **A) Positive control diploids plated on DDO/X/A plates.** This agar selected for both bait and prey plasmids (-Trp, -Leu) and the interaction of bait and prey. Distinct colonies with a diameter of around 2 mm and their intense blue color confirmed the activation of all reporters by the positive controls. **B) GRN-FL plated on SD/X agar plates.** The single dropout agar (-Trp) selected for the bait vector, X-alpha-Gal detected the activation of the MEL1 reporter. The distinct colonies showed the presence of the bait vector, the blue color indicated auto-activation through the GRN-FL bait. **C) GRN-FL plated on SD/X/A agar plates.** The single dropout agar (-Trp) selected for the bait vector, X-alpha-Gal and Aureobasidin A detected the activation of the reporter genes MEL1 and AUR1. The fact that colonies were able to grow on the SD/X/A plates confirmed the strong auto-activating capabilities of GRN-FL as AUR1 is a very stringent selection marker.

The reason for the observed auto-activation of the GRN-FL bait was likely that certain domains or folds within the GRN protein interacted non-specifically with transcription factors and thereby activated the reporter genes. One possible way to avoid auto-activation by a bait protein is to identify the responsible protein domain(s) and remove it from the bait construct. Since GRN is comprised of 7.5 repeat domains separated by spacer regions a series of deletion mutants was cloned and evaluated for auto-activation. In total, 12 GRN constructs were generated by progressively deleting domains from the N- and C-terminus. The first six fragments that were cloned started with the P and G domains (N-terminus) and sequentially became longer towards the C-terminus. The fragments 7 to 12 started with the domains D and E at the C-terminus of GRN and become longer towards the N-terminus (see figure 4.17).

	Domains	AA	Cloned by	SD /A_{250}
FL	P_G_F_B_A_C_D_E	18-594		
1	P_G	18-120		
2	P_G_F	18-185	PCR	
3	P_G_F_B	18-271		
4	P_G_F_B_A	18-354		
5	P_G_F_B_A_C	18-433		
6	P_G_F_B_A_C_D	18-513		
7	D_E	447-594		
8	C_D_E	363-594	Ligation	
9	A_C_D_E	280-594		
10	B_A_C_D_E	205-594		
11	F_B_A_C_D_E	122-594		
12	G_F_B_A_C_D_E	57-594		
	APP c-term	649-695		
	pGBKT7			

Figure 4.17: Identification of granulin domain F as the auto-activating domain in the GRN-FL bait. 12 different fragments of the human GRN protein were cloned into the pGBKT7 bait vector and tested for auto-activation by transformation into Y2H Gold cells and plating on SD/A agar plates (-Trp/Aureobasidin A). Without auto-activation, colonies are not able to grow on agar with Aureobasidin A. As indicated in green, this was the case for all baits lacking the granulin domain F. No growth was also observed after transformation of the yeast with the APP C-terminus bait construct or the empty pGBKT7 vector. Indicated in red are all baits that were able to grow on the Aureobasidin A containing agar and, consequently, auto-activated the AUR1 reporter gene. The N-terminal fragment constructs (1-6) were generated through the introduction of stop codons by mutagenesis PCR. The C-terminal fragment constructs (7-12) were cloned and ligated via the EcoRI and BamHI restriction sites. FL: full-length, SD: single dropout (here: -Trp), A_{250}: 250ng/ml Aureobasidin A.

All 12 GRN bait constructs were transformed into Y2H Gold cells and tested for auto-activation by plating on SD/X agar plates that selected for the presence of a bait plasmid (-Trp) and for the activation of the stringent reporter gene AUR1. If the bait protein is able to auto-activate the AUR1 reporter, the yeast cells are able to grow on agar plates containing Aureobasidin A even in the absence of an interacting prey protein. Evaluation of the different GRN fragments clearly showed that all bait constructs that contained the granulin domain F auto-activated the AUR1 reporter. On the other hand, for all baits without the granulin domain F no auto-activation of the AUR1 reporter was detected. All cells transformed with those fragments that lacked the granulin domain F were sensitive to Aureobasidin A and no

colonies appeared on SD/A agar plates (see figure 4.17). Notably, these included the fragment F8 consisting of the granulin domains C, D and E, which is identical to a GRN bait that had been previously used for a Y2H screen (Hoque et al., 2003).

Consequently, a GRN mutant with a deletion of the F domain (deltaF-GRN) was cloned. This mutant was preferred to fragment 10 in Figure 4.17 in order to use the GRN bait with the smallest deletion possible to prevent the loss of any potential protein interaction domains. The new bait construct was sequenced to confirm the deletion and transformed into Y2H Gold cells. Plated on SD/A plates no growth was observed showing that yeast cells containing the deltaF-GRN bait construct did not auto-activate the AUR1 reporter and were sensitive to Aureobasidin A treatment as expected. Next, expression of the deltaF-GRN deletion mutant was confirmed by Western blotting. In lysates of yeast transformed with the respective bait constructs the expression of the bait proteins was detected. The deltaF-GRN bait was detected at an approximate size of 100 kDa, which was the expected size for a fusion protein of the Gal4 DNA-binding domain with the deltaF-GRN deletion mutant (Figure 4.18 B). The expression of the other GRN bait fragments F8, F10 and F11 was also confirmed (Figure 4.18 B).

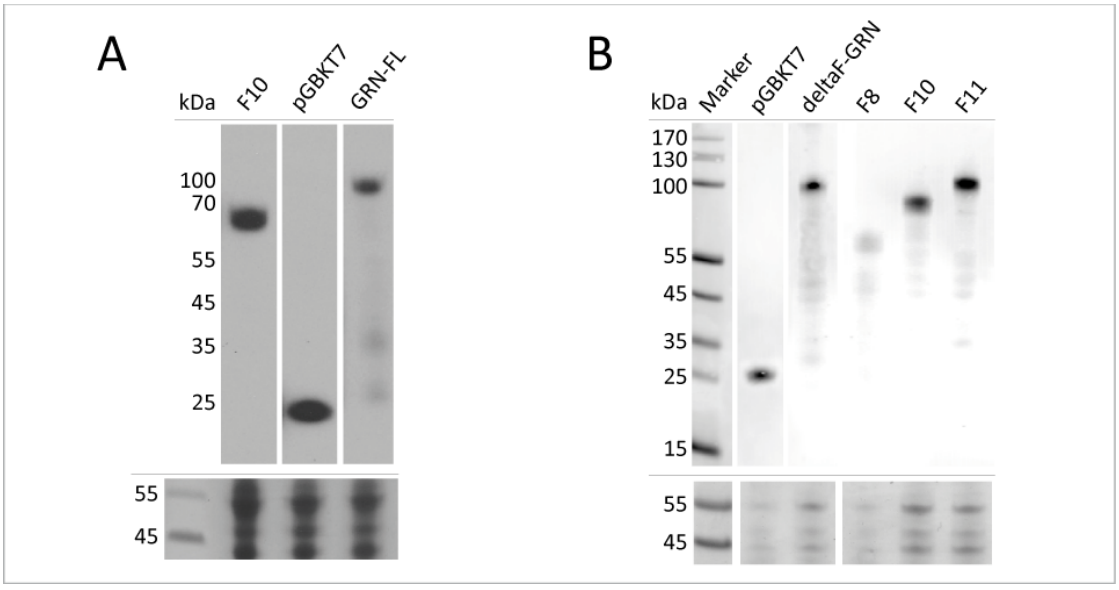

Figure 4.18: Expression of the different GRN bait proteins. Lysates were prepared from overnight yeast cultures previously transformed with the respective GRN bait plasmids. The samples were subjected to Western blot analysis with anti-Myc antibody (Calbiochem). **A) Western blot analysis of GRN-FL and fragment 10 (B-A-C-D-E).** The F10 bait protein was detected at the expected size of approximately 65 kDa and the GRN-FL bait protein at the expected size of >80kDa. The protein translated from the empty pGBKT7 vector was the GAL4 DNA-binding domain with a Myc-epitope tag with a size of approximately 25kDa. Below a Coomassie staining is shown as a loading control. **B) Western blot analysis of the deltaF-GRN bait protein.** Expression of the deletion mutant lacking the granulin domain F was detected at the expected size of 100kDa and showed a signal intensity similar to the empty plasmid. The GRN fragments F8, F10 and F11 were also expressed and detected at the expected sizes (52kDa, 70kDa, 77kDa). Signals were recorded on a Licor Odyssey Clx Imaging system. Below, a Coomassie stained loading control is shown.

After establishing a GRN bait-protein suitable for the Y2H assay, the actual screen with the deltaF-GRN deletion mutant against the prey library was performed. The commercial, pre-transformed cDNA library used for this screen was constructed from male human brain tissue and transformed into the yeast strain Y187 (Mate&Plate^{TM} library, Clontech, Lot number: 9100082A). To reduce the number of highly represented mRNA transcripts in favor of transcripts with low copy number the cDNA library was normalized prior to library construction. A 1ml aliquot of the library contained >5x10^7 cfu/ml and 3.2x10^6 independent cDNA clones ligated into the pGADT7-RecAB prey plasmid. For the library screening, 5ml of 2x(-Trp) medium were inoculated with 3 Y2H Gold colonies carrying the deltaF-GRN bait construct and incubated at 30°C until the OD_{600} reached 0,8 (approximately 20 hours). The suspension was centrifuged and the pelleted cells resuspended in 5ml fresh medium. This resulted in a cell density of >1x10^8 per ml. This culture was combined with 1 ml Y187 library strain in a sterile flask. Then 45 ml 2xYPDA liquid medium were added, containing 50 µg/ml kanamycin. For the mating process the flask was incubated at 30°C for over 24 hours shaking slowly (40rpm).

The incubation of the mating culture was stopped when yeast zygotes (3-lobed structures, comprising the two parental cells and a budding diploid daughter cell) could be observed under a phase contrast microscope. The mated cells were pelleted, washed and finally resuspended in 10ml 0.5xYPDA liquid medium. 200µl aliquots of this mating culture were plated on 150mm DDO/X/A_{250} agar plates. From these plates fast growing blue colonies were picked after 5 days and re-streaked on the most stringent QDO/X/A_{250} plates. Positive and negative control diploids were always included. The quadruple dropout plates (-Trp, -Leu, -His, -Ade, containing X-α-Gal and Aureobasidin A) selected for the presence of both the bait and the prey plasmid and the expression of all 4 Gal4-controlled reporter genes in the Y2H Gold yeast strain (HIS3, ADE2, MEL1, AUR1). Positive clones growing on the QDO/X/A_{250} plates were further analyzed by colony PCR as described above for the APP C-terminus Y2H screen, and diploids containing only one prey plasmid were sequenced (see figure 4.19 B).

For a complete evaluation of a Y2H screen it is important to determine the total number of individual yeast colonies that were screened and to calculate the efficiency of the mating process. A sufficient number of diploids indicates that every cDNA represented in the library had the chance to interact with the bait. Using the normalized prey library, a Y2H screen has to include more than 1 million diploids to allow the detection of all possible genuine interactions (MatchmakerManual). A serial dilution of the mating solution was plated on different dropout agar plates and incubated at 30°C for 3 days. The appearing colonies were counted and the number of colonies per milliliter was calculated (cfu/ml). Colonies that grew on the (-Leu) agar plates represented the viability of cells that contained the prey library,

whereas colony numbers on (-Trp) agar plates represented the viability of the bait culture. The number of colonies growing on DDO agar correlated to the viability of the diploids and showed the efficiency of the mating. From these viabilities, it was calculated that a total of $6x10^6$ diploids had been plated after the mating on the DDO/X/A selection plates, meaning that $6x10^6$ clones had been screened (cfu/ml diploids x resuspension volume). From the viability of the diploids and the viability of the limiting mating partner, a mating efficiency of 8% was determined ([number of diploids per ml/ number of limiting partner per ml] x 100). These data confirmed that the number of colonies screened and the mating efficiency in the deltaF-GRN Y2H screen had been sufficient.

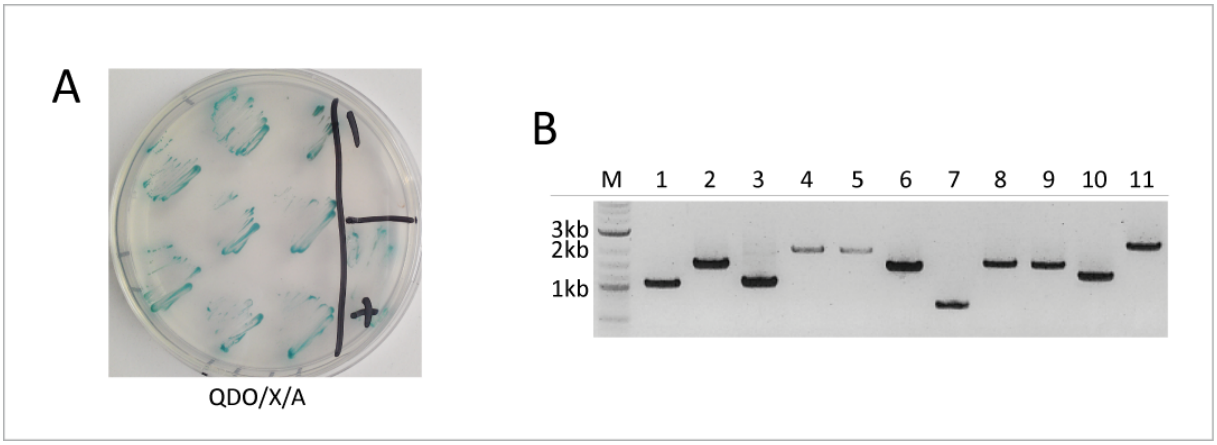

Figure 4.19: Y2H screen with the deltaF-GRN bait. A) Re-streaking of positive clones on QDO/X/A agar plates. The stringency of selection was increased for positive clones that grew on the DDO/X/A agar by plating them on the quadruple dropout QDO/X/A agar plates. These plates also contained the colorless chromogenic substrate X-α-Gal, and viable growing yeast colonies expressing the reporter gene MEL1 encoding α-galactosidase hydrolyzed X-α-Gal into a blue product (blue color of positive clones). **B) Colony PCR analysis of positive diploids.** The positive diploids from the QDO/X/A plates were analyzed via colony PCR using primers flanking the insert of the prey plasmid. Visualized on agarose gels the amplified DNA showed the size of the respective prey cDNA inserts. Shown here are the prey clones 1 to 11. (QDO: quadruple dropout, DDO: double dropout, X: X-α-Gal, A: Aureobasidin A, M: marker)

More than 400 positive clones were analyzed by colony PCR and then sequenced. No frequently recurring identical prey clones could be identified by the comparison of insert sizes and their digestion pattern after digestion with the restriction enzymes AluI and HaeIII. In fact, the sequencing data identified 323 different proteins that were subsequently categorized and rated following different criteria. First, the obtained sequences were analyzed using the nucleotide database of the National Center for Biotechnology Information (NCBI) and the Basic Local Alignment Search Tool (BLAST) (*www.ncbi.nlm.gov*). With these results a first ranking was created omitting e.g. mitochondrial proteins, as it is not possible for GRN, which is located in the secretory pathway, to interact with mitochondrial proteins in an intact cell.

Second, the exact nucleotide sequence in the prey plasmids was checked and only inserts cloned in frame with the GAL4 DNA-activation domain were chosen for further analysis. This drastically reduced the number of potentially interacting proteins to 52. These prey plasmids were rescued from the respective diploids and amplified in bacteria to test them in co-transformation experiments in Y2H Gold cells. Through this assay, false positive hits caused by auto-activation of the reporter genes by the prey proteins could be identified and excluded (as described above for the APP C-terminus screen). Third, the last exclusion criterion was the exact cellular localization of the prey protein domain captured in the screen. GRN is directed into the secretory pathway of the cell and then secreted into the extracellular space. Consequently, proteins that are located in the nucleus or the cytosol cannot interact with GRN (excluded in the first step). However, this also applies to captured prey proteins that are transmembrane proteins. The extracellular domain of transmembrane proteins could possibly interact with GRN, but if the identified interaction domain is located within the cytoplasmic tail these proteins can be excluded as valid interaction partners. Although the detected interaction in the artificial environment of the Y2H screen might real they are most likely not physiological interaction partners in the compartmentalized environment of a living cell.

Table 4.3: Validation experiments with rescued prey plasmids by co-transformation. In a total of 413 analyzed diploids, sequences encoding 323 different individual proteins were detected. Only 10 of these prey clones were 1) in frame with the Gal4 DNA-activating domain, 2) encoded a protein domain localized in the same cellular compartment as GRN, and 3) did not auto-activate the reporter genes when retransformed into Y2H Gold cells. The co-transformation experiments confirmed the final 10 candidates as true positives as no colonies grew on DDO/X/A plates. Zinc finger proteins were captured with high frequency, but they turned out to be false positives as they could activate the reporter genes independently of the bait protein. The GABARAPL2 clone was tested as a member of the final candidate list and it showed no auto-activation. However, this protein is known to occur in many Y2H screens and has been designated a sticky prey. The DAZ associated protein 2 clones did not result in auto-activation in the co-transformation experiment. However, they were not in frame with the Gal4 DNA-activating domain and thereby excluded. The mitochondrial calcium uptake 1 protein is an example for a prey protein that was cloned in frame and displayed no auto-activation of the reporter genes, but was disregarded as a plausible interaction partner because of its cellular localization. (DDO: double dropout, X: X-a-Gal, A: Aureobasidin A)

Plasmid 1	Plasmid 2	DDO/X		DDO/X/A		Validated as
final candidate	deltaF-GRN	Yes	blue	Yes	blue	positive
final candidate	pGBKT7	Yes	white	No		
Zinc finger protein	deltaF-GRN	Yes	blue	Yes	blue	false positive
Zinc finger protein	pGBKT7	Yes	blue	Yes	blue	
GABA receptor-associated protein-like 2	deltaF-GRN	Yes	blue	Yes	blue	sticky prey
GABA receptor-associated protein-like 2	pGBKT7	Yes	white	No		
DAZ associated protein 2	deltaF-GRN	Yes	blue	Yes	blue	not in frame
DAZ associated protein 2	pGBKT7	Yes	white	No		
mitochondrial calcium uptake 1	deltaF-GRN	Yes	blue	Yes	blue	interaction in Y2H only
mitochondrial calcium uptake 1	pGBKT7	Yes	white	No		

With these criteria, the number of candidate interaction partners was reduced to a total of 10 proteins – all of them were cloned in frame, none of them caused auto-activation of the reporter genes, and all of these prey clones encoded a protein domain that could possibly interact with GRN within the cell. In the co-transformation validation experiments, all 10 candidates, when combined with the empty bait plasmid, displayed growth on the DDO agar (selecting for the presence of both plasmids) and no colonies appeared on the DDO/X/A plates, which selected for the activation of the reporter genes. In contrast, distinct blue colonies appeared on both types of agar when the prey candidate plasmids were co-transformed with the plasmid containing the deltaF-GRN bait. Therefore, these clones were classified as true positive hits (Figure 4.3).

Zinc finger proteins were also tested in co-transformation validation experiments as they appeared frequently among all sequenced positive diploids. Testing these candidates was supported by controversial findings that GRN might function as a transcriptional co-repressor of cell cycle genes in the nucleus (Hoque et al., 2003). In total 20 different zinc finger proteins were captured, a result that was strikingly different from the APP C-terminus screen where no zinc finger proteins appeared. However, all prey proteins containing a zinc finger domain showed strong auto-activation of the reporter genes in the absence of the deltaF-GRN bait protein and were identified as false positives.

The GABA receptor-associated protein like 2 (GABARAPL2) is a prey known to appear in many Y2H screens and has been designated a “sticky prey”. Co-transfecting the GABARAPL2 prey plasmid with the empty pGBKT7 plasmid into Y2H Gold cells did not result in auto-activation. In addition, the GABARAPL2 cDNA was captured only once, a fact that would argue against it being a sticky prey in this screen. In addition, the GABARAPL2 cDNA was captured only once, a fact that would argue against it being a sticky prey in this screen. Furthermore, it is located in the golgi, a compartment where it would have the chance to interact with GRN. Therefore, this prey was kept in the list of candidates that possibly bind to GRN. Whether the GABARAPL2 protein is indeed a false positive result can only be clarified in future co-immunoprecipitation (Co-IP) experiments or other protein-protein interaction assays.

Another example of a sticky prey was the DAZ associated protein 2 (DAZAP2). In these prey clones the captured cDNA fragment was not cloned in frame with the Gal4 DNA-activating domain. This frame shift leads to a changed amino acid sequence and the translation of a non-natural protein. Such proteins likely lack proper folding, which promotes non-specific protein-protein interactions with the bait protein and activation of the reporter genes. This type of a false positive hit, which is different from an auto-activating prey protein, can easily be excluded through sequencing of the prey plasmid. Typically for a sticky prey, DAZAP2 appeared with high frequency in the screen.

Physiological functions and diseases that are associated with GRN include inflammatory responses (Tang et al., 2011; Yin et al., 2010a), defense against oxidative stress (Piscopo et al., 2010; Sato et al., 2014), tumor progression (Matsumura et al., 2006; Miyanishi et al., 2007) and neurodegenerative diseases like Alzheimer's disease (Brouwers et al., 2008; Knopman and Roberts, 2011; Rademakers et al., 2007), Parkinson's disease (Rademakers et al., 2012), and frontotemporal dementia (Cruts et al., 2012). For several of the final 10 candidates of the Y2H-screen, a great overlap of their assigned functions and their roles in diseases with GRN can be found. These proteins included Versican, Selenoprotein P, Dickkopf WNT signaling pathway inhibitor (DKK1) and Phospholipase A2 (table 4.4; see also the discussion section for further information on the candidate proteins).

Table 4.4: Putative interaction partners of GRN identified in the Y2H screen. This list of proteins represents the final candidates of the Y2H screen with the deltaF-GRN bait.

Name	Gene	Function	Localization	Associated diseases
Versican	VCAN	controling structure and function of neurons and synapses	mature brain/ extracellular Matrix	inflammation, malignant transformation and tumor progression, AD progression, PD, HD
Selenoprotein P	SEPP1	defense against oxidative stress, selenium storage	ubiquitously/ secreted	inflammation, protection against cancer and neurodegeneration
dickkopf WNT signaling pathway inhibitor 1	DKK1	Wnt signaling inhibitor	ubiquitously/ secreted	glioblastoma, AD, FTD (GRN deficiency)
Phospholipase A2	PLA2 G12A	releases arachidonic acid and lysophospholipids from phospholipids	ubiquitously/ secreted	inflammation, AD, MS, FTD
TIMP metallopeptidase inhibitor 4	TIMP4	tissue remodeling, wound healing, synaptic plasticity, neuronal cell differentiation	brain (astrocytes, macrophages)/ secreted	inflammation, inhibits tumor growth and invasion
Leucine rich repeat neuronal 3	LRRN3	mediates MAPK phosphorylation	brain/ transmembrane	cognitive abilities
T-cell lymphoma invasion and metastasis 2	TIAM2	modulates activity of RHO-like GTPases, connects extracellular signalling to cytoskeletal actions	ubiquituosly/ intracellular	liver cancer
Neurexin	NRXN1	synaptic cell adhesion, synaptic strength and maturation	neurons/ transmembrane	Schizophrenia, Autism, Tourette syndrom, AD
transmembrane protein with EGF-like and two follastin-like domains	TMEFF2	cell growth, differentiation, apoptosis; activates Akt and Erk signaling	brain/ transmembrane	tumor suppressor, AD
GABA receptor-associated protein-like 2	GABA RAPL2	protein transport, formation of the autophagosome	ubiquitously/ Golgi, cytopl. vesicles	defense against oxidative stress

4.4. Preliminary Validation of Y2H Hits

The putative interaction between GRN and two of the candidate proteins from the Y2H screen was further investigated by functional assays and by co-immunoprecipitation (Co-IP).

DKK1 is a secreted protein that could potentially interact with GRN in the secretory pathway or the extracellular space, and interaction between GRN and the WNT signaling pathway has been proposed (de la Encarnacion et al., 2016; Raitano et al., 2015; Rosen et al., 2011). There are four different DKK members in the human genome and they have different activities (Wu et al., 2000). DKK1 is a negative regulator of Wnt signaling (Glinka et al., 1998; Niehrs, 1999). It is secreted and interacts in the extracellular space with the Wnt co-receptor LRP (Bafico et al., 2001; Mao et al., 2001; Semenov et al., 2001). After binding of the growth factor Wnt to its receptor Frizzled (FZD), the activated receptor forms a complex with either LRP5 or 6 and stimulates the canonical Wnt-beta-catenin pathway. DKK1 is thought to inhibit this stimulation by disrupting the FZD-LRP complex (Bafico et al., 2001) A well-known downstream target of the canonical Wnt pathway is a protein called β-catenin. Upon activation of the pathway, β-catenin degradation is reduced and the protein accumulates in the cytosol. This increase in β-catenin levels is easily detectable via Western blot analysis (Corr, 2008; Metcalfe and Bienz, 2011; van Noort et al., 2002).

To investigate a possible effect of GRN on the canonical Wnt pathway through interaction with DKK, the human monocyte cell line THP-1 was treated for 24 hours with recombinant Wnt3a, DKK1, GRN or granulins (grn) or combinations of these proteins, followed by cell lysis and Western blot analysis of β-catenin levels (Figure 4.20). As expected, the agonist Wnt3a caused a significant increase of β-catenin levels in the treated cells compared to the untreated control cells. Treatment with the antagonist DKK1 alone did not show an effect on β-catenin levels. However, DKK1 blocked the increase in β-catenin levels by Wnt3a when applied in combination (Figure 4.20 B, 1-4). Treatment of THP-1 cells with GRN or grn alone had no effect on β-catenin levels (Figure 4.20 B, 5-6). When GRN or grn were applied in combination with Wnt3a, the β-catenin levels were increased to similar levels as with Wnt3a treatment alone (Figure 4.20 B, 7-8). Importantly, when Wnt3a, DKK1 and GRN or grn were applied in the same experiment (Figure 4.20 B, 9-10), DKK1 was still able to antagonize the actions of Wnt3a and the β-catenin levels were comparable to the untreated control cells or cells treated with the combination of DKK1 and Wnt3a. Taken together, these experiments did not show any effects of recombinant GRN or grn on the Wnt pathway. In addition, they failed to provide evidence for any functional interaction with DKK1, as DKK1 was still able to antagonize Wnt signaling in the presence of GRN or grn. Obviously, these experiments do not rule a physical interaction between GRN and DKK1 as suggested by the results of the

Y2H screening. However, if such an interaction occurs, it does not seem to affect the function of DKK1 in the canonical Wnt signaling pathway.

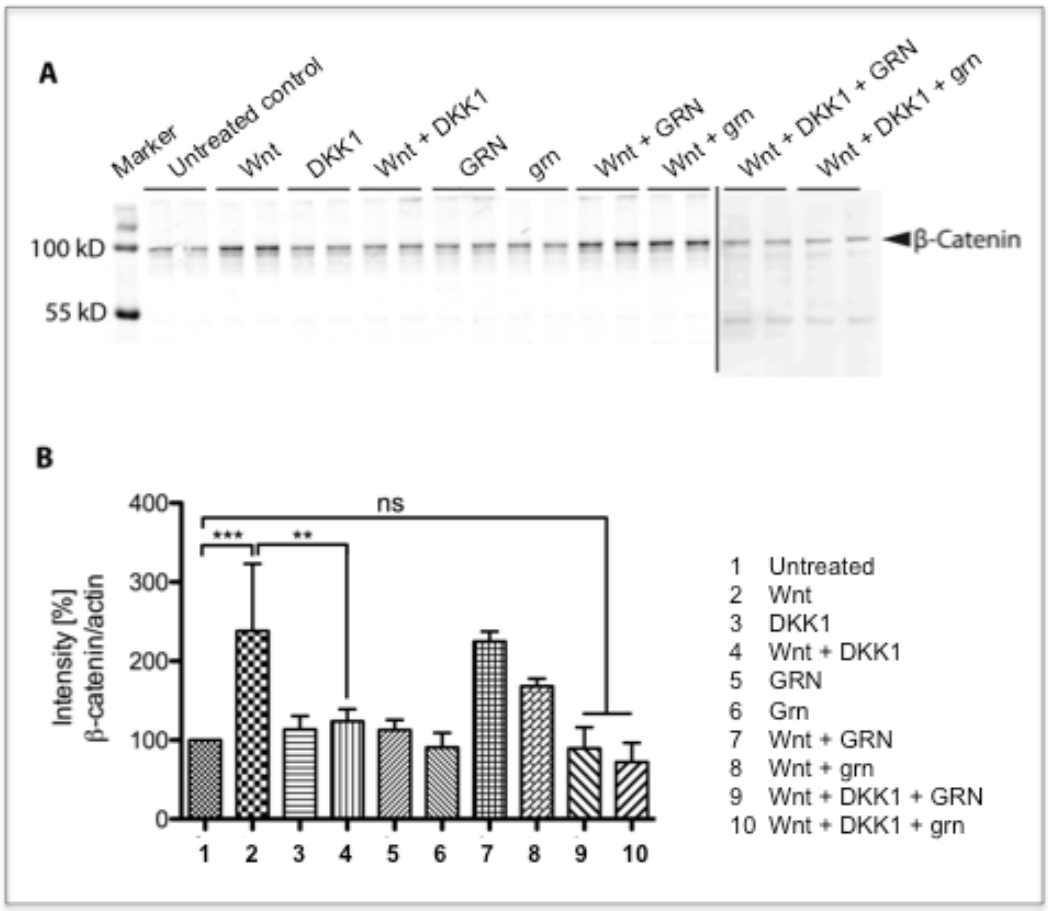

Figure 4.20: Wnt signaling assay **A) β-catenin protein levels as determined by Western blotting.** 2.5 x 10^5 THP-1 cells were seeded in 500 µL RPMI buffer in 24-well cell culture plates. After 24 h the cells were treated with Wnt3a (250 ng/µL), Dkk1 (1 µg/µL), GRN (1 µM), or grn (1 µM), and combinations thereof. After additional 24 h of incubation, the cells were harvested and lysed in 40 µL RIPA buffer. 8 µg of total protein were loaded per lane onto a 12 % BisTris-SDS-PAGE. The Western blots were probed with an antibody against β-catenin (BD Biosciences). **B) Quantification of β-catenin protein levels.** β-catenin signals from Western blot membranes were quantified with the ImageStudio software from LI-COR Biosciences and normalized to actin protein levels. Data were analyzed by one-way ANOVA with Tukey post-tests in GraphPad Prism software. Results from 3 independent experiments with 2 technical replicates per condition are shown.

The second hit from the deltaF-GRN Y2H screen that was further investigated was the transmembrane protein with EGF-like and two follastin-like domains (TMEFF2). TMEFF2 is a type-I transmembrane protein with a receptor-like structure and a large, glycosylated extracellular domain. TMEFF2 is exclusively expressed in the brain and the prostate and is able to activate both the PI3K/Akt and MAPK/ERK signaling pathways (Chen and Ruiz-Echevarria, 2013). Co-IP experiments were performed in order to validate the interaction between GRN and TMEFF2. A TMEFF2 cDNA was purchased, amplified by PCR and cloned into the pLHCX retroviral vector via HindIII and ClaI restriction sites. A C-terminal V5 tag was

added for easier detection and immunoprecipitation. Murine hippocampal HT22 cells were transiently transfected with the pLHCX-TMEFF-V5 construct and cell lysates were prepared. The lysates were pre-incubated with protein A/G agarose beads to capture non-specifically binding proteins in the lysates. Recombinant full-length GRN was added to the cleared lysates and the mixture was incubated to enable binding of GRN to TMEFF2. Subsequently, anti-V5 antibody was coupled to NHS-Sepharose and added to immunoprecipitate the V5-tagged TMEFF2. The immunoprecipitated material was eluted by boiling the sepharose and analyzed by Western blotting with anti-V5 and anti-GRN antibodies (Figure 4.21).

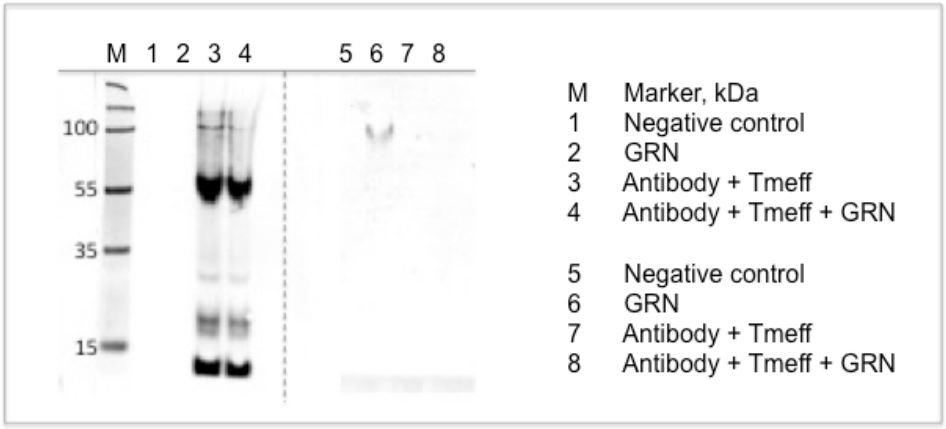

Figure 4.21: CoIP experiment to validate the putative interaction between GRN and TMEFF2. Recombinant GRN protein was incubated with cell lysates of HT22 cells transiently transfected with the pLHCX-TMEFF2-V5 construct. The mixture was immunoprecipitated with anti-V5 antibody coupled to NHS-Sepharose, and the precipitated material was analyzed by Western blotting with anti-V5 (lanes 1-4) or with anti-GRN antibodies (lanes 5-8). The TMEFF2 protein was detected at > 55 kDa only in lysates of transfected HT22 cells (lanes 3, 4) but not in control cells (lanes 1, 2). Weak unspecific binding of GRN to the NHS-Sepharose was detected when GRN was incubated with only the beads (lane 6). When GRN was incubated with cell lysates from TMEFF2 transfected cells, no GRN protein was detected after immunoprecipitation with anti-V5 antibody (lane 8), indicating no interaction between GRN and TMEFF2.

The Western blot analysis showed that the TMEFF protein was successfully expressed in the transfected cells (Figure 4.21, lane 3+4). Furthermore, only weak non-specific binding of GRN to the sepharose beads occured (lane 6). However, after incubation of transfected cell lysates with recombinant GRN and immunoprecipitation with anti-V5 antibody, no GRN protein was detected in the immunoprecipitated material (8). This indicated that GRN and TMEFF2 did not interact under the specific experimental conditions.

5. Discussion

The overexpression and purification of human recombinant GRN as well as the application of the purified protein in different assays has been reported in several studies. For the purification, in most cases a C-terminal 6xHis tag and NiNtA column material was employed (Gao et al., 2010; Gass et al., 2012a; Monami et al., 2006). Other laboratories purified GRN from cell culture supernatants after labeling with ^{35}S cysteine using ultrafiltration units and subsequent fractionation with a reverse-phased HPLC (He et al., 2003; Kessenbrock et al., 2008). The advantage of this technique is that it does not rely on a protein tag for purification, given the fact that fusing a peptide tag to the GRN protein is an artificial change to the native protein and always harbors the risk of interference with protein structure and binding to interaction partners. However, many laboratories have successfully used C-terminally tagged GRN protein in bioactivity assays. As a cellular system for expression, mostly transiently or stably transfected Hek293 or Cos7 cells have been used, and the secreted GRN was purified from conditioned serum-free medium. Consequently, the experimental outline to purify the recombinant GRN in this study was loosely based on these successful examples.

Unexpectedly, the purification procedure, although described many times by various laboratories, was not trivial to reproduce. In a first attempt at purification, human GRN was expressed from the pCDNA3 expression plasmid with three C-terminal tags, namely V5, 6xHis, and GB1. Initially, IgG coupled beads were used to purify the GRN protein via its GB1 tag. The construct was transfected either transiently or stably into Cos1 cells and the cells were incubated with serum-containing medium to collect the secreted GRN protein. However, this strategy was not successful yielding very low protein concentrations and insufficient purity. Hence, several changes were made to improve the expression and purification procedure. First, a different cell line was used for the expression of GRN. A Hek293T cell line stably transfected with the GRN-6xHis-V5-GB1 construct showed markedly stronger expression of the recombinant protein as compared to the COS1 cell line. Second, the affinity resin was changed. In subsequent experiments GRN was purified with NiNtA agarose via its His-tag. Third, a peristaltic pump drive was used to allow very slow application of medium onto the column to prevent the wash-out of bound GRN. However, the commercial NiNtA column connected to the pump drive was only useable with GRN in serum-free medium. This limitation was due to the fact that bovine serum albumin as the major protein component in serum-containing medium was getting trapped in the column and that elongated or harsher washes eliminated the bound GRN. This seemed like a reasonable

modification to the purification method as most publications that had previously reported the purification of recombinant GRN had also used serum-free medium to collect the protein (Gao et al., 2010; Gass et al., 2012a; He et al., 2003; Kessenbrock et al., 2008; Monami et al., 2006). However, during these experiments it was observed that GRN protein purified from serum-free medium had a smaller size on Western blots compared to GRN protein purified from complete medium (see figure 4.6). GRN is known to have multiple N-glycosylation sites (Songsrirote et al., 2010; Zhou et al., 1993) and reduced glycosylation as the result of expression in serum-free medium would reduce the molecular weight of the protein (Zhou et al., 1993). This was subsequently proven in de-glycosylation assays in which GRN expressed in serum-containing and serum-free conditions and separated on SDS-gels was reduced to the same molecular weight. Since reduced glycosylation might impair the bioactivity of the recombinant protein (Deribe et al., 2010), it was decided to further optimize the GRN purification procedure for serum-containing medium. This made it necessary to apply the NiNtA agarose in batch mode instead of the automated loading of the NiNtA column with the peristaltic pump. Finally, to improve the affinity of the recombinant protein to the NiNtA resin and to allow harsher washing conditions, the 6xHis-V5-GB1 tag was replaced with a 12xHis tag at the C-terminus of GRN and new stable Hek293T cells were generated with a retroviral expression system. This optimized purification protocol resulted in highly pure and concentrated recombinant protein. The determination of exact protein concentrations was now possible and enabled the quantitatively accurate treatment of cells with recombinant GRN in the subsequent bioactivity assays.

In vitro assays with cultured cell lines of various origins have played an important role in discovering and understanding the biological functions of the GRN protein and the proteolytically derived granulin peptides. Most consistently, a mitogenic effect of GRN has been reported in many studies in response to either GRN overexpression or exogenous treatment with purified recombinant GRN (He and Bateman, 1999; Monami et al., 2009; Wang et al., 2003). In addition, it has also been shown that the depletion of endogenous GRN expression with antisense methods, or the inactivation of secreted GRN with anti-GRN antibodies resulted in reduced cell proliferation of various cancer cell lines (Cheung et al., 2004; Ho et al., 2008; Liu et al., 2007; Lu and Serrero, 2000). To establish a bioactivity assay for our recombinant GRN protein expressed in HEK293 cells, we tried to reproduce the mitogenic effect of purified recombinant GRN protein on SW13 cells, which was previously shown by He and Bateman (He and Bateman, 1999). However, no mitogenic effects of GRN were observed under conditions precisely matching the experiments described by He and Bateman (He and Bateman, 1999). Even with an elongation of the treatment period (from 3 to 5 days) and significantly increased GRN protein concentrations (from 70 nM to 1 µM)

compared to the protocol by He and Bateman, no significant effect on the growth of the cells was seen. Stimulating SW13 cells with recombinant GRN protein would model the paracrine influence of extracellular GRN on neighboring cells and tissues. In addition, GRN has been proposed to support the survival of cells in an autocrine fashion. For example Ryan et al. used the motor neuron cell line NSC34 and compared cells with stable overexpression of GRN fused at the C-terminus to GFP to empty vector control cells. In these experiments, overexpression of the GRN fusion protein resulted in markedly increased survival of NSC34 cells and a strongly reduced number of apoptotic cells in long-term serum-free cultures (Ryan et al., 2009). Similarly, GRN was shown to support the survival of primary motor neurons in culture (Gao et al., 2010; Ryan et al., 2009; Van Damme et al., 2008). We used Hek293T cells with stable expression of GRN-12xHis and compared them to the parental Hek293T cells either growing under serum-free conditions or in serum-containing medium. No differences in survival were observed. The reasons for the failure to reproduce the results from the literature are currently unknown. Generally, it is not unusual that different batches of a purified protein display different levels of bioactivity. For example, Jian et al. reported that different batches of GRN purchased from R&D Systems showed different binding affinities to TNFR in solid phase binding assay (Jian et al., 2013). Variations in binding and bioactivity were also observed for recombinant batches of perlecan, which has been identified as a GRN interaction partner, when purified from different cell types or using different expression systems (Gonzalez et al., 2003; Knox et al., 2005; Knox et al., 2002; Whitelock et al., 1999). With our purification protocol it was possible to express GRN in complete medium, to generate GRN protein batches of high purity, and to precisely determine the concentrations of the recombinant protein. Consequently, the proliferation assays were performed with recombinant GRN protein of high purity and with exact treatment concentrations. Furthermore, purification via a C-terminal His-tag using NiNtA had also been previously used to successfully generate bioactive GRN protein (Gao et al., 2010; Monami et al., 2006) and even a GRN-GFP fusion protein was able to support the survival of cells (Ryan et al., 2009). Obviously, the choice of the specific cell line can have a major impact on the outcome of proliferation or survival assays. In the survival assay, we used HEK293 cells, which like SW13 cells are of epithelial origin but whose response to GRN had not been previously investigated. In summary, our experiments clearly demonstrate that it is not trivial to express and purify GRN and to prove its bioactivity *in vitro*.

GRN might also be involved in the generation of reactive oxygen species and it has been proposed to protect cells from oxidative stress. Kessenbrock et al. have described that GRN bound to the cell surface of neutrophils prevents these cells from initiating an oxidative burst. In neutrophils, reactive oxygen species are produced by the membrane-bound NADPH

oxidase complex and are released into the extracellular space to kill pathogens such as invading bacteria (Kessenbrock et al., 2008; Nathan and Shiloh, 2000). When GRN is cleaved by neutrophil elastase or other protease into granulins, NADPH oxidase becomes activated and the oxidative burst by neutrophily proceeds. Other studies have shown that GRN was able to protect rat primary cortical neurons from H_2O_2 or the oxidative stress inducing toxin MPP, the active derivative of 1-methyl-4-phenyl-1,2,3,6- tetrahydropyridine (MPTP). This prompted us to test whether GRN might be able to protect the murine hippocampal cell line HT22 from oxidative stress induced by excessive concentrations of extracellular glutamate (Davis and Maher, 1994). HT22 cells express the system x_c antiporter responsible for the import of extracellular cystine in exchange for glutamate. Cystine is used by cells to synthesize glutathione, which is an essential molecule in the cellular antioxidant defense system. Treatment of HT22 cells with mM concentrations of glutamate blocks the system x_c antiporter and cystine can no longer be imported into the cell. This results in low intracellular levels of glutathione that are not sufficient to eliminate accumulating reactive oxygen species (ROS), finally leading to cell death (Lewerenz et al., 2013). In this assay we were indeed able to observe protective effects of the recombinant GRN protein. After failing to detect any protective activity of the full-length GRN protein, granulin peptides were generated by *in vitro* proteolysis of GRN with neutrophil elastase (NE). Treated with granulins, the HT22 cells were able to survive glutamate concentrations of up to 1.5 mM, a glutamate concentration that killed around 50% of the untreated control cells. While it is surprising that not the full-length GRN protein but the granulin peptides were protective in this assay, other studies have reported similar findings. Gass et al. have reported that GRN is able to promote neurite outgrowth and branching in primary neuronal cultures (Gass et al., 2012a; Van Damme et al., 2008). They also proposed that this neurotrophic function of GRN is dependent on cleavage of GRN into granulin peptides as no effect was observed when the cells were treated with recombinant GRN in the presence of SLPI, which binds to GRN and blocks its proteolysis (Gass et al., 2012a; Van Damme et al., 2008). Similar effects were also reported by Van Damme et al. in a survival assay with rat cortical neurons and motor neurons. These cells were treated either with recombinant full-length GRN or a commercially available granulin E peptide under serum-free condition. Both proteins supported neuronal survival but the supportive effect of full-length GRN was abolished when SLPI was added (Gass et al., 2012a; Van Damme et al., 2008). One possible explanation for the observed bioactivity of both full-length GRN and granulin peptides in these bioassays is that certain cell lines might have the ability to cleave the precursor protein into the granulin peptides. However, when we treated HT22 cells with full-length GRN and analyzed the tissue culture supernatants at the end of the glutamate toxicity experiments by Western blotting, no granulins or GRN fragments could be detected (see figure 4.2.4). Thus, HT22 cells might not

be able to cleave GRN and this could potentially explain why only granulin peptides but not full-length GRN were able to protect the cells from oxidative stress. Aside from this issue, important questions about the actions of GRN in this bioassay remain. First, it is unclear which of the granulin domains is responsible for the protective effects, and whether a single domain is sufficient or whether several granulin peptides have synergistic protective effects. To address this question, individual granulin domains could be expressed and purified in HEK293 cells in a similar fashion to the full-length GRN protein, and the recombinant peptides could then be tested individually or in combination in the HT22 assay. Second, the intracellular signaling events through which granulin peptides protect HT22 cells from the oxidative glutamate toxicity are unknown. One possibility is that granulins are able to directly suppress increased ROS production after glutamate treatment. This could me mechanistically similar to the previously reported control by GRN over the oxidative burst in neutrophils (Kessenbrock et al., 2008; Nathan and Shiloh, 2000). Alternatively, granulins might stimulate other signaling pathways that indirectly promote cellular survival. It has been demonstrated that activation of protein kinase C can protect HT22 cells from glutamate toxicity and that downstream activation of ERK1/ERK2 was essential for cell protection (Maher, 2001). Intriguingly, ERK1/ERK2 activation by GRN has been previously reported in several different cell types (Feng et al., 2010; Gao et al., 2010; Xu et al., 2011) but it is unclear whether granulins are also able to stimulate this pathway. Finally, it is not known how granulins interact with the cell surface of HT22 cells. Granulins are small peptides but their size of around 6 kDa makes it unlikely that they enter cells by diffusion. Instead, a cell surface receptor is likely involved that could be shared with the full-length GRN protein or might be unique to the granulin peptides. Importantly, it might be possible to adapt the HT22 bioassay for genetic screening by RNA interference (RNAi) to identify a granulin receptor in future studies.

Various techniques exist to detect protein-protein interactions including co-immunoprecipitation (Co-IP), tandem affinity purification (TAP), surface plasmon resonance spectroscopy, fluorescence resonance energy transfer (FRET), and mass spectrometry. Not all of these methods are suitable to detect novel protein-protein interactions, and some require laborious optimization and the availability of highly expensive equipment. To search for novel interaction partners of GRN, the choice was made to use the Y2H system. The Y2H is a cell-based technique, in which a protein of interest is screened against a cDNA library encoding unknown proteins. First, as described in chapter 4.3, the experimental set-up was tested with a bait protein for which strong interaction partners are known, the cytosolic C-terminus of the amyloid precursor protein (APP). Importantly, the APP C-terminus had previously been used successfully in several Y2H screens to detect novel and known interaction partners of APP like Fe65, its homolog FE65L1, X11 and JIP-1 (Hao et al., 2011)

(Duilio et al., 1998; Guenette et al., 1996; Zambrano et al., 1997). In accordance with Hao *et al*., the C-terminal 46 amino acids of APP were cloned in the bait vector and expression of the bait protein in yeast was confirmed by Western blotting. The bait protein was screened against a normalized human brain library and positive yeast colonies were analyzed by DNA sequencing. Out of 105 sequenced individual clones 5 encoded parts of the Fe65L1 protein in frame with the activation domain of the prey plasmid. All 5 clones showed substantial sequence overlap and contained the complete sequence of the PTB2 domain of Fe65L1, which had been found to interact with an Asn-Pro-X-Tyr motif at the C-terminus of APP (McLoughlin and Miller, 2008) (Duilio et al., 1998; Guenette et al., 1996; Zambrano et al., 1997). Taken together, the APP C-terminus test screen showed that the Y2H system was successfully established in the laboratory. The screen also showed that a careful analysis of positive clones is essential. The reporter genes used in the Y2H system can be auto-activated by prey proteins through various mechanisms. Retransformation control experiments revealed that two positive hits from the APP C-terminus screening, PGM1 and COP9 activated the reporter genes independently of the bait protein, leading to a false positive read-out.

To screen for interaction partners of GRN, the human full-length GRN sequence lacking the N-terminal signal sequence (first 17 amino acids) was cloned into the bait vector (GRN-FL bait), and its expression was confirmed by Western Blot analysis of yeast cell lysates. The usability of this protein for the Y2H screen was investigated by checking the activation status of the Y2H reporter genes in the absence of any prey protein. Therefore, Y2H Gold cells were transformed with the GRN-FL bait plasmid and plated on selection plates. Unfortunately, the GRN-FL bait protein showed full activation of the Aureobasidin reporter, which selects for resistance against the antibiotic Aureobasidin A and is considered the most stringent reporter in the Matchmaker® Gold Y2H system. To circumvent this problem, an Aureobasidin A gradient was tested ranging from 125-500ng/ml. However, even at the highest Aureobasidin A concentration the number of yeast colonies that appeared on the plate was not reduced, which made it impossible to screen the GRN-FL bait. In order to identify the auto-activating domain and to remove it from the bait, 12 deletion mutants were generated and tested for auto-activation. The evaluation of the different GRN fragments revealed that all bait constructs containing the granulin domain F auto-activated the Aureobasidin A reporter. To obtain the most complete GRN bait possible, a deletion mutant exclusively lacking the auto-activating domain F was cloned and tested. This bait was detectable by Western blotting and showed no auto-activation of the Y2H reporter genes. In the subsequent screening against the cDNA library constructed from male human brain tissue, more than 400 positive diploids were analyzed by colony PCR and sequenced to

identify the captured prey proteins. The sequencing data identified 323 different proteins that were categorized and rated. Only for 10 of these proteins the following criteria were fulfilled: 1) The prey cDNA fragments were cloned in frame with the Gal4 DNA-activation domain of the prey expression vector. 2) The protein fragments encoded by the prey clones displayed a cellular localization that would allow interaction with GRN in the secretory pathway or in the extracellular space. 3) The prey clones were not auto-activating when retransformed into Y2H Gold cells. Co-transformation experiments confirmed the final candidates as true positives as no colonies grew on selection plates when the empty bait plasmid was co-transformed with the respective prey plasmids. The following proteins were identified as potential interaction partner of GRN in the Y2H screen:

Versican (VCAN)

Versican, also known as chondroitin sulfate proteoglycan 2, is the largest member of the lectican protein family. It has a molecular mass of over 1000 kDa and consists of N- and C-terminal globular domains and two chondroitin sulfate domains. At least four isoforms exist, but versican V2 is the main constituent of the mature brain extracellular matrix (ECM) (Schmalfeldt et al., 1998). V1, mainly expressed in late embryonic development, and V2, mainly expressed in the mature brain, seem to have mostly opposing functions, with a central role in controlling the structure and function of neurons and synapses. V2 has an inhibitory effect on neurite and axonal outgrowth (Dours-Zimmermann et al., 2009; Schmalfeldt et al., 1998) and overexpression causes apoptotic sensitivity (LaPierre et al., 2007; Sheng et al., 2005). V2 accumulation leads to disruption of cell adhesion (DeWitt et al., 1993). In contrast, V1 enhances cell proliferation, protects from apoptosis and induces neuronal differentiation (LaPierre et al., 2007; Sheng et al., 2005; Wu et al., 2009). Versican also plays a key role in inflammation through the interaction with chemokines and the adhesion molecules on the surface of inflammatory leukocytes (Kim et al., 2009). In cancer, Versican might play a role in malignant transformation, tumor progression and metastasis, and increased expression has been observed in a variety of malignant tumors (Du et al., 2013). Furthermore, *in vitro* studies have shown that chondroitin sulfate chains and glycosaminoglycans promote the aggregation of Aβ peptides (Castillo et al., 1999; Cotman et al., 2000; McLaurin et al., 1999; van Horssen et al., 2003). In summary, versican appears to have some functional overlap with GRN and neurodegenerative diseases. However, no connection between GRN and versican has been made so far.

Selenoprotein P (SEPP1)

Selenoprotein P is a secreted glycoprotein and a unique member of the selenoprotein family as it contains multiple selenocysteine residues (Burk and Hill, 2009). This protein family is

one of the primary lines of defense against oxidative stress. In the CNS, SEPP1 binds to the apolipoprotein E receptor-2 and is taken up into neurons, delivering selenium for selenoprotein synthesis (Burk et al., 2007). Selenoprotein synthesis is especially important for the proper function of parvalbumin (PV) interneurons. These inhibitory GABAergic neurons coordinate brain activity via synchronizing spike activities within neuronal populations and by restricting the firing rates of pyramidal neurons (Freund and Katona, 2007; Wulff et al., 2009). PV interneurons are particularly sensitive to oxidative stress (Behrens et al., 2007; Kinney et al., 2006) and SEPP1 knock-out mice showed impairments in contextual fear extinction, latent inhibition and sensorimotor gating (Pitts et al., 2012). Inflammation might alter the activity of the SEPP1 promoter, which interacts with cytokine and growth factor pathways (Al-Taie et al., 2002; Dreher et al., 1997; Mostert et al., 2001). The absence of SEPP1 increases the risk of several cancers like lung cancer, prostate cancer or breast cancer (Epplein et al., 2014; Geybels et al., 2014; Pellatt et al., 2013). SEPP1 is ubiquitously expressed and is thought to serve as a storage tool for selenium in the brain. The importance of selenium in the brain is supported by the fact that the organism maintains brain selenium at the expense of other tissues (Nakayama et al., 2007) and by the observation of serious brain injury after a selenium deficit (Hill et al., 2004). Loss of functional SEPP1 was shown to cause severe selenium deficiency leading to neurodegeneration (Valentine et al., 2008). Consequently, this protein is very important for the CNS and has potential functional overlap with GRN in inflammation, oxidative stress, cancer and neurodegeneration.

Dickkopf Wnt signaling pathway inhibitor 1 (DKK1)

DKK1 is a secreted protein and an antagonist of the Wnt signaling pathway. The Wnt signaling pathway was first identified in carcinogenesis but was subsequently discovered to regulate important processes during embryogenesis like axis determination (Ulloa and Briscoe, 2007; Zou, 2004), cell fate specification (Gilbert et al., 2010; Nusse, 2008), proliferation (Kaldis and Pagano, 2009; Willert and Jones, 2006) and migration (Schambony et al., 2004). The pathway is activated by binding of a soluble Wnt ligand to a Frizzled receptor at the cell surface. Signaling is facilitated by co-receptors including the lipoprotein receptor-related proteins 5 and 6 (LRP5, LRP6). After signal transduction from Frizzled to the cytoplasmic phospho-protein Dishevelled, the signal can branch into several different pathways (Habas and Dawid, 2005). DKK1 acts as an antagonist of Wnt signaling by binding LRP5/LRP6 and blocking their co-receptor function. Growing evidence connects the Wnt signaling pathway to FTD and also directly to GRN (Rosen et al., 2011; Wexler et al., 2011; Wiedau-Pazos et al., 2009). In cultured cells, down regulation of GRN expression resulted in enhanced Wnt signaling and this was accompanied by up regulation of the Wnt receptor

Frizzled-2 (FZD2) (Rosen et al., 2011). Hence, the potential interaction between GRN and DKK1 could provide another connection between GRN and the Wnt signaling pathway.

Phospholipase A2 (PLA2G12A)

The general function of this phospholipase is to release arachidonic acid and lysophospholipids from phospholipids. Subsequent modification of arachidonic acid by cyclooxygenases leads to the generation of eicosanoids including prostaglandins and leukotrienes. These molecules are known as inflammatory mediators (Dennis, 1994). The activity of the enzyme is tightly regulated. It is activated upon phosphorylation through MAPK and inhibited through the release of lipocortin, which is stimulated by glucocorticoids (Leslie, 1997). Secreted PLA2 is believed to contribute to various inflammatory diseases and has been shown to exert increased activity in the CSF of AD patients and multiple sclerosis (MS) patients (Chalbot et al., 2011). The enzyme has been suggested as a biomarker for leakage of the blood brain barrier (Chalbot et al., 2011).

TIMP metallopeptidase inhibitor (TIMP4)

Matrix metalloproteinases are zinc dependent endopeptidases involved in the degradation of the extracellular matrix. MMPs cleave cell surface receptors and inactivate chemokine/cytokine activation. Furthermore, they are involved in biological processes like proliferation, migration, differentiation, angiogenesis, apoptosis and host defense (Van Lint and Libert, 2007). Due to their important role in tissue remodeling, they are also thought to be important for metastasis, rheumathoid arthritis and chronic cardiovascular diseases (Snoek-van Beurden and Von den Hoff, 2005). The specific endogenous tissue inhibitors of metalloproteinases (TIMPs) inhibit the MMPs and include TIMP-1 to -4. They irreversibly inactivate MMPs by binding to their catalytic zinc cofactor (Clark et al., 2008). They are involved in immune responses, inflammatory actions, wound healing, angiogenesis and tumorigenesis (Bourboulia and Stetler-Stevenson, 2010; Lambert et al., 2004; Pilcher et al., 1999). Specific for the CNS is their involvement in synaptic plasticity and neuronal cell differentiation (Candelario-Jalil et al., 2009; Crocker et al., 2004). TIMP-4 expression is inducible and the 25kDa protein is secreted and soluble (Gomez et al., 1997; Swarnakar et al., 2011). TIMP-4 expression has been detected in the brain, heart, ovary and skeletal muscle (Leco et al., 1997; Melendez-Zajgla et al., 2008). TIMP4 overexpression was shown to inhibit growth and invasion of tumor cells (Lee et al., 2006; Wang et al., 1997). Paradoxically, TIMP4 was strongly expressed in human gliomas, possibly representing a defense mechanism as in functional studies TIMP-4 had only shown tumor suppressing features (Groft et al., 2001).

Leucine rich repeat neuronal 3 (LRRN3)

Leucine-rich repeat (LRR) domain proteins contain highly hydrophobic amino acids and a repeat structure consisting of about 24 residues (Rothberg et al., 1990). Neuronal LRRs (LRRN) have been proposed to function as adhesion molecules or as soluble receptors. However, not much is known about their biological activities. One study showed that stimulation of cells with low concentrations of epidermal growth factor (EGF) resulted in LRRN3 mediated MAPK phosphorylation (Fukamachi et al., 2002). LRRN3 is a highly conserved type I transmembrane protein of 80kDa containing 12 leucine-rich repeats. Highest expression is found in the brain, predominantly in the cerebral cortex, hippocampus, cerebellar cortex and paraflocculus, suggesting functions in cognition, language, memory and oculomotor behavior. Furthermore, it was shown that low expression of LRRN3 in neuroblastomas correlated with a poor prognosis of patients (Akter et al., 2011).

T-Cell Lymphoma Invasion and Metastasis 2 (TIAM2)

This 190kDa protein is a guanine nucleotide exchange factor, which modulates the activity of Rho-like GTPases and connects extracellular signaling to cytoskeletal changes. TIAM2 was shown to mediate lamellipodia and growth cone formation in embryonic hippocampal neurons (Matsuo et al., 2003), to regulate cell migration (Rooney et al., 2010) especially of cortical neurons (Kawauchi et al., 2003), to promote neurite growth (Goto et al., 2011; Matsuo et al., 2002), and to enhance proliferation and invasion of liver cancer cells (Chen et al., 2012).

Neurexin (NRXN1)

Neurexin is a presynaptic transmembrane protein involved in synaptic cell adhesion. The intracellular domain interacts with proteins involved in exocytosis (Li et al., 2006), while the extracellular part of neurexin interacts with proteins in the synaptic cleft, mainly neuroligins. This interaction connects two neurons and results in the formation of a synapse (Scheiffele et al., 2000). Neurexins enable signaling across the synapse and are structurally similar to other proteins responsible for axon guidance and synaptogenesis. Neurexins are expressed by neurons of every receptor type and become concentrated at presynaptic terminals when neurons mature. Expression of neurexin can be induced by neuroligin, and neurexin can induce the expression of neuroligin (Knight et al., 2011). This protein pair was found to be important for synapse maturation and strength, but they are not required for synaptic formation (Knight et al., 2011). Furthermore, they can induce neurite outgrowth (Gjorlund et al., 2012). Mutations in neurexin are linked to schizophrenia, autism and intellectual disability. A neurexin deletion was shown to cause Tourette syndrome (Duong et al., 2012; Sudhof, 2008; Walsh et al., 2008).

Transmembrane Protein with EGF-like and Two Follastin-like Domains (TMEFF2)

TMEFF2, also known as Tomoregulin-2, is a type-I transmembrane protein with two follastin modules, a unique epidermal growth factor (EGF) domain, and a short, highly conserved cytoplasmic tail. It is predominantly expressed in the brain and might function as a neurotrophic factor. TMEFF2 was found to stimulate phosphorylation of the ErB-4 receptor, suggesting a role in cell growth, differentiation or apoptosis (Uchida et al., 1999). Furthermore, it might act as a survival factor for hippocampal and mesencephalic neurons and promote cancer progression (Glynne-Jones et al., 2001; Horie et al., 2000; Mohler et al., 2002; Young et al., 2001). However, more recent studies have reported TMEFF to be downregulated in cancer and tumor cell lines, indicating that TMEFF could be a tumor suppressor that inhibits cell migration and invasion by its cytoplasmic tail (Chen et al., 2014). TMEFF2 was also shown to activate Akt and ERK signaling (Chen and Ruiz-Echevarria, 2013). Amyloid plaques in Alzheimer's disease contain high levels of TMEFF2 that might contribute to plaque formation and disease progression (Siegel et al., 2006).

GABA receptor-associated protein-like 2 (GABARAPL2)

GABARAPL2 is a ubiquitin-like protein that is part of the ATG8 conjugation system, which is necessary for the formation of the autophagosome (Kraft et al., 2012; Slobodkin and Elazar, 2013). GABARAPL2 is also involved in mitochondrial autophagy (mitophagy), which leads to the selective degradation of dysfunctional mitochondria as a defense mechanism against reactive oxygen species (Ambivero et al., 2014; Frank et al., 2012). GABARAPL2 is a well-known false positive hit in Y2H screens. However, it did not show auto-activation in our experiments and could represent a promising interaction partner as GRN appears to regulate lysosomal biogenesis and function (Kao et al., 2017).

Evidently, the results of the Y2H screen have to be further validated. GRN is a secreted protein whose folding is very likely dependent on the formation of intermolecular cysteine bridges. These post-transitional modifications cannot occur in the reducing environment of the yeast nucleus. This means that secreted proteins are generally less suitable for Y2H screening, and that the GRN bait protein might have been partially or largely unfolded during the screening procedure. Nevertheless, several Y2H screens with GRN as a bait protein had been previously reported (Altmann et al., 2016; Hoque et al., 2003; Tang et al., 2011). The results of the Y2H screen confirmed a very large proportion of non-specific interactions. The vast majority of these were caused by prey cDNA clones that were not in frame with the Gal4 DNA-activation domain. This led to the translation of non-natural proteins that are likely unfolded with a high tendency to bind non-specifically to the bait protein. In addition, many

zinc finger transcription factors were identified, which caused auto-activation of the Y2H reporter genes in re-transformation experiments. Beyond that a smaller number of proteins were excluded because their cellular localization outside of the secretory pathway made an interaction with GRN improbable. For 2 of the 10 remaining candidate proteins preliminary validation experiments were performed that did not provide evidence for functional or physical interaction with GRN. For DKK1, a functional interaction with GRN was tested in a Wnt signaling activation assay. In this assay, treatment of a human monocyte cell line THP-1 with the known Wnt ligand Wnt3a resulted in post-translational stabilization of β-catenin, which is a central signaling molecule in the Wnt pathway. Treatment of THP-1 cells with DKK1, an antagonist of Wnt signaling (Glinka et al., 1998; Niehrs, 1999), blocked β-catenin accumulation as expected. However, treatment with GRN or granulins alone did not affect β-catenin protein levels and treatment in combination with Wnt3a and DKK1 did not reveal synergistic or antagonistic effects. These experiments addressed only one outcome of Wnt signaling and they did not exclude a physical interaction between DKK1 and GRN. Further bindings studies either with recombinant GRN and DKK1 *in vitro* or by co-transfection of both proteins into mammalian cells followed by co-immunoprecipitation experiments are clearly warranted. In addition, an interaction between GRN and TMEFF2 was investigated by co-immunoprecipitation. TMEFF2 is an attractive candidate protein, it has a receptor-like structure and it was shown to facilitate AKT and ERK signaling, two signaling pathways that were also stimulated by GRN in different cell lines (Chen and Ruiz-Echevarria, 2013) (Cuevas-Antonio et al., 2010; He et al., 2002; He et al., 2003; Ho et al., 2008; Lu and Serrero, 2001; Monami et al., 2009; Monami et al., 2006; Youn et al., 2009; Zanocco-Marani et al., 1999) (Kleinberger et al., 2010). HT22 cells with stable overexpression of V5-tagged TMEFF2 were generated and cell lysates were incubated with recombinant GRN. While overexpression of TMEFF2 could be confirmed by Western blotting, immunoprecipitation of TMEFF2 with anti-V5 antibody did not result in co-precipitation of GRN. These results did not support interaction between GRN and TMEFF2. However, it should be pointed out that the binding studies were performed with recombinant GRN, which might have lower affinity to physiological binding partners. Co-transfection experiments with GRN and TMEFF2 might circumvent this issue. In addition, only a limited number of buffer conditions were tested in the co-immunoprecipitation experiments. Therefore, the negative results should not be regarded as definitive.

In summary, to establish the Y2H method in our laboratory, the APP C-terminus was used as a bait and screened against a human brain cDNA library. In this screen, FE65L1, a known adapter protein that interacts with the APP C-terminus through a PTB domain, was repeatedly isolated, indicating that the multi-step Y2H procedure was successfully implemented. In the Y2H screen with GRN as a bait protein, a high background of non-

specific interactions was observed and only 10 proteins were classified as true positive hits with a cellular localization that would allow interaction with GRN in the secretory pathway or the extracellular space. Of these 10 candidate proteins, none had been described as an interaction partner of GRN before. However, 3 of 10 proteins had a receptor-like structure (TMEFF2, Neurexin, LRRN3), and for some of the candidate proteins functional overlap with GRN and involvement in cancer and neurodegenerative diseases had been previously described. Confirmation of GRN binding partners or receptors within this set of candidate proteins could lead to a better understanding of the physiological functions of GRN, and could provide a starting-point for the development of novel therapeutic interventions for neurodegenerative diseases and cognitive decline.

6. References

Ahmed, Z. (2007). Progranulin in frontotemporal lobar degeneration and neuroinflammation. Journal of neuroinflammation *4*, 7.

Ahmed, Z., Sheng, H., Xu, Y.F., Lin, W.L., Innes, A.E., Gass, J., Yu, X., Wuertzer, C.A., Hou, H., Chiba, S.*, et al.* (2010). Accelerated lipofuscinosis and ubiquitination in granulin knockout mice suggest a role for progranulin in successful aging. The American journal of pathology *177*, 311-324.

Akter, J., Takatori, A., Hossain, M.S., Ozaki, T., Nakazawa, A., Ohira, M., Suenaga, Y., and Nakagawara, A. (2011). Expression of NLRR3 orphan receptor gene is negatively regulated by MYCN and Miz-1, and its downregulation is associated with unfavorable outcome in neuroblastoma. Clinical cancer research : an official journal of the American Association for Cancer Research *17*, 6681-6692.

Al-Taie, O.H., Seufert, J., Mork, H., Treis, H., Mentrup, B., Thalheimer, A., Starostik, P., Abel, J., Scheurlen, M., Kohrle, J.*, et al.* (2002). A complex DNA-repeat structure within the Selenoprotein P promoter contains a functionally relevant polymorphism and is genetically unstable under conditions of mismatch repair deficiency. European journal of human genetics : EJHG *10*, 499-504.

Almeida, S., Zhang, Z., Coppola, G., Mao, W., Futai, K., Karydas, A., Geschwind, M.D., Tartaglia, M.C., Gao, F., Gianni, D.*, et al.* (2012). Induced pluripotent stem cell models of progranulin-deficient frontotemporal dementia uncover specific reversible neuronal defects. Cell reports *2*, 789-798.

Altmann, C., Hardt, S., Fischer, C., Heidler, J., Lim, H.Y., Haussler, A., Albuquerque, B., Zimmer, B., Moser, C., Behrends, C.*, et al.* (2016). Progranulin overexpression in sensory neurons attenuates neuropathic pain in mice: Role of autophagy. Neurobiology of disease *96*, 294-311.

Ambivero, C.T., Cilenti, L., Main, S., and Zervos, A.S. (2014). Mulan E3 ubiquitin ligase interacts with multiple E2 conjugating enzymes and participates in mitophagy by recruiting GABARAP. Cellular signalling *26*, 2921-2929.

Andersen, J.K. (2004). Oxidative stress in neurodegeneration: cause or consequence? Nature medicine *10 Suppl*, S18-25.

Ash, P.E., Zhang, Y.J., Roberts, C.M., Saldi, T., Hutter, H., Buratti, E., Petrucelli, L., and Link, C.D. (2010). Neurotoxic effects of TDP-43 overexpression in C. elegans. Human molecular genetics *19*, 3206-3218.

Ashcroft, G.S., Lei, K., Jin, W., Longenecker, G., Kulkarni, A.B., Greenwell-Wild, T., Hale-Donze, H., McGrady, G., Song, X.Y., and Wahl, S.M. (2000). Secretory leukocyte protease inhibitor mediates non-redundant functions necessary for normal wound healing. Nature medicine *6*, 1147-1153.

Baba, T., Hoff, H.B., 3rd, Nemoto, H., Lee, H., Orth, J., Arai, Y., and Gerton, G.L. (1993). Acrogranin, an acrosomal cysteine-rich glycoprotein, is the precursor of the growth-modulating peptides, granulins, and epithelins, and is expressed in somatic as well as male germ cells. Molecular reproduction and development *34*, 233-243.

Bafico, A., Liu, G., Yaniv, A., Gazit, A., and Aaronson, S.A. (2001). Novel mechanism of Wnt signalling inhibition mediated by Dickkopf-1 interaction with LRP6/Arrow. Nature cell biology *3*, 683-686.

Baker, M., Mackenzie, I.R., Pickering-Brown, S.M., Gass, J., Rademakers, R., Lindholm, C., Snowden, J., Adamson, J., Sadovnick, A.D., Rollinson, S.*, et al.* (2006). Mutations in progranulin cause tau-negative frontotemporal dementia linked to chromosome 17. Nature *442*, 916-919.

Bannai, S. (1986). Exchange of cystine and glutamate across plasma membrane of human fibroblasts. The Journal of biological chemistry *261*, 2256-2263.

Bannai, S., and Kitamura, E. (1981). Role of proton dissociation in the transport of cystine and glutamate in human diploid fibroblasts in culture. The Journal of biological chemistry *256*, 5770-5772.

Banzhaf-Strathmann, J., Claus, R., Mucke, O., Rentzsch, K., van der Zee, J., Engelborghs, S., De Deyn, P.P., Cruts, M., van Broeckhoven, C., Plass, C.*, et al.* (2013). Promoter DNA methylation regulates progranulin expression and is altered in FTLD. Acta neuropathologica communications *1*, 16.

Bateman, A., and Bennett, H.P. (2009). The granulin gene family: from cancer to dementia. BioEssays : news and reviews in molecular, cellular and developmental biology *31*, 1245-1254.

Behrens, M.M., Ali, S.S., Dao, D.N., Lucero, J., Shekhtman, G., Quick, K.L., and Dugan, L.L. (2007). Ketamine-induced loss of phenotype of fast-spiking interneurons is mediated by NADPH-oxidase. Science *318*, 1645-1647.

Benussi, L., Binetti, G., Sina, E., Gigola, L., Bettecken, T., Meitinger, T., and Ghidoni, R. (2008). A novel deletion in progranulin gene is associated with FTDP-17 and CBS. Neurobiology of aging *29*, 427-435.

Benussi, L., Ghidoni, R., Pegoiani, E., Moretti, D.V., Zanetti, O., and Binetti, G. (2009). Progranulin Leu271LeufsX10 is one of the most common FTLD and CBS associated mutations worldwide. Neurobiology of disease *33*, 379-385.

Bhandari, V. (1996). Structural and functional analysis of a promoter of the human granulin/epithelin gene. The Biochemical journal *319 (Pt 2)*, 441-447.

Bhandari, V., and Bateman, A. (1992). Structure and chromosomal location of the human granulin gene. Biochemical and biophysical research communications *188*, 57-63.

Bishop, N.A., Lu, T., and Yankner, B.A. (2010). Neural mechanisms of ageing and cognitive decline. Nature 464, 529-535.

Boeve, B.F., Baker, M., Dickson, D.W., Parisi, J.E., Giannini, C., Josephs, K.A., Hutton, M., Pickering-Brown, S.M., Rademakers, R., Tang-Wai, D.*, et al.* (2006). Frontotemporal dementia and parkinsonism associated with the IVS1+1G->A mutation in progranulin: a clinicopathologic study. Brain : a journal of neurology *129*, 3103-3114.

Borg, J.P., Ooi, J., Levy, E., and Margolis, B. (1996). The phosphotyrosine interaction domains of X11 and FE65 bind to distinct sites on the YENPTY motif of amyloid precursor protein. Molecular and cellular biology *16*, 6229-6241.

Bourboulia, D., and Stetler-Stevenson, W.G. (2010). Matrix metalloproteinases (MMPs) and tissue inhibitors of metalloproteinases (TIMPs): Positive and negative regulators in tumor cell adhesion. Seminars in cancer biology *20*, 161-168.

Brieger, K., Schiavone, S., Miller, F.J., Jr., and Krause, K.H. (2012). Reactive oxygen species: from health to disease. Swiss medical weekly *142*, w13659.

Brouwers, N., Sleegers, K., Engelborghs, S., Maurer-Stroh, S., Gijselinck, I., van der Zee, J., Pickut, B.A., Van den Broeck, M., Mattheijssens, M., Peeters, K.*, et al.* (2008). Genetic variability in progranulin contributes to risk for clinically diagnosed Alzheimer disease. Neurology *71*, 656-664.

Burk, R.F., and Hill, K.E. (2009). Selenoprotein P-expression, functions, and roles in mammals. Biochimica et biophysica acta *1790*, 1441-1447.

Burk, R.F., Hill, K.E., Olson, G.E., Weeber, E.J., Motley, A.K., Winfrey, V.P., and Austin, L.M. (2007). Deletion of apolipoprotein E receptor-2 in mice lowers brain selenium and causes severe neurological dysfunction and death when a low-selenium diet is fed. The Journal of neuroscience : the official journal of the Society for Neuroscience *27*, 6207-6211.

Candelario-Jalil, E., Yang, Y., and Rosenberg, G.A. (2009). Diverse roles of matrix metalloproteinases and tissue inhibitors of metalloproteinases in neuroinflammation and cerebral ischemia. Neuroscience *158*, 983-994.

Capell, A., Liebscher, S., Fellerer, K., Brouwers, N., Willem, M., Lammich, S., Gijselinck, I., Bittner, T., Carlson, A.M., Sasse, F.*, et al.* (2011). Rescue of progranulin deficiency associated with frontotemporal lobar degeneration by alkalizing reagents and inhibition of vacuolar ATPase. The Journal of neuroscience : the official journal of the Society for Neuroscience *31*, 1885-1894.

Carecchio, M., Fenoglio, C., De Riz, M., Guidi, I., Comi, C., Cortini, F., Venturelli, E., Restelli, I., Cantoni, C., Bresolin, N.*, et al.* (2009). Progranulin plasma levels as potential biomarker for the identification of GRN deletion carriers. A case with atypical onset as clinical amnestic Mild Cognitive Impairment converted to Alzheimer's disease. Journal of the neurological sciences *287*, 291-293.

Carrasquillo, M.M., Nicholson, A.M., Finch, N., Gibbs, J.R., Baker, M., Rutherford, N.J., Hunter, T.A., DeJesus-Hernandez, M., Bisceglio, G.D., Mackenzie, I.R.*, et al.* (2010). Genome-wide screen identifies rs646776 near sortilin as a regulator of progranulin levels in human plasma. American journal of human genetics *87*, 890-897.

Castillo, G.M., Lukito, W., Wight, T.N., and Snow, A.D. (1999). The sulfate moieties of glycosaminoglycans are critical for the enhancement of beta-amyloid protein fibril formation. Journal of neurochemistry *72*, 1681-1687.

Cenik, B., Sephton, C.F., Dewey, C.M., Xian, X., Wei, S., Yu, K., Niu, W., Coppola, G., Coughlin, S.E., Lee, S.E.*, et al.* (2011). Suberoylanilide hydroxamic acid (vorinostat) up-regulates progranulin transcription: rational therapeutic approach to frontotemporal dementia. The Journal of biological chemistry *286*, 16101-16108.

Chalbot, S., Zetterberg, H., Blennow, K., Fladby, T., Andreasen, N., Grundke-Iqbal, I., and Iqbal, K. (2011). Blood-cerebrospinal fluid barrier permeability in Alzheimer's disease. Journal of Alzheimer's disease : JAD *25*, 505-515.

Chen, J.S., Su, I.J., Leu, Y.W., Young, K.C., and Sun, H.S. (2012). Expression of T-cell lymphoma invasion and metastasis 2 (TIAM2) promotes proliferation and invasion of liver cancer. International journal of cancer Journal international du cancer *130*, 1302-1313.

Chen, X., Chang, J., Deng, Q., Xu, J., Nguyen, T.A., Martens, L.H., Cenik, B., Taylor, G., Hudson, K.F., Chung, J.*, et al.* (2013). Progranulin does not bind tumor necrosis factor (TNF) receptors and is not a direct regulator of TNF-dependent signaling or bioactivity in immune or neuronal cells. The Journal of neuroscience : the official journal of the Society for Neuroscience *33*, 9202-9213.

Chen, X., Corbin, J.M., Tipton, G.J., Yang, L.V., Asch, A.S., and Ruiz-Echevarria, M.J. (2014). The TMEFF2 tumor suppressor modulates integrin expression, RhoA activation and migration of prostate cancer cells. Biochimica et biophysica acta *1843*, 1216-1224.

Chen, X., and Ruiz-Echevarria, M.J. (2013). TMEFF2 modulates the AKT and ERK signaling pathways. International journal of biochemistry and molecular biology *4*, 83-94.

Chen-Plotkin, A.S., Geser, F., Plotkin, J.B., Clark, C.M., Kwong, L.K., Yuan, W., Grossman, M., Van Deerlin, V.M., Trojanowski, J.Q., and Lee, V.M. (2008). Variations in the progranulin gene affect global gene expression in frontotemporal lobar degeneration. Human molecular genetics *17*, 1349-1362.

Cheng, Y., and Patel, D.J. (2004). An efficient system for small protein expression and refolding. Biochemical and biophysical research communications *317*, 401-405.

Cheung, S.T., Cheung, P.F., Cheng, C.K., Wong, N.C., and Fan, S.T. (2011). Granulin-epithelin precursor and ATP-dependent binding cassette (ABC)B5 regulate liver cancer cell chemoresistance. Gastroenterology *140*, 344-355.

Cheung, S.T., Wong, S.Y., Leung, K.L., Chen, X., So, S., Ng, I.O., and Fan, S.T. (2004). Granulin-epithelin precursor overexpression promotes growth and invasion of hepatocellular carcinoma. Clinical cancer research : an official journal of the American Association for Cancer Research *10*, 7629-7636.

Chow, T.W., Miller, B.L., Hayashi, V.N., and Geschwind, D.H. (1999). Inheritance of frontotemporal dementia. Archives of neurology *56*, 817-822.

Clark, I.M., Swingler, T.E., Sampieri, C.L., and Edwards, D.R. (2008). The regulation of matrix metalloproteinases and their inhibitors. The international journal of biochemistry & cell biology *40*, 1362-1378.

Coppola, G., Karydas, A., Rademakers, R., Wang, Q., Baker, M., Hutton, M., Miller, B.L., and Geschwind, D.H. (2008). Gene expression study on peripheral blood identifies progranulin mutations. Annals of neurology *64*, 92-96.

Corr, M. (2008). Wnt-beta-catenin signaling in the pathogenesis of osteoarthritis. Nature clinical practice Rheumatology *4*, 550-556.

Cotman, S.L., Halfter, W., and Cole, G.J. (2000). Agrin binds to beta-amyloid (Abeta), accelerates abeta fibril formation, and is localized to Abeta deposits in Alzheimer's disease brain. Molecular and cellular neurosciences *15*, 183-198.

Crocker, S.J., Pagenstecher, A., and Campbell, I.L. (2004). The TIMPs tango with MMPs and more in the central nervous system. Journal of neuroscience research *75*, 1-11.

Cruts, M., Gijselinck, I., van der Zee, J., Engelborghs, S., Wils, H., Pirici, D., Rademakers, R., Vandenberghe, R., Dermaut, B., Martin, J.J.*, et al.* (2006). Null mutations in progranulin cause ubiquitin-positive frontotemporal dementia linked to chromosome 17q21. Nature *442*, 920-924.

Cruts, M., Theuns, J., and Van Broeckhoven, C. (2012). Locus-specific mutation databases for neurodegenerative brain diseases. Human mutation *33*, 1340-1344.

Cruts, M., and Van Broeckhoven, C. (2008). Loss of progranulin function in frontotemporal lobar degeneration. Trends in genetics : TIG *24*, 186-194.

Cuevas-Antonio, R., Cancino, C., Arechavaleta-Velasco, F., Andrade, A., Barron, L., Estrada, I., Fernandez, R.L., Olguin, V., Ruiz, S., Imani, F.*, et al.* (2010). Expression of progranulin (Acrogranin/PCDGF/Granulin-Epithelin Precursor) in benign and malignant ovarian tumors and activation of MAPK signaling in ovarian cancer cell line. Cancer investigation *28*, 452-458.

Culouscou, J.M., Carlton, G.W., and Shoyab, M. (1993). Biochemical analysis of the epithelin receptor. The Journal of biological chemistry *268*, 10458-10462.

Czirr, E., and Wyss-Coray, T. (2012). The immunology of neurodegeneration. The Journal of clinical investigation *122*, 1156-1163.

D'Autreaux, B., and Toledano, M.B. (2007). ROS as signalling molecules: mechanisms that generate specificity in ROS homeostasis. Nature reviews Molecular cell biology *8*, 813-824.

Daniel, R., Daniels, E., He, Z., and Bateman, A. (2003). Progranulin (acrogranin/PC cell-derived growth factor/granulin-epithelin precursor) is expressed in the placenta, epidermis, microvasculature, and brain during murine development. Developmental dynamics : an official publication of the American Association of Anatomists *227*, 593-599.

Daniel, R., He, Z., Carmichael, K.P., Halper, J., and Bateman, A. (2000). Cellular localization of gene expression for progranulin. The journal of histochemistry and cytochemistry : official journal of the Histochemistry Society *48*, 999-1009.

Davis, J.B., and Maher, P. (1994). Protein kinase C activation inhibits glutamate-induced cytotoxicity in a neuronal cell line. Brain research *652*, 169-173.

Day, B.W., Stringer, B.W., and Boyd, A.W. (2014). Eph receptors as therapeutic targets in glioblastoma. British journal of cancer *111*, 1255-1261.

de la Encarnacion, A., Alquezar, C., and Martin-Requero, A. (2016). Increased Wnt Signaling and Reduced Viability in a Neuronal Model of Progranulin-Deficient Frontotemporal Lobar Degeneration. Molecular neurobiology *53*, 7107-7118.

De Muynck, L., Herdewyn, S., Beel, S., Scheveneels, W., Van Den Bosch, L., Robberecht, W., and Van Damme, P. (2013). The neurotrophic properties of progranulin depend on the granulin E domain but do not require sortilin binding. Neurobiology of aging *34*, 2541-2547.

De Muynck, L., and Van Damme, P. (2011). Cellular effects of progranulin in health and disease. Journal of molecular neuroscience : MN *45*, 549-560.

DeJesus-Hernandez, M., Mackenzie, I.R., Boeve, B.F., Boxer, A.L., Baker, M., Rutherford, N.J., Nicholson, A.M., Finch, N.A., Flynn, H., Adamson, J.*, et al.* (2011). Expanded GGGGCC hexanucleotide repeat in noncoding region of C9ORF72 causes chromosome 9p-linked FTD and ALS. Neuron *72*, 245-256.

Dennis, E.A. (1994). Diversity of group types, regulation, and function of phospholipase A2. The Journal of biological chemistry *269*, 13057-13060.

Deribe, Y.L., Pawson, T., and Dikic, I. (2010). Post-translational modifications in signal integration. Nat Struct Mol Biol *17*, 666-672.

DeWitt, D.A., Silver, J., Canning, D.R., and Perry, G. (1993). Chondroitin sulfate proteoglycans are associated with the lesions of Alzheimer's disease. Experimental neurology *121*, 149-152.

Donald, C.D., Laddu, A., Chandham, P., Lim, S.D., Cohen, C., Amin, M., Gerton, G.L., Marshall, F.F., and Petros, J.A. (2001). Expression of progranulin and the epithelin/granulin precursor acrogranin correlates with neoplastic state in renal epithelium. Anticancer research *21*, 3739-3742.

Dormann, D., Capell, A., Carlson, A.M., Shankaran, S.S., Rodde, R., Neumann, M., Kremmer, E., Matsuwaki, T., Yamanouchi, K., Nishihara, M.*, et al.* (2009). Proteolytic processing of TAR DNA binding protein-43 by caspases produces C-terminal fragments with disease defining properties independent of progranulin. Journal of neurochemistry *110*, 1082-1094.

Dours-Zimmermann, M.T., Maurer, K., Rauch, U., Stoffel, W., Fassler, R., and Zimmermann, D.R. (2009). Versican V2 assembles the extracellular matrix surrounding the nodes of ranvier in the CNS. The Journal of neuroscience : the official journal of the Society for Neuroscience *29*, 7731-7742.

Dreher, I., Jakobs, T.C., and Kohrle, J. (1997). Cloning and characterization of the human selenoprotein P promoter. Response of selenoprotein P expression to cytokines in liver cells. The Journal of biological chemistry *272*, 29364-29371.

Du, W.W., Yang, W., and Yee, A.J. (2013). Roles of versican in cancer biology--tumorigenesis, progression and metastasis. Histology and histopathology *28*, 701-713.

Duilio, A., Faraonio, R., Minopoli, G., Zambrano, N., and Russo, T. (1998). Fe65L2: a new member of the Fe65 protein family interacting with the intracellular domain of the Alzheimer's beta-amyloid precursor protein. The Biochemical journal *330 (Pt 1)*, 513-519.

Duong, L., Klitten, L.L., Moller, R.S., Ingason, A., Jakobsen, K.D., Skjodt, C., Didriksen, M., Hjalgrim, H., Werge, T., and Tommerup, N. (2012). Mutations in NRXN1 in a family multiply affected with brain disorders: NRXN1 mutations and brain disorders. American journal of medical genetics Part B, Neuropsychiatric genetics : the official publication of the International Society of Psychiatric Genetics *159B*, 354-358.

Egland, K.A., Vincent, J.J., Strausberg, R., Lee, B., and Pastan, I. (2003). Discovery of the breast cancer gene BASE using a molecular approach to enrich for genes encoding membrane and secreted proteins. Proceedings of the National Academy of Sciences of the United States of America *100*, 1099-1104.

Elkabets, M., Gifford, A.M., Scheel, C., Nilsson, B., Reinhardt, F., Bray, M.A., Carpenter, A.E., Jirstrom, K., Magnusson, K., Ebert, B.L.*, et al.* (2011). Human tumors instigate granulin-expressing hematopoietic cells that promote malignancy by activating stromal fibroblasts in mice. The Journal of clinical investigation *121*, 784-799.

Epplein, M., Burk, R.F., Cai, Q., Hargreaves, M.K., and Blot, W.J. (2014). A Prospective Study of Plasma Selenoprotein P and Lung Cancer Risk Among Low-Income Adults. Cancer epidemiology, biomarkers & prevention : a publication of the American Association for Cancer Research, cosponsored by the American Society of Preventive Oncology.

Eriksen, J.L., and Mackenzie, I.R. (2008). Progranulin: normal function and role in neurodegeneration. Journal of neurochemistry *104*, 287-297.

Feng, J.Q., Guo, F.J., Jiang, B.C., Zhang, Y., Frenkel, S., Wang, D.W., Tang, W., Xie, Y., and Liu, C.J. (2010). Granulin epithelin precursor: a bone morphogenic protein 2-inducible growth factor that activates Erk1/2 signaling and JunB transcription factor in chondrogenesis. FASEB journal : official publication of the Federation of American Societies for Experimental Biology *24*, 1879-1892.

Fenton, T.R., and Gout, I.T. (2011). Functions and regulation of the 70kDa ribosomal S6 kinases. The international journal of biochemistry & cell biology *43*, 47-59.

Finch, N., Baker, M., Crook, R., Swanson, K., Kuntz, K., Surtees, R., Bisceglio, G., Rovelet-Lecrux, A., Boeve, B., Petersen, R.C.*, et al.* (2009). Plasma progranulin levels predict progranulin mutation status in frontotemporal dementia patients and asymptomatic family members. Brain : a journal of neurology *132*, 583-591.

Fiore, F., Zambrano, N., Minopoli, G., Donini, V., Duilio, A., and Russo, T. (1995). The regions of the Fe65 protein homologous to the phosphotyrosine interaction/phosphotyrosine binding domain of Shc bind the intracellular domain of the Alzheimer's amyloid precursor protein. The Journal of biological chemistry *270*, 30853-30856.

Frank, M., Duvezin-Caubet, S., Koob, S., Occhipinti, A., Jagasia, R., Petcherski, A., Ruonala, M.O., Priault, M., Salin, B., and Reichert, A.S. (2012). Mitophagy is triggered by mild oxidative stress in a mitochondrial fission dependent manner. Biochimica et biophysica acta *1823*, 2297-2310.

Freund, T.F., and Katona, I. (2007). Perisomatic inhibition. Neuron *56*, 33-42.

Fukamachi, K., Matsuoka, Y., Ohno, H., Hamaguchi, T., and Tsuda, H. (2002). Neuronal leucine-rich repeat protein-3 amplifies MAPK activation by epidermal growth factor through a carboxyl-terminal region containing endocytosis motifs. The Journal of biological chemistry *277*, 43549-43552.

Galimberti, D., D'Addario, C., Dell'osso, B., Fenoglio, C., Marcone, A., Cerami, C., Cappa, S.F., Palazzo, M.C., Arosio, B., Mari, D.*, et al.* (2013). Progranulin gene (GRN) promoter methylation is increased in patients with sporadic frontotemporal lobar degeneration. Neurological sciences : official journal of the Italian Neurological Society and of the Italian Society of Clinical Neurophysiology *34*, 899-903.

Gao, X., Joselin, A.P., Wang, L., Kar, A., Ray, P., Bateman, A., Goate, A.M., and Wu, J.Y. (2010). Progranulin promotes neurite outgrowth and neuronal differentiation by regulating GSK-3beta. Protein & cell *1*, 552-562.

Gass, J., Lee, W.C., Cook, C., Finch, N., Stetler, C., Jansen-West, K., Lewis, J., Link, C.D., Rademakers, R., Nykjaer, A.*, et al.* (2012a). Progranulin regulates neuronal outgrowth independent of sortilin. Molecular neurodegeneration *7*, 33.

Gass, J., Prudencio, M., Stetler, C., and Petrucelli, L. (2012b). Progranulin: an emerging target for FTLD therapies. Brain research *1462*, 118-128.

Gerst, J.L., Siedlak, S.L., Nunomura, A., Castellani, R., Perry, G., and Smith, M.A. (1999). Role of oxidative stress in frontotemporal dementia. Dementia and geriatric cognitive disorders *10 Suppl 1*, 85-87.

Geybels, M.S., van den Brandt, P.A., Schouten, L.J., van Schooten, F.J., van Breda, S.G., Rayman, M.P., Green, F.R., and Verhage, B.A. (2014). Selenoprotein gene variants, toenail selenium levels, and risk for advanced prostate cancer. Journal of the National Cancer Institute *106*, dju003.

Ghidoni, R. (2008). Low plasma progranulin levels predict progranulin mutations in frontotemporal lobar degeneration. Neurology *71*, 1235-1239.

Ghoshal, N., Dearborn, J.T., Wozniak, D.F., and Cairns, N.J. (2012). Core features of frontotemporal dementia recapitulated in progranulin knockout mice. Neurobiology of disease *45*, 395-408.

Gilbert, A.M., Bursavich, M.G., Alon, N., Bhat, B.M., Bex, F.J., Cain, M., Coleburn, V., Gironda, V., Green, P., Hauze, D.B.*, et al.* (2010). Hit to lead studies on (hetero)arylpyrimidines--agonists of the canonical Wnt-beta-catenin cellular messaging system. Bioorganic & medicinal chemistry letters *20*, 366-370.

Gjorlund, M.D., Nielsen, J., Pankratova, S., Li, S., Korshunova, I., Bock, E., and Berezin, V. (2012). Neuroligin-1 induces neurite outgrowth through interaction with neurexin-1beta and activation of fibroblast growth factor receptor-1. FASEB journal : official publication of the Federation of American Societies for Experimental Biology *26*, 4174-4186.

Glinka, A., Wu, W., Delius, H., Monaghan, A.P., Blumenstock, C., and Niehrs, C. (1998). Dickkopf-1 is a member of a new family of secreted proteins and functions in head induction. Nature *391*, 357-362.

Glynne-Jones, E., Harper, M.E., Seery, L.T., James, R., Anglin, I., Morgan, H.E., Taylor, K.M., Gee, J.M., and Nicholson, R.I. (2001). TENB2, a proteoglycan identified in prostate cancer that is associated with disease progression and androgen independence. International journal of cancer Journal international du cancer *94*, 178-184.

Gochenauer, G.E., and Robinson, M.B. (2001). Dibutyryl-cAMP (dbcAMP) up-regulates astrocytic chloride-dependent L-[3H]glutamate transport and expression of both system xc(-) subunits. Journal of neurochemistry *78*, 276-286.

Goldman, J.S., Farmer, J.M., Wood, E.M., Johnson, J.K., Boxer, A., Neuhaus, J., Lomen-Hoerth, C., Wilhelmsen, K.C., Lee, V.M., Grossman, M.*, et al.* (2005). Comparison of family histories in FTLD subtypes and related tauopathies. Neurology *65*, 1817-1819.

Gomez, D.E., Alonso, D.F., Yoshiji, H., and Thorgeirsson, U.P. (1997). Tissue inhibitors of metalloproteinases: structure, regulation and biological functions. European journal of cell biology *74*, 111-122.

Gonzalez, E.M., Mongiat, M., Slater, S.J., Baffa, R., and Iozzo, R.V. (2003). A novel interaction between perlecan protein core and progranulin: potential effects on tumor growth. The Journal of biological chemistry *278*, 38113-38116.

Goto, A., Hoshino, M., Matsuda, M., and Nakamura, T. (2011). Phosphorylation of STEF/Tiam2 by protein kinase A is critical for Rac1 activation and neurite outgrowth in dibutyryl cAMP-treated PC12D cells. Molecular biology of the cell *22*, 1780-1790.

Gotzl, J.K., Mori, K., Damme, M., Fellerer, K., Tahirovic, S., Kleinberger, G., Janssens, J., van der Zee, J., Lang, C.M., Kremmer, E.*, et al.* (2014). Common pathobiochemical hallmarks of progranulin-associated frontotemporal lobar degeneration and neuronal ceroid lipofuscinosis. Acta neuropathologica *127*, 845-860.

Groft, L.L., Muzik, H., Rewcastle, N.B., Johnston, R.N., Knauper, V., Lafleur, M.A., Forsyth, P.A., and Edwards, D.R. (2001). Differential expression and localization of TIMP-1 and TIMP-4 in human gliomas. British journal of cancer *85*, 55-63.

Gronenborn, A.M., Filpula, D.R., Essig, N.Z., Achari, A., Whitlow, M., Wingfield, P.T., and Clore, G.M. (1991). A novel, highly stable fold of the immunoglobulin binding domain of streptococcal protein G. Science *253*, 657-661.

Guenette, S.Y., Chen, J., Jondro, P.D., and Tanzi, R.E. (1996). Association of a novel human FE65-like protein with the cytoplasmic domain of the beta-amyloid precursor protein. Proceedings of the National Academy of Sciences of the United States of America *93*, 10832-10837.

Guerra, R.R., Kriazhev, L., Hernandez-Blazquez, F.J., and Bateman, A. (2007). Progranulin is a stress-response factor in fibroblasts subjected to hypoxia and acidosis. Growth Factors *25*, 280-285.

Guo, A., Tapia, L., Bamji, S.X., Cynader, M.S., and Jia, W. (2010). Progranulin deficiency leads to enhanced cell vulnerability and TDP-43 translocation in primary neuronal cultures. Brain research *1366*, 1-8.

Habas, R., and Dawid, I.B. (2005). Dishevelled and Wnt signaling: is the nucleus the final frontier? Journal of biology *4*, 2.

Hancock, J.F. (1992). COS Cell Expression. Methods Mol Biol *8*, 153-158.

Hanisch, U.K., and Kettenmann, H. (2007). Microglia: active sensor and versatile effector cells in the normal and pathologic brain. Nature neuroscience *10*, 1387-1394.

Hao, Y., Perkinton, M.S., Chan, W.W., Chan, H.Y., Miller, C.C., and Lau, K.F. (2011). GULP1 is a novel APP-interacting protein that alters APP processing. The Biochemical journal *436*, 631-639.

He, Z., and Bateman, A. (1999). Progranulin gene expression regulates epithelial cell growth and promotes tumor growth in vivo. Cancer research *59*, 3222-3229.

He, Z., Ismail, A., Kriazhev, L., Sadvakassova, G., and Bateman, A. (2002). Progranulin (PC-cell-derived growth factor/acrogranin) regulates invasion and cell survival. Cancer research *62*, 5590-5596.

He, Z., Ong, C.H., Halper, J., and Bateman, A. (2003). Progranulin is a mediator of the wound response. Nature medicine *9*, 225-229.

Hill, K.E., Zhou, J., McMahan, W.J., Motley, A.K., and Burk, R.F. (2004). Neurological dysfunction occurs in mice with targeted deletion of the selenoprotein P gene. The Journal of nutrition *134*, 157-161.

Ho, J.C., Ip, Y.C., Cheung, S.T., Lee, Y.T., Chan, K.F., Wong, S.Y., and Fan, S.T. (2008). Granulin-epithelin precursor as a therapeutic target for hepatocellular carcinoma. Hepatology *47*, 1524-1532.

Holler, C.J., Taylor, G., McEachin, Z.T., Deng, Q., Watkins, W.J., Hudson, K., Easley, C.A., Hu, W.T., Hales, C.M., Rossoll, W*., et al.* (2016). Trehalose upregulates progranulin expression in human and mouse models of GRN haploinsufficiency: a novel therapeutic lead to treat frontotemporal dementia. Molecular neurodegeneration *11*, 46.

Hoque, M., Young, T.M., Lee, C.G., Serrero, G., Mathews, M.B., and Pe'ery, T. (2003). The growth factor granulin interacts with cyclin T1 and modulates P-TEFb-dependent transcription. Molecular and cellular biology *23*, 1688-1702.

Horie, M., Mitsumoto, Y., Kyushiki, H., Kanemoto, N., Watanabe, A., Taniguchi, Y., Nishino, N., Okamoto, T., Kondo, M., Mori, T*., et al.* (2000). Identification and characterization of TMEFF2, a novel survival factor for hippocampal and mesencephalic neurons. Genomics *67*, 146-152.

Hrabal, R., Chen, Z., James, S., Bennett, H.P., and Ni, F. (1996). The hairpin stack fold, a novel protein architecture for a new family of protein growth factors. Nature structural biology *3*, 747-752.

Hu, F., Padukkavidana, T., Vaegter, C.B., Brady, O.A., Zheng, Y., Mackenzie, I.R., Feldman, H.H., Nykjaer, A., and Strittmatter, S.M. (2010). Sortilin-mediated endocytosis determines levels of the frontotemporal dementia protein, progranulin. Neuron *68*, 654-667.

Huang, T.T., Zou, Y., and Corniola, R. (2012). Oxidative stress and adult neurogenesis--effects of radiation and superoxide dismutase deficiency. Seminars in cell & developmental biology *23*, 738-744.

Hwang, C., Sinskey, A.J., and Lodish, H.F. (1992). Oxidized redox state of glutathione in the endoplasmic reticulum. Science *257*, 1496-1502.

Jia, Y. (2009). Analysis of the neuroprotective function and the N-glycosylation of progranulin (PGRN) (University of British Columbia).

Jian, J., Zhao, S., Tian, Q., Gonzalez-Gugel, E., Mundra, J.J., Uddin, S.M., Liu, B., Richbourgh, B., Brunetti, R., and Liu, C.J. (2013). Progranulin directly binds to the CRD2 and CRD3 of TNFR extracellular domains. FEBS letters *587*, 3428-3436.

Jiang, H., Guo, W., Liang, X., and Rao, Y. (2005). Both the establishment and the maintenance of neuronal polarity require active mechanisms: critical roles of GSK-3beta and its upstream regulators. Cell *120*, 123-135.

Jiao, J., Herl, L.D., Farese, R.V., and Gao, F.B. (2010). MicroRNA-29b regulates the expression level of human progranulin, a secreted glycoprotein implicated in frontotemporal dementia. PloS one *5*, e10551.

Jones, M.B., Michener, C.M., Blanchette, J.O., Kuznetsov, V.A., Raffeld, M., Serrero, G., Emmert-Buck, M.R., Petricoin, E.F., Krizman, D.B., Liotta, L.A*., et al.* (2003). The granulin-epithelin precursor/PC-cell-derived growth factor is a growth factor for epithelial ovarian cancer. Clinical cancer research : an official journal of the American Association for Cancer Research *9*, 44-51.

Josephs, K.A., Ahmed, Z., Katsuse, O., Parisi, J.F., Boeve, B.F., Knopman, D.S., Petersen, R.C., Davies, P., Duara, R., Graff-Radford, N.R*., et al.* (2007). Neuropathologic features of frontotemporal lobar degeneration with

ubiquitin-positive inclusions with progranulin gene (PGRN) mutations. Journal of neuropathology and experimental neurology *66*, 142-151.

Josephs, K.A., Whitwell, J.L., Weigand, S.D., Murray, M.E., Tosakulwong, N., Liesinger, A.M., Petrucelli, L., Senjem, M.L., Knopman, D.S., Boeve, B.F.*, et al.* (2014). TDP-43 is a key player in the clinical features associated with Alzheimer's disease. Acta neuropathologica.

Kaldis, P., and Pagano, M. (2009). Wnt signaling in mitosis. Developmental cell *17*, 749-750.

Kanazawa, M., Kawamura, K., Takahashi, T., Miura, M., Tanaka, Y., Koyama, M., Toriyabe, M., Igarashi, H., Nakada, T., Nishihara, M.*, et al.* (2015). Multiple therapeutic effects of progranulin on experimental acute ischaemic stroke. Brain : a journal of neurology *138*, 1932-1948.

Kao, A.W., Eisenhut, R.J., Martens, L.H., Nakamura, A., Huang, A., Bagley, J.A., Zhou, P., de Luis, A., Neukomm, L.J., Cabello, J.*, et al.* (2011). A neurodegenerative disease mutation that accelerates the clearance of apoptotic cells. Proceedings of the National Academy of Sciences of the United States of America *108*, 4441-4446.

Kao, A.W., McKay, A., Singh, P.P., Brunet, A., and Huang, E.J. (2017). Progranulin, lysosomal regulation and neurodegenerative disease. Nat Rev Neurosci *18*, 325-333.

Kaplowitz, N., Aw, T.Y., and Ookhtens, M. (1985). The regulation of hepatic glutathione. Annual review of pharmacology and toxicology *25*, 715-744.

Karageorgiou, E., and Miller, B.L. (2014). Frontotemporal lobar degeneration: a clinical approach. Semin Neurol *34*, 189-201.

Kawauchi, T., Chihama, K., Nabeshima, Y., and Hoshino, M. (2003). The in vivo roles of STEF/Tiam1, Rac1 and JNK in cortical neuronal migration. The EMBO journal *22*, 4190-4201.

Kayasuga, Y., Chiba, S., Suzuki, M., Kikusui, T., Matsuwaki, T., Yamanouchi, K., Kotaki, H., Horai, R., Iwakura, Y., and Nishihara, M. (2007). Alteration of behavioural phenotype in mice by targeted disruption of the progranulin gene. Behavioural brain research *185*, 110-118.

Kelley, B.J., Haidar, W., Boeve, B.F., Baker, M., Graff-Radford, N.R., Krefft, T., Frank, A.R., Jack, C.R., Jr., Shiung, M., Knopman, D.S.*, et al.* (2009). Prominent phenotypic variability associated with mutations in Progranulin. Neurobiology of aging *30*, 739-751.

Kessenbrock, K., Frohlich, L., Sixt, M., Lammermann, T., Pfister, H., Bateman, A., Belaaouaj, A., Ring, J., Ollert, M., Fassler, R.*, et al.* (2008). Proteinase 3 and neutrophil elastase enhance inflammation in mice by inactivating antiinflammatory progranulin. The Journal of clinical investigation *118*, 2438-2447.

Kim, S., Takahashi, H., Lin, W.W., Descargues, P., Grivennikov, S., Kim, Y., Luo, J.L., and Karin, M. (2009). Carcinoma-produced factors activate myeloid cells through TLR2 to stimulate metastasis. Nature *457*, 102-106.

Kinney, J.W., Davis, C.N., Tabarean, I., Conti, B., Bartfai, T., and Behrens, M.M. (2006). A specific role for NR2A-containing NMDA receptors in the maintenance of parvalbumin and GAD67 immunoreactivity in cultured interneurons. The Journal of neuroscience : the official journal of the Society for Neuroscience *26*, 1604-1615.

Kleinberger, G., Wils, H., Ponsaerts, P., Joris, G., Timmermans, J.P., Van Broeckhoven, C., and Kumar-Singh, S. (2010). Increased caspase activation and decreased TDP-43 solubility in progranulin knockout cortical cultures. Journal of neurochemistry *115*, 735-747.

Knight, D., Xie, W., and Boulianne, G.L. (2011). Neurexins and neuroligins: recent insights from invertebrates. Molecular neurobiology *44*, 426-440.

Knopman, D.S., and Roberts, R.O. (2011). Estimating the number of persons with frontotemporal lobar degeneration in the US population. Journal of molecular neuroscience : MN *45*, 330-335.

Knox, S., Fosang, A.J., Last, K., Melrose, J., and Whitelock, J. (2005). Perlecan from human epithelial cells is a hybrid heparan/chondroitin/keratan sulfate proteoglycan. FEBS letters *579*, 5019-5023.

Knox, S., Merry, C., Stringer, S., Melrose, J., and Whitelock, J. (2002). Not all perlecans are created equal: interactions with fibroblast growth factor (FGF) 2 and FGF receptors. The Journal of biological chemistry *277*, 14657-14665.

Kojima, Y., Ono, K., Inoue, K., Takagi, Y., Kikuta, K., Nishimura, M., Yoshida, Y., Nakashima, Y., Matsumae, H., Furukawa, Y.*, et al.* (2009). Progranulin expression in advanced human atherosclerotic plaque. Atherosclerosis *206*, 102-108.

Kong, W.J., Zhang, S.L., Chen, X., Zhang, S., Wang, Y.J., Zhang, D., and Sun, Y. (2007). PC cell-derived growth factor overexpression promotes proliferation and survival of laryngeal carcinoma. Anti-cancer drugs *18*, 29-40.

Kraft, C., Kijanska, M., Kalie, E., Siergiejuk, E., Lee, S.S., Semplicio, G., Stoffel, I., Brezovich, A., Verma, M., Hansmann, I.*, et al.* (2012). Binding of the Atg1/ULK1 kinase to the ubiquitin-like protein Atg8 regulates autophagy. The EMBO journal *31*, 3691-3703.

Lambert, E., Dasse, E., Haye, B., and Petitfrere, E. (2004). TIMPs as multifacial proteins. Critical reviews in oncology/hematology *49*, 187-198.

LaPierre, D.P., Lee, D.Y., Li, S.Z., Xie, Y.Z., Zhong, L., Sheng, W., Deng, Z., and Yang, B.B. (2007). The ability of versican to simultaneously cause apoptotic resistance and sensitivity. Cancer research *67*, 4742-4750.

Le Ber, I., Camuzat, A., Hannequin, D., Pasquier, F., Guedj, E., Rovelet-Lecrux, A., Hahn-Barma, V., van der Zee, J., Clot, F., Bakchine, S.*, et al.* (2008). Phenotype variability in progranulin mutation carriers: a clinical, neuropsychological, imaging and genetic study. Brain : a journal of neurology *131*, 732-746.

Leco, K.J., Apte, S.S., Taniguchi, G.T., Hawkes, S.P., Khokha, R., Schultz, G.A., and Edwards, D.R. (1997). Murine tissue inhibitor of metalloproteinases-4 (Timp-4): cDNA isolation and expression in adult mouse tissues. FEBS letters *401*, 213-217.

Lee, S., Desai, K.K., Iczkowski, K.A., Newcomer, R.G., Wu, K.J., Zhao, Y.G., Tan, W.W., Roycik, M.D., and Sang, Q.X. (2006). Coordinated peak expression of MMP-26 and TIMP-4 in preinvasive human prostate tumor. Cell research *16*, 750-758.

Lee, W.C., Almeida, S., Prudencio, M., Caulfield, T.R., Zhang, Y.J., Tay, W.M., Bauer, P.O., Chew, J., Sasaguri, H., Jansen-West, K.R.*, et al.* (2014). Targeted manipulation of the sortilin-progranulin axis rescues progranulin haploinsufficiency. Human molecular genetics *23*, 1467-1478.

Leslie, C.C. (1997). Properties and regulation of cytosolic phospholipase A2. The Journal of biological chemistry *272*, 16709-16712.

Lewerenz, J., Hewett, S.J., Huang, Y., Lambros, M., Gout, P.W., Kalivas, P.W., Massie, A., Smolders, I., Methner, A., Pergande, M.*, et al.* (2013). The cystine/glutamate antiporter system x(c)(-) in health and disease: from molecular mechanisms to novel therapeutic opportunities. Antioxid Redox Signal *18*, 522-555.

Li, X., Zhang, J., Cao, Z., Wu, J., and Shi, Y. (2006). Solution structure of GOPC PDZ domain and its interaction with the C-terminal motif of neuroligin. Protein science : a publication of the Protein Society *15*, 2149-2158.

Liachko, N.F., Guthrie, C.R., and Kraemer, B.C. (2010). Phosphorylation promotes neurotoxicity in a Caenorhabditis elegans model of TDP-43 proteinopathy. The Journal of neuroscience : the official journal of the Society for Neuroscience *30*, 16208-16219.

Liau, L.M., Lallone, R.L., Seitz, R.S., Buznikov, A., Gregg, J.P., Kornblum, H.I., Nelson, S.F., and Bronstein, J.M. (2000). Identification of a human glioma-associated growth factor gene, granulin, using differential immuno-absorption. Cancer research *60*, 1353-1360.

Liu, H., Wang, H., Shenvi, S., Hagen, T.M., and Liu, R.M. (2004). Glutathione metabolism during aging and in Alzheimer disease. Annals of the New York Academy of Sciences *1019*, 346-349.

Liu, Y., Xi, L., Liao, G., Wang, W., Tian, X., Wang, B., Chen, G., Han, Z., Wu, M., Wang, S.*, et al.* (2007). Inhibition of PC cell-derived growth factor (PCDGF)/granulin-epithelin precursor (GEP) decreased cell proliferation and invasion through downregulation of cyclin D and CDK4 and inactivation of MMP-2. BMC cancer *7*, 22.

Lopez-Otin, C., Blasco, M.A., Partridge, L., Serrano, M., and Kroemer, G. (2013). The hallmarks of aging. Cell 153, 1194-1217.

Lu, R., and Serrero, G. (2000). Inhibition of PC cell-derived growth factor (PCDGF, epithelin/granulin precursor) expression by antisense PCDGF cDNA transfection inhibits tumorigenicity of the human breast carcinoma cell line MDA-MB-468. Proceedings of the National Academy of Sciences of the United States of America *97*, 3993-3998.

Lu, R., and Serrero, G. (2001). Mediation of estrogen mitogenic effect in human breast cancer MCF-7 cells by PC-cell-derived growth factor (PCDGF/granulin precursor). Proceedings of the National Academy of Sciences of the United States of America *98*, 142-147.

Lui, H., Zhang, J., Makinson, S.R., Cahill, M.K., Kelley, K.W., Huang, H.Y., Shang, Y., Oldham, M.C., Martens, L.H., Gao, F.*, et al.* (2016). Progranulin Deficiency Promotes Circuit-Specific Synaptic Pruning by Microglia via Complement Activation. Cell *165*, 921-935.

Mackenzie, I.R., Baker, M., Pickering-Brown, S., Hsiung, G.Y., Lindholm, C., Dwosh, E., Gass, J., Cannon, A., Rademakers, R., Hutton, M.*, et al.* (2006). The neuropathology of frontotemporal lobar degeneration caused by mutations in the progranulin gene. Brain : a journal of neurology *129*, 3081-3090.

Maher, P. (2001). How protein kinase C activation protects nerve cells from oxidative stress-induced cell death. The Journal of neuroscience : the official journal of the Society for Neuroscience *21*, 2929-2938.

Makowske, M., and Christensen, H.N. (1982). Contrasts in transport systems for anionic amino acids in hepatocytes and a hepatoma cell line HTC. The Journal of biological chemistry *257*, 5663-5670.

Mao, B., Wu, W., Li, Y., Hoppe, D., Stannek, P., Glinka, A., and Niehrs, C. (2001). LDL-receptor-related protein 6 is a receptor for Dickkopf proteins. Nature *411*, 321-325.

Markert, J.M., Fuller, C.M., Gillespie, G.Y., Bubien, J.K., McLean, L.A., Hong, R.L., Lee, K., Gullans, S.R., Mapstone, T.B., and Benos, D.J. (2001). Differential gene expression profiling in human brain tumors. Physiological genomics *5*, 21-33.

Martin, J.A., Craft, D.K., Su, J.H., Kim, R.C., and Cotman, C.W. (2001). Astrocytes degenerate in frontotemporal dementia: possible relation to hypoperfusion. Neurobiology of aging *22*, 195-207.

MatchmakerManual, C. Matchmaker Gold Yeast Two-Hybrid System User Manual. *PT4084-1 Version PR033493*.

Matsubara, T., Mita, A., Minami, K., Hosooka, T., Kitazawa, S., Takahashi, K., Tamori, Y., Yokoi, N., Watanabe, M., Matsuo, E.*, et al.* (2012). PGRN is a key adipokine mediating high fat diet-induced insulin resistance and obesity through IL-6 in adipose tissue. Cell metabolism *15*, 38-50.

Matsuda, J., Yoneshige, A., and Suzuki, K. (2007). The function of sphingolipids in the nervous system: lessons learnt from mouse models of specific sphingolipid activator protein deficiencies. Journal of neurochemistry *103 Suppl 1*, 32-38.

Matsumura, N., Mandai, M., Miyanishi, M., Fukuhara, K., Baba, T., Higuchi, T., Kariya, M., Takakura, K., and Fujii, S. (2006). Oncogenic property of acrogranin in human uterine leiomyosarcoma: direct evidence of genetic contribution in in vivo tumorigenesis. Clinical cancer research : an official journal of the American Association for Cancer Research *12*, 1402-1411.

Matsuo, N., Hoshino, M., Yoshizawa, M., and Nabeshima, Y. (2002). Characterization of STEF, a guanine nucleotide exchange factor for Rac1, required for neurite growth. The Journal of biological chemistry *277*, 2860-2868.

Matsuo, N., Terao, M., Nabeshima, Y., and Hoshino, M. (2003). Roles of STEF/Tiam1, guanine nucleotide exchange factors for Rac1, in regulation of growth cone morphology. Molecular and cellular neurosciences *24*, 69-81.

Matsuwaki, T., Asakura, R., Suzuki, M., Yamanouchi, K., and Nishihara, M. (2011). Age-dependent changes in progranulin expression in the mouse brain. The Journal of reproduction and development *57*, 113-119.

McLaurin, J., Franklin, T., Zhang, X., Deng, J., and Fraser, P.E. (1999). Interactions of Alzheimer amyloid-beta peptides with glycosaminoglycans effects on fibril nucleation and growth. European journal of biochemistry / FEBS *266*, 1101-1110.

McLoughlin, D.M., and Miller, C.C. (1996). The intracellular cytoplasmic domain of the Alzheimer's disease amyloid precursor protein interacts with phosphotyrosine-binding domain proteins in the yeast two-hybrid system. FEBS letters *397*, 197-200.

McLoughlin, D.M., and Miller, C.C. (2008). The FE65 proteins and Alzheimer's disease. Journal of neuroscience research *86*, 744-754.

Melendez-Zajgla, J., Del Pozo, L., Ceballos, G., and Maldonado, V. (2008). Tissue inhibitor of metalloproteinases-4. The road less traveled. Molecular cancer *7*, 85.

Meredith, M.J., and Reed, D.J. (1982). Status of the mitochondrial pool of glutathione in the isolated hepatocyte. The Journal of biological chemistry *257*, 3747-3753.

Mesulam, M., Johnson, N., Krefft, T.A., Gass, J.M., Cannon, A.D., Adamson, J.L., Bigio, E.H., Weintraub, S., Dickson, D.W., Hutton, M.L.*, et al.* (2007). Progranulin mutations in primary progressive aphasia: the PPA1 and PPA3 families. Archives of neurology *64*, 43-47.

Metcalfe, C., and Bienz, M. (2011). Inhibition of GSK3 by Wnt signalling--two contrasting models. Journal of cell science *124*, 3537-3544.

Minami, S.S., Min, S.W., Krabbe, G., Wang, C., Zhou, Y., Asgarov, R., Li, Y., Martens, L.H., Elia, L.P., Ward, M.E.*, et al.* (2014). Progranulin protects against amyloid beta deposition and toxicity in Alzheimer's disease mouse models. Nature medicine *20*, 1157-1164.

Minich, T., Riemer, J., Schulz, J.B., Wielinga, P., Wijnholds, J., and Dringen, R. (2006). The multidrug resistance protein 1 (Mrp1), but not Mrp5, mediates export of glutathione and glutathione disulfide from brain astrocytes. Journal of neurochemistry *97*, 373-384.

Miyanishi, M., Mandai, M., Matsumura, N., Yamaguchi, K., Hamanishi, J., Higuchi, T., Takakura, K., and Fujii, S. (2007). Immortalized ovarian surface epithelial cells acquire tumorigenicity by Acrogranin gene overexpression. Oncology reports *17*, 329-333.

Mohler, J.L., Morris, T.L., Ford, O.H., 3rd, Alvey, R.F., Sakamoto, C., and Gregory, C.W. (2002). Identification of differentially expressed genes associated with androgen-independent growth of prostate cancer. The Prostate *51*, 247-255.

Moisse, K., Volkening, K., Leystra-Lantz, C., Welch, I., Hill, T., and Strong, M.J. (2009). Divergent patterns of cytosolic TDP-43 and neuronal progranulin expression following axotomy: implications for TDP-43 in the physiological response to neuronal injury. Brain research *1249*, 202-211.

Monami, G., Emiliozzi, V., Bitto, A., Lovat, F., Xu, S.Q., Goldoni, S., Fassan, M., Serrero, G., Gomella, L.G., Baffa, R.*, et al.* (2009). Proepithelin regulates prostate cancer cell biology by promoting cell growth, migration, and anchorage-independent growth. The American journal of pathology *174*, 1037-1047.

Monami, G., Gonzalez, E.M., Hellman, M., Gomella, L.G., Baffa, R., Iozzo, R.V., and Morrione, A. (2006). Proepithelin promotes migration and invasion of 5637 bladder cancer cells through the activation of ERK1/2 and the formation of a paxillin/FAK/ERK complex. Cancer research *66*, 7103-7110.

Mostert, V., Wolff, S., Dreher, I., Kohrle, J., and Abel, J. (2001). Identification of an element within the promoter of human selenoprotein P responsive to transforming growth factor-beta. European journal of biochemistry / FEBS *268*, 6176-6181.

Murphy, T.H., Miyamoto, M., Sastre, A., Schnaar, R.L., and Coyle, J.T. (1989). Glutamate toxicity in a neuronal cell line involves inhibition of cystine transport leading to oxidative stress. Neuron *2*, 1547-1558.

Nakayama, A., Hill, K.E., Austin, L.M., Motley, A.K., and Burk, R.F. (2007). All regions of mouse brain are dependent on selenoprotein P for maintenance of selenium. The Journal of nutrition *137*, 690-693.

Naphade, S.B., Kigerl, K.A., Jakeman, L.B., Kostyk, S.K., Popovich, P.G., and Kuret, J. (2010). Progranulin expression is upregulated after spinal contusion in mice. Acta neuropathologica *119*, 123-133.

Nathan, C., and Shiloh, M.U. (2000). Reactive oxygen and nitrogen intermediates in the relationship between mammalian hosts and microbial pathogens. Proceedings of the National Academy of Sciences of the United States of America *97*, 8841-8848.

Neill, T., Buraschi, S., Goyal, A., Sharpe, C., Natkanski, E., Schaefer, L., Morrione, A., and Iozzo, R.V. (2016). EphA2 is a functional receptor for the growth factor progranulin. The Journal of cell biology *215*, 687-703.

Nicholson, A.M., Finch, N.A., Almeida, M., Perkerson, R.B., van Blitterswijk, M., Wojtas, A., Cenik, B., Rotondo, S., Inskeep, V., Almasy, L.*, et al.* (2016). Prosaposin is a regulator of progranulin levels and oligomerization. Nat Commun *7*, 11992.

Niehrs, C. (1999). Head in the WNT: the molecular nature of Spemann's head organizer. Trends in genetics : TIG *15*, 314-319.

Noble, W., Planel, E., Zehr, C., Olm, V., Meyerson, J., Suleman, F., Gaynor, K., Wang, L., LaFrancois, J., Feinstein, B.*, et al.* (2005). Inhibition of glycogen synthase kinase-3 by lithium correlates with reduced tauopathy and degeneration in vivo. Proceedings of the National Academy of Sciences of the United States of America *102*, 6990-6995.

Nusse, R. (2008). Wnt signaling and stem cell control. Cell research *18*, 523-527.

Nykjaer, A., and Willnow, T.E. (2012). Sortilin: a receptor to regulate neuronal viability and function. Trends in neurosciences *35*, 261-270.

O'Brien, J.S., and Kishimoto, Y. (1991). Saposin proteins: structure, function, and role in human lysosomal storage disorders. FASEB journal : official publication of the Federation of American Societies for Experimental Biology *5*, 301-308.

Oakley, H., Cole, S.L., Logan, S., Maus, E., Shao, P., Craft, J., Guillozet-Bongaarts, A., Ohno, M., Disterhoft, J., Van Eldik, L.*, et al.* (2006). Intraneuronal beta-amyloid aggregates, neurodegeneration, and neuron loss in transgenic mice with five familial Alzheimer's disease mutations: potential factors in amyloid plaque formation. The Journal of neuroscience : the official journal of the Society for Neuroscience *26*, 10129-10140.

Okura, H., Yamashita, S., Ohama, T., Saga, A., Yamamoto-Kakuta, A., Hamada, Y., Sougawa, N., Ohyama, R., Sawa, Y., and Matsuyama, A. (2010). HDL/apolipoprotein A-I binds to macrophage-derived progranulin and suppresses its conversion into proinflammatory granulins. Journal of atherosclerosis and thrombosis *17*, 568-577.

Parnell, P.G. (1992). Transforming growth factor e: amino acid analysis and partial amino acid sequence. Growth Factors *7*, 65-72.

Patel, S.A., Warren, B.A., Rhoderick, J.F., and Bridges, R.J. (2004). Differentiation of substrate and non-substrate inhibitors of transport system xc(-): an obligate exchanger of L-glutamate and L-cystine. Neuropharmacology *46*, 273-284.

Pellatt, A.J., Wolff, R.K., John, E.M., Torres-Mejia, G., Hines, L.M., Baumgartner, K.B., Giuliano, A.R., Lundgreen, A., and Slattery, M.L. (2013). SEPP1 influences breast cancer risk among women with greater native american ancestry: the breast cancer health disparities study. PloS one *8*, e80554.

Pereson, S., Wils, H., Kleinberger, G., McGowan, E., Vandewoestyne, M., Van Broeck, B., Joris, G., Cuijt, I., Deforce, D., Hutton, M.*, et al.* (2009). Progranulin expression correlates with dense-core amyloid plaque burden in Alzheimer disease mouse models. The Journal of pathology *219*, 173-181.

Petkau, T.L., and Leavitt, B.R. (2014). Progranulin in neurodegenerative disease. Trends in neurosciences *37*, 388-398.

Petkau, T.L., Neal, S.J., Orban, P.C., MacDonald, J.L., Hill, A.M., Lu, G., Feldman, H.H., Mackenzie, I.R., and Leavitt, B.R. (2010). Progranulin expression in the developing and adult murine brain. The Journal of comparative neurology *518*, 3931-3947.

Pilcher, B.K., Wang, M., Qin, X.J., Parks, W.C., Senior, R.M., and Welgus, H.G. (1999). Role of matrix metalloproteinases and their inhibition in cutaneous wound healing and allergic contact hypersensitivity. Annals of the New York Academy of Sciences *878*, 12-24.

Piscopo, P., Rivabene, R., Adduci, A., Mallozzi, C., Malvezzi-Campeggi, L., Crestini, A., and Confaloni, A. (2010). Hypoxia induces up-regulation of progranulin in neuroblastoma cell lines. Neurochem Int *57*, 893-898.

Pitts, M.W., Raman, A.V., Hashimoto, A.C., Todorovic, C., Nichols, R.A., and Berry, M.J. (2012). Deletion of selenoprotein P results in impaired function of parvalbumin interneurons and alterations in fear learning and sensorimotor gating. Neuroscience *208*, 58-68.

Pizarro, G.O., Zhou, X.C., Koch, A., Gharib, M., Raval, S., Bible, K., and Jones, M.B. (2007). Prosurvival function of the granulin-epithelin precursor is important in tumor progression and chemoresponse. International journal of cancer Journal international du cancer *120*, 2339-2343.

Plowman, G.D., Green, J.M., Neubauer, M.G., Buckley, S.D., McDonald, V.L., Todaro, G.J., and Shoyab, M. (1992). The epithelin precursor encodes two proteins with opposing activities on epithelial cell growth. The Journal of biological chemistry *267*, 13073-13078.

Puschmann, A. (2013). Monogenic Parkinson's disease and parkinsonism: clinical phenotypes and frequencies of known mutations. Parkinsonism & related disorders *19*, 407-415.

Qi, X., and Grabowski, G.A. (2001). Differential membrane interactions of saposins A and C: implications for the functional specificity. The Journal of biological chemistry *276*, 27010-27017.

Rademakers, R., Baker, M., Gass, J., Adamson, J., Huey, E.D., Momeni, P., Spina, S., Coppola, G., Karydas, A.M., Stewart, H.*, et al.* (2007). Phenotypic variability associated with progranulin haploinsufficiency in patients with the common 1477C-->T (Arg493X) mutation: an international initiative. Lancet neurology *6*, 857-868.

Rademakers, R., Cruts, M., and van Broeckhoven, C. (2004). The role of tau (MAPT) in frontotemporal dementia and related tauopathies. Human mutation *24*, 277-295.

Rademakers, R., Neumann, M., and Mackenzie, I.R. (2012). Advances in understanding the molecular basis of frontotemporal dementia. Nature reviews Neurology *8*, 423-434.

Rademakers, R., and Rovelet-Lecrux, A. (2009). Recent insights into the molecular genetics of dementia. Trends in neurosciences *32*, 451-461.

Raitano, S., Ordovas, L., De Muynck, L., Guo, W., Espuny-Camacho, I., Geraerts, M., Khurana, S., Vanuytsel, K., Toth, B.I., Voets, T.*, et al.* (2015). Restoration of progranulin expression rescues cortical neuron generation in an induced pluripotent stem cell model of frontotemporal dementia. Stem Cell Reports *4*, 16-24.

Renton, A.E., Majounie, E., Waite, A., Simon-Sanchez, J., Rollinson, S., Gibbs, J.R., Schymick, J.C., Laaksovirta, H., van Swieten, J.C., Myllykangas, L.*, et al.* (2011). A hexanucleotide repeat expansion in C9ORF72 is the cause of chromosome 9p21-linked ALS-FTD. Neuron *72*, 257-268.

Rooney, C., White, G., Nazgiewicz, A., Woodcock, S.A., Anderson, K.I., Ballestrem, C., and Malliri, A. (2010). The Rac activator STEF (Tiam2) regulates cell migration by microtubule-mediated focal adhesion disassembly. EMBO reports *11*, 292-298.

Rosen, E.Y., Wexler, E.M., Versano, R., Coppola, G., Gao, F., Winden, K.D., Oldham, M.C., Martens, L.H., Zhou, P., Farese, R.V., Jr.*, et al.* (2011). Functional genomic analyses identify pathways dysregulated by progranulin deficiency, implicating Wnt signaling. Neuron *71*, 1030-1042.

Rothberg, J.M., Jacobs, J.R., Goodman, C.S., and Artavanis-Tsakonas, S. (1990). slit: an extracellular protein necessary for development of midline glia and commissural axon pathways contains both EGF and LRR domains. Genes & development *4*, 2169-2187.

Ryan, C.L., Baranowski, D.C., Chitramuthu, B.P., Malik, S., Li, Z., Cao, M., Minotti, S., Durham, H.D., Kay, D.G., Shaw, C.A.*, et al.* (2009). Progranulin is expressed within motor neurons and promotes neuronal cell survival. BMC neuroscience *10*, 130.

Sato, K., Yamanaka, Y., Ishii, M., Ishibashi, K., Ogura, Y., Ohtani-Kaneko, R., Nishihara, M., and Nedachi, T. (2014). Dual cell protective mechanisms activated by differing levels of oxidative stress in HT22 murine hippocampal cells. Bioscience, biotechnology, and biochemistry *78*, 1495-1503.

Schambony, A., Kunz, M., and Gradl, D. (2004). Cross-regulation of Wnt signaling and cell adhesion. Differentiation; research in biological diversity *72*, 307-318.

Scheiffele, P., Fan, J., Choih, J., Fetter, R., and Serafini, T. (2000). Neuroligin expressed in nonneuronal cells triggers presynaptic development in contacting axons. Cell *101*, 657-669.

Schmalfeldt, M., Dours-Zimmermann, M.T., Winterhalter, K.H., and Zimmermann, D.R. (1998). Versican V2 is a major extracellular matrix component of the mature bovine brain. The Journal of biological chemistry *273*, 15758-15764.

Seelaar, H., Kamphorst, W., Rosso, S.M., Azmani, A., Masdjedi, R., de Koning, I., Maat-Kievit, J.A., Anar, B., Donker Kaat, L., Breedveld, G.J.*, et al.* (2008). Distinct genetic forms of frontotemporal dementia. Neurology *71*, 1220-1226.

Sekhar, R.V., Patel, S.G., Guthikonda, A.P., Reid, M., Balasubramanyam, A., Taffet, G.E., and Jahoor, F. (2011). Deficient synthesis of glutathione underlies oxidative stress in aging and can be corrected by dietary cysteine and glycine supplementation. The American journal of clinical nutrition *94*, 847-853.

Semenov, M.V., Tamai, K., Brott, B.K., Kuhl, M., Sokol, S., and He, X. (2001). Head inducer Dickkopf-1 is a ligand for Wnt coreceptor LRP6. Current biology : CB *11*, 951-961.

Sephton, C.F., Cenik, B., Cenik, B.K., Herz, J., and Yu, G. (2012). TDP-43 in central nervous system development and function: clues to TDP-43-associated neurodegeneration. Biological chemistry *393*, 589-594.

Sheng, W., Wang, G., Wang, Y., Liang, J., Wen, J., Zheng, P.S., Wu, Y., Lee, V., Slingerland, J., Dumont, D.*, et al.* (2005). The roles of versican V1 and V2 isoforms in cell proliferation and apoptosis. Molecular biology of the cell *16*, 1330-1340.

Shukla, V., Mishra, S.K., and Pant, H.C. (2011). Oxidative stress in neurodegeneration. Advances in pharmacological sciences *2011*, 572634.

Siegel, D.A., Davies, P., Dobrenis, K., and Huang, M. (2006). Tomoregulin-2 is found extensively in plaques in Alzheimer's disease brain. Journal of neurochemistry *98*, 34-44.

Sjobring, U., Bjorck, L., and Kastern, W. (1991). Streptococcal protein G. Gene structure and protein binding properties. The Journal of biological chemistry *266*, 399-405.

Skibinski, G., Parkinson, N.J., Brown, J.M., Chakrabarti, L., Lloyd, S.L., Hummerich, H., Nielsen, J.E., Hodges, J.R., Spillantini, M.G., Thusgaard, T.*, et al.* (2005). Mutations in the endosomal ESCRTIII-complex subunit CHMP2B in frontotemporal dementia. Nature genetics *37*, 806-808.

Sleegers, K., Brouwers, N., Van Damme, P., Engelborghs, S., Gijselinck, I., van der Zee, J., Peeters, K., Mattheijssens, M., Cruts, M., Vandenberghe, R.*, et al.* (2009). Serum biomarker for progranulin-associated frontotemporal lobar degeneration. Annals of neurology *65*, 603-609.

Slobodkin, M.R., and Elazar, Z. (2013). The Atg8 family: multifunctional ubiquitin-like key regulators of autophagy. Essays Biochem *55*, 51-64.

Smith, K.R., Damiano, J., Franceschetti, S., Carpenter, S., Canafoglia, L., Morbin, M., Rossi, G., Pareyson, D., Mole, S.E., Staropoli, J.F.*, et al.* (2012). Strikingly different clinicopathological phenotypes determined by progranulin-mutation dosage. American journal of human genetics *90*, 1102-1107.

Snoek-van Beurden, P.A., and Von den Hoff, J.W. (2005). Zymographic techniques for the analysis of matrix metalloproteinases and their inhibitors. BioTechniques *38*, 73-83.

Sommer, L.A., Meier, M.A., and Dames, S.A. (2012). A fast and simple method for probing the interaction of peptides and proteins with lipids and membrane-mimetics using GB1 fusion proteins and NMR spectroscopy. Protein science : a publication of the Protein Society *21*, 1566-1570.

Songsrirote, K., Li, Z., Ashford, D., Bateman, A., and Thomas-Oates, J. (2010). Development and application of mass spectrometric methods for the analysis of progranulin N-glycosylation. Journal of proteomics *73*, 1479-1490.

Sudhof, T.C. (2008). Neuroligins and neurexins link synaptic function to cognitive disease. Nature *455*, 903-911.

Sulston, J.E., Schierenberg, E., White, J.G., and Thomson, J.N. (1983). The embryonic cell lineage of the nematode Caenorhabditis elegans. Developmental biology *100*, 64-119.

Swarnakar, S., Paul, S., Singh, L.P., and Reiter, R.J. (2011). Matrix metalloproteinases in health and disease: regulation by melatonin. Journal of pineal research *50*, 8-20.

Tan, S., Sagara, Y., Liu, Y., Maher, P., and Schubert, D. (1998). The regulation of reactive oxygen species production during programmed cell death. The Journal of cell biology *141*, 1423-1432.

Tan, S., Schubert, D., and Maher, P. (2001). Oxytosis: A novel form of programmed cell death. Current topics in medicinal chemistry *1*, 497-506.

Tanaka, Y., Suzuki, G., Matsuwaki, T., Hosokawa, M., Serrano, G., Beach, T.G., Yamanouchi, K., Hasegawa, M., and Nishihara, M. (2017). Progranulin regulates lysosomal function and biogenesis through acidification of lysosomes. Human molecular genetics *26*, 969-988.

Tang, W., Lu, Y., Tian, Q.Y., Zhang, Y., Guo, F.J., Liu, G.Y., Syed, N.M., Lai, Y., Lin, E.A., Kong, L.*, et al.* (2011). The growth factor progranulin binds to TNF receptors and is therapeutic against inflammatory arthritis in mice. Science *332*, 478-484.

Tangkeangsirisin, W., and Serrero, G. (2004). PC cell-derived growth factor (PCDGF/GP88, progranulin) stimulates migration, invasiveness and VEGF expression in breast cancer cells. Carcinogenesis *25*, 1587-1592.

Tapaneeyakorn, S., Ross, S., Attrill, H., and Watts, A. (2010). Heterologous high yield expression and purification of neurotensin and its functional fragment in Escherichia coli. Protein expression and purification *74*, 65-68.

Tapia, L., Milnerwood, A., Guo, A., Mills, F., Yoshida, E., Vasuta, C., Mackenzie, I.R., Raymond, L., Cynader, M., Jia, W.*, et al.* (2011). Progranulin deficiency decreases gross neural connectivity but enhances transmission at individual synapses. The Journal of neuroscience : the official journal of the Society for Neuroscience *31*, 11126-11132.

Toh, H., Chitramuthu, B.P., Bennett, H.P., and Bateman, A. (2011). Structure, function, and mechanism of progranulin; the brain and beyond. Journal of molecular neuroscience : MN *45*, 538-548.

Tolkatchev, D., Malik, S., Vinogradova, A., Wang, P., Chen, Z., Xu, P., Bennett, H.P., Bateman, A., and Ni, F. (2008). Structure dissection of human progranulin identifies well-folded granulin/epithelin modules with unique functional activities. Protein science : a publication of the Protein Society *17*, 711-724.

Uchida, T., Wada, K., Akamatsu, T., Yonezawa, M., Noguchi, H., Mizoguchi, A., Kasuga, M., and Sakamoto, C. (1999). A novel epidermal growth factor-like molecule containing two follistatin modules stimulates tyrosine phosphorylation of erbB-4 in MKN28 gastric cancer cells. Biochemical and biophysical research communications *266*, 593-602.

Ulloa, F., and Briscoe, J. (2007). Morphogens and the control of cell proliferation and patterning in the spinal cord. Cell Cycle *6*, 2640-2649.

Valentine, W.M., Abel, T.W., Hill, K.E., Austin, L.M., and Burk, R.F. (2008). Neurodegeneration in mice resulting from loss of functional selenoprotein P or its receptor apolipoprotein E receptor 2. Journal of neuropathology and experimental neurology *67*, 68-77.

Valko, M., Morris, H., and Cronin, M.T. (2005). Metals, toxicity and oxidative stress. Current medicinal chemistry *12*, 1161-1208.

Van Damme, P., Van Hoecke, A., Lambrechts, D., Vanacker, P., Bogaert, E., van Swieten, J., Carmeliet, P., Van Den Bosch, L., and Robberecht, W. (2008). Progranulin functions as a neurotrophic factor to regulate neurite outgrowth and enhance neuronal survival. The Journal of cell biology *181*, 37-41.

van Horssen, J., Wesseling, P., van den Heuvel, L.P., de Waal, R.M., and Verbeek, M.M. (2003). Heparan sulphate proteoglycans in Alzheimer's disease and amyloid-related disorders. Lancet neurology *2*, 482-492.

Van Kampen, J.M., Baranowski, D., and Kay, D.G. (2014). Progranulin gene delivery protects dopaminergic neurons in a mouse model of Parkinson's disease. PloS one *9*, e97032.

Van Lint, P., and Libert, C. (2007). Chemokine and cytokine processing by matrix metalloproteinases and its effect on leukocyte migration and inflammation. Journal of leukocyte biology *82*, 1375-1381.

van Noort, M., Meeldijk, J., van der Zee, R., Destree, O., and Clevers, H. (2002). Wnt signaling controls the phosphorylation status of beta-catenin. The Journal of biological chemistry *277*, 17901-17905.

Walsh, T., McClellan, J.M., McCarthy, S.E., Addington, A.M., Pierce, S.B., Cooper, G.M., Nord, A.S., Kusenda, M., Malhotra, D., Bhandari, A.*, et al.* (2008). Rare structural variants disrupt multiple genes in neurodevelopmental pathways in schizophrenia. Science *320*, 539-543.

Wang, M., Li, G., Yin, J., Lin, T., and Zhang, J. (2012). Progranulin overexpression predicts overall survival in patients with glioblastoma. Med Oncol *29*, 2423-2431.

Wang, M., Liu, Y.E., Greene, J., Sheng, S., Fuchs, A., Rosen, E.M., and Shi, Y.E. (1997). Inhibition of tumor growth and metastasis of human breast cancer cells transfected with tissue inhibitor of metalloproteinase 4. Oncogene *14*, 2767-2774.

Wang, W., Hayashi, J., Kim, W.E., and Serrero, G. (2003). PC cell-derived growth factor (granulin precursor) expression and action in human multiple myeloma. Clinical cancer research : an official journal of the American Association for Cancer Research *9*, 2221-2228.

Watts, G.D., Wymer, J., Kovach, M.J., Mehta, S.G., Mumm, S., Darvish, D., Pestronk, A., Whyte, M.P., and Kimonis, V.E. (2004). Inclusion body myopathy associated with Paget disease of bone and frontotemporal dementia is caused by mutant valosin-containing protein. Nature genetics *36*, 377-381.

Wexler, E.M., Rosen, E., Lu, D., Osborn, G.E., Martin, E., Raybould, H., and Geschwind, D.H. (2011). Genome-wide analysis of a Wnt1-regulated transcriptional network implicates neurodegenerative pathways. Science signaling *4*, ra65.

Whitelock, J.M., Graham, L.D., Melrose, J., Murdoch, A.D., Iozzo, R.V., and Underwood, P.A. (1999). Human perlecan immunopurified from different endothelial cell sources has different adhesive properties for vascular cells. Matrix Biol *18*, 163-178.

Wiedau-Pazos, M., Wong, E., Solomon, E., Alarcon, M., and Geschwind, D.H. (2009). Wnt-pathway activation during the early stage of neurodegeneration in FTDP-17 mice. Neurobiology of aging *30*, 14-21.

Willert, K., and Jones, K.A. (2006). Wnt signaling: is the party in the nucleus? Genes & development *20*, 1394-1404.

Wu, W., Glinka, A., Delius, H., and Niehrs, C. (2000). Mutual antagonism between dickkopf1 and dickkopf2 regulates Wnt/beta-catenin signalling. Current biology : CB *10*, 1611-1614.

Wu, Y., Sheng, W., Dong, H., Lapierre, D., Wan, Y., Lu, W.Y., and Yang, B.B. (2009). Versican isoforms modulate expression and function of nicotinic acetylcholine receptors. International journal of physiology, pathophysiology and pharmacology *1*, 64-75.

Wulff, P., Schonewille, M., Renzi, M., Viltono, L., Sassoe-Pognetto, M., Badura, A., Gao, Z., Hoebeek, F.E., van Dorp, S., Wisden, W.*, et al.* (2009). Synaptic inhibition of Purkinje cells mediates consolidation of vestibulo-cerebellar motor learning. Nature neuroscience *12*, 1042-1049.

Xia, X., and Serrero, G. (1998). Identification of cell surface binding sites for PC-cell-derived growth factor, PCDGF, (epithelin/granulin precursor) on epithelial cells and fibroblasts. Biochemical and biophysical research communications *245*, 539-543.

Xu, J., Xilouri, M., Bruban, J., Shioi, J., Shao, Z., Papazoglou, I., Vekrellis, K., and Robakis, N.K. (2011). Extracellular progranulin protects cortical neurons from toxic insults by activating survival signaling. Neurobiology of aging *32*, 2326 e2325-2316.

Yin, F., Banerjee, R., Thomas, B., Zhou, P., Qian, L., Jia, T., Ma, X., Ma, Y., Iadecola, C., Beal, M.F.*, et al.* (2010a). Exaggerated inflammation, impaired host defense, and neuropathology in progranulin-deficient mice. The Journal of experimental medicine *207*, 117-128.

Yin, F., Dumont, M., Banerjee, R., Ma, Y., Li, H., Lin, M.T., Beal, M.F., Nathan, C., Thomas, B., and Ding, A. (2010b). Behavioral deficits and progressive neuropathology in progranulin-deficient mice: a mouse model of frontotemporal dementia. FASEB journal : official publication of the Federation of American Societies for Experimental Biology *24*, 4639-4647.

Yoo, H.J., Hwang, S.Y., Hong, H.C., Choi, H.Y., Yang, S.J., Choi, D.S., Baik, S.H., Bluher, M., Youn, B.S., and Choi, K.M. (2013). Implication of progranulin and C1q/TNF-related protein-3 (CTRP3) on inflammation and atherosclerosis in subjects with or without metabolic syndrome. PloS one *8*, e55744.

Youn, B.S., Bang, S.I., Kloting, N., Park, J.W., Lee, N., Oh, J.E., Pi, K.B., Lee, T.H., Ruschke, K., Fasshauer, M.*, et al.* (2009). Serum progranulin concentrations may be associated with macrophage infiltration into omental adipose tissue. Diabetes *58*, 627-636.

Young, J., Biden, K.G., Simms, L.A., Huggard, P., Karamatic, R., Eyre, H.J., Sutherland, G.R., Herath, N., Barker, M., Anderson, G.J.*, et al.* (2001). HPP1: a transmembrane protein-encoding gene commonly methylated in colorectal polyps and cancers. Proceedings of the National Academy of Sciences of the United States of America *98*, 265-270.

Zambrano, N., Buxbaum, J.D., Minopoli, G., Fiore, F., De Candia, P., De Renzis, S., Faraonio, R., Sabo, S., Cheetham, J., Sudol, M.*, et al.* (1997). Interaction of the phosphotyrosine interaction/phosphotyrosine binding-related domains of Fe65 with wild-type and mutant Alzheimer's beta-amyloid precursor proteins. The Journal of biological chemistry *272*, 6399-6405.

Zanocco-Marani, T., Bateman, A., Romano, G., Valentinis, B., He, Z.H., and Baserga, R. (1999). Biological activities and signaling pathways of the granulin/epithelin precursor. Cancer research *59*, 5331-5340.

Zhang, H., and Serrero, G. (1998). Inhibition of tumorigenicity of the teratoma PC cell line by transfection with antisense cDNA for PC cell-derived growth factor (PCDGF, epithelin/granulin precursor). Proceedings of the National Academy of Sciences of the United States of America *95*, 14202-14207.

Zhang, Y.J., Xu, Y.F., Dickey, C.A., Buratti, E., Baralle, F., Bailey, R., Pickering-Brown, S., Dickson, D., and Petrucelli, L. (2007). Progranulin mediates caspase-dependent cleavage of TAR DNA binding protein-43. The Journal of neuroscience : the official journal of the Society for Neuroscience *27*, 10530-10534.

Zhao, Y.P., Tian, Q.Y., and Liu, C.J. (2013). Progranulin deficiency exaggerates, whereas progranulin-derived Atsttrin attenuates, severity of dermatitis in mice. FEBS letters *587*, 1805-1810.

Zheng, H., and Koo, E.H. (2011). Biology and pathophysiology of the amyloid precursor protein. Molecular neurodegeneration *6*, 27.

Zheng, Y., Brady, O.A., Meng, P.S., Mao, Y., and Hu, F. (2011). C-terminus of progranulin interacts with the beta-propeller region of sortilin to regulate progranulin trafficking. PloS one *6*, e21023.

Zhou, J., Gao, G., Crabb, J.W., and Serrero, G. (1993). Purification of an autocrine growth factor homologous with mouse epithelin precursor from a highly tumorigenic cell line. The Journal of biological chemistry *268*, 10863-10869.

Zhou, X., Sun, L., Bastos de Oliveira, F., Qi, X., Brown, W.J., Smolka, M.B., Sun, Y., and Hu, F. (2015). Prosaposin facilitates sortilin-independent lysosomal trafficking of progranulin. The Journal of cell biology *210*, 991-1002.

Zhu, J., Nathan, C., Jin, W., Sim, D., Ashcroft, G.S., Wahl, S.M., Lacomis, L., Erdjument-Bromage, H., Tempst, P., Wright, C.D.*, et al.* (2002). Conversion of proepithelin to epithelins: roles of SLPI and elastase in host defense and wound repair. Cell *111*, 867-878.

Zhu, Y., Carvey, P.M., and Ling, Z. (2006). Age-related changes in glutathione and glutathione-related enzymes in rat brain. Brain research *1090*, 35-44.

Zou, Y. (2004). Wnt signaling in axon guidance. Trends in neurosciences *27*, 528-532.

7. Acknowledgements

First, I would like to thank my thesis advisor Prof. Dr. Sascha Weggen of the Institute of Neuropathology at the University Hospital Düsseldorf for the opportunity to work on this project.

I would also like to thank my second advisor Prof. Dr. Vlada Urlacher of the Institute of Biochemistry at the Heinrich-Heine University Düsseldorf for supporting my thesis.

Special thanks goes to the supporting energy from all my friends and colleagues, everybody a one-of-a-kind-expert.